UNCLASSIFIED

LOCKHEED MARTIN ENERGY RESEARCH LIBRARIES
3 4456 0511511 2

CENTRAL RESEARCH LIBRARY
DOCUMENT COLLECTION

ORNL-2277
Physics and Mathematics Cy. 4

A MONTE CARLO CALCULATION OF AIR-SCATTERED NEUTRONS

C. D. Zerby

OAK RIDGE NATIONAL LABORATORY
CENTRAL RESEARCH LIBRARY
CIRCULATION SECTION
4500N ROOM 175
LIBRARY LOAN COPY
DO NOT TRANSFER TO ANOTHER PERSON.
if you wish someone else to see this report, send in name with report and the library will arrange a loan.
ORNL-118 (6-97)

OAK RIDGE NATIONAL LABORATORY
OPERATED BY
UNION CARBIDE NUCLEAR COMPANY
A Division of Union Carbide and Carbon Corporation
UCC
POST OFFICE BOX X · OAK RIDGE, TENNESSEE

UNCLASSIFIED

Printed in USA. Price 65 cents. Available from the

Office of Technical Services
U. S. Department of Commerce
Washington 25, D. C.

LEGAL NOTICE

This report was prepared as an account of Government sponsored work. Neither the United States, nor the Commission, nor any person acting on behalf of the Commission:

A. Makes any warranty or representation, express or implied, with respect to the accuracy, completeness, or usefulness of the information contained in this report, or that the use of any information, apparatus, method, or process disclosed in this report may not infringe privately owned rights; or

B. Assumes any liabilities with respect to the use of, or for damages resulting from the use of any information, apparatus, method, or process disclosed in this report.

As used in the above, "person acting on behalf of the Commission" includes any employee or contractor of the Commission to the extent that such employee or contractor prepares, handles or distributes, or provides access to, any information pursuant to his employment or contract with the Commission.

UNCLASSIFIED

ORNL-2277

Contract No. W-7405-eng-26

Applied Nuclear Physics Division

A MONTE CARLO CALCULATION OF AIR-SCATTERED NEUTRONS

C. D. Zerby

Date Issued

APR 23 1957

OAK RIDGE NATIONAL LABORATORY
Operated by
UNION CARBIDE NUCLEAR COMPANY
A Division of Union Carbide and Carbon Corporation
Post Office Box X
Oak Ridge, Tennessee

UNCLASSIFIED

LOCKHEED MARTIN ENERGY RESEARCH LIBRARIES

3 4456 0511511 2

INTERNAL DISTRIBUTION

1. C. E. Center
2. Biology Library
3. Health Physics Library
4-5. Central Research Library
6. Reactor Experimental Engineering Library
7-26. Laboratory Records Department
27. Laboratory Records, ORNL R.C.
28. A. M. Weinberg
29. L. B. Emlet (K-25)
30. J. P. Murray (Y-12)
31. J. A. Swartout
32. E. H. Taylor
33. E. D. Shipley
34. A. H. Snell
35. M. L. Nelson
36. W. H. Jordan
37. S. J. Cromer
38. G. E. Boyd
39. R. A. Charpie
40. S. C. Lind
41. F. L. Culler
42. A. Hollaender
43. J. H. Frye, Jr.
44. M. T. Kelley
45. R. S. Livingston
46. K. Z. Morgan
47. T. A. Lincoln
48. A. S. Householder
49. C. P. Keim
50. C. S. Harrill
51. C. E. Winters
52. D. S. Billington
53. D. W. Cardwell
54. E. M. King
55. E. P. Blizard
56. D. D. Cowen
57. M. J. Skinner
58. R. B. Murray
59. R. R. Dickison
60. J. A. Harvey
61. A. Simon
62. F. C. Maienschein
63. L. A. Bowman
64. J. Hilgeman
65-69. C. D. Zerby
70. G. C. Williams
71. ORNL - Y-12 Technical Library, Document Reference Section

EXTERNAL DISTRIBUTION

72. R. F. Bacher, California Institute of Technology
73. Division of Research and Development, AEC, ORO
74-648. Given distribution as shown in TID-4500 under Physics and Mathematics category (100 copies - OTS)

TABLE OF CONTENTS

CHAPTER		PAGE
ABSTRACT		iii
I.	INTRODUCTION	1
	General Introduction	1
	Organization of the Report	2
II.	PROBLEM ANALYSIS AND PROCEDURES	3
	Composition of Air and Cross Sections	3
	Geometry	5
	General Formulation of the Monte Carlo Problem	7
	Distribution Sampling and Generation of a Neutron History	16
	Computation of the Neutron Current at the Detector Point and Its Variance	26
	Computation of the Tissue Dose Rate at the Detector Point	29
III.	TESTING THE CALCULATION	35
	Testing of the Single Scattering Current from a Monodirectional Source	35
	Comparisons of the Monte Carlo Solution Against Numerical Solutions of the One-Velocity Boltzmann Equation	36
	Comparison of the Monte Carlo Solution Against a Moments Method Solution	41
IV.	RESULTS	49
APPENDIX A		61
Appendix B		65

ABSTRACT

A description is given of a Monte Carlo calculation to determine the angular distribution and energy spectrum of air-scattered neutrons. The calculation was programmed for computation on the ORACLE. The particular form of Monte Carlo calculation used involved the integration of the Boltzmann equation and is described in some detail. The problem was idealized to have the source in an infinite body of air and used isotropic scattering in the center-of-mass system. The results for the total neutron flux and tissue dose rate at a source-detector separation distance of 64 ft are presented. The source in this case was a point which emitted a line beam of monoenergetic neutrons.

CHAPTER I. INTRODUCTION

General Introduction

It is very difficult to conceive of an experiment or apparatus using or containing sources of nuclear radiation which does not permit some fraction of the radiation to escape to the surrounding air. A knowledge of the distribution of the radiation, once it enters the air, can be of great importance if the intensity is high and there is a need for personnel protection or estimating material damage. Unfortunately, it is not a simple matter to determine the distribution from experiment for general cases which can be applied to design problems. This means one must depend on calculations to provide the information, and the purpose of this report is to present some calculations which can be useful in the general case. In particular, this report deals with distribution of neutrons emitted into an infinite body of air. The Monte Carlo method of calculation was used.

In order to maintain generality it was decided to make a parameter study involving a line beam of monoenergetic neutrons from a point source. The results of such a calculation can be integrated to make up any arbitrary source distribution.[1]

There have been several calculations to determine the distribution of neutrons in air. The most noteable of these was done by Holland and Richards[2] who used the moments method of solution for a monoenergetic, isotropic point source in air. For the case of line beams, most calculations

---

1. C. D. Zerby, Transmission of Obliquely Incident Gamma-Radiation Through Stratified Slab Barriers, ORNL-224, Vol. 1 (1956) App. B.
2. S. S. Holland P. I. Richards, J. Appl. Phys. 27, 1042 (1956).

have used single scattering theory. Some examples of this type of calculation have been given by Weller and Workman.[3]

Organization of the Report

The main text of this report deals with the processes and procedures incorporated into the Monte Carlo problem which was coded for calculation on the ORACLE, a high speed automatic digital computor located at the Oak Ridge National Laboratory. Chapter II contains most of this material. Chapter III presents the results of some test calculations which were run for the purposes of evaluating the accuracy of the Monte Carlo technique used. Chapter IV presents the results of a parameter study at a source-detector separation distance of 64 ft where the radiation was emitted from a monoenergetic line beam point source.

Appendix B is a self-consistent entity which provides a record of the final code for the ORACLE; along with this is a complete description of its operation and use. The reader who does not have access to the ORACLE will find little interest in this appendix except in those paragraphs dealing with the input data which will give an idea of the versatility of the code.

---

3. G. S. Weller and B. J. Workman, Single Scattering of Neutrons in Air, CVAC-211T (1954).

CHAPTER II. PROBLEM ANALYSIS AND PROCEDURES

Composition of Air and Cross Sections

The composition of dry air at sea level conditions as given in the Handbook of Chemistry and Physics[4] is repeated in Table 1. Since the main elements of the air are nitrogen and oxygen and the other elements altogether make up less than one percent of the volume of the air, it was decided to consider the effects of nitrogen and oxygen only in the calculation. Using the volume percents given in Table 1 and normalizing to a unit volume resulted in the weight percentages of nitrogen and oxygen of 76.5 and 23.5, respectively. These weight percents were used for every density of dry air.

Table 1. Composition of Dry Air, Mean Percentages by Volume, at Sea Level Conditions

N_2	78.03	H_2	0.01
O_2	20.99	Ne	0.0012
A	0.94	He	0.0004
CO_2	0.03		

The total cross sections for oxygen, nitrogen, and hydrogen were taken from the graphs presented in the report BNL-325.[5] The hydrogen total cross sections were included so that moisture could be added to the air. The total cross sections for oxygen and nitrogen were included as a table for

4. C. H. Hodgman, Editor, Handbook of Chemistry and Physics, 33rd Edition, Chemical Rubber Publishing Company, Cleveland, 1951, p. 2817.
5. D. J. Hughes and J. A. Harvey, Neutron Cross Sections, BNL-325 (1955).

neutron energies above 0.10 Mev. The values of the cross sections were included at energy intervals of 0.025 Mev between 0.10 and 2.5 Mev, at intervals of 0.10 Mev between 2.5 and 7.5 Mev, and at intervals of 2.0 Mev between 7.5 and 31.5 Mev. Cross sections required from this table were obtained by linear interpolation. Below 0.10 Mev analytic expressions fit to the data were used. The total cross section for hydrogen was obtained with a series of rational polynomials fit to the data.

Although the total cross sections were included up to neutron energies of 15 Mev, it was not intended that the calculation be general enough to include sources of such a high energy. For this reason, stimulated by the lack of information, it was decided to consider the total cross section as being identical with the scattering cross section except at very low energy where the (n,γ) reaction becomes of some importance. The absorption cross section for nitrogen and hydrogen at low energy was obtained in the calculation by taking the absorption cross section at thermal energy (0.025 ev) and assuming a $1/v$ dependence.

The scattering probability was taken as isotropic in the center of mass system which is correct only for hydrogen at the energies of interest in this problem; however, it is nearly correct in the case of oxygen and nitrogen over much of the low energy range. The decision to include the scattering as isotropic in the center of mass system was made because of the lack of experimental data giving the anisotropy of scattering. It appeared to be reasonable to go ahead with this procedure and prove a technique of calculating first and alter or recode the problem later as data became available.

Geometry

The geometry of the source and detector are shown in Fig. 1. The source of radiation was taken as a point located on a black sphere with diameter d. The radiation emitted from the source point was assumed to have an axis of symmetry perpendicular to the surface of the sphere which pointed at an angle θ_o with respect to the source detector axis. The distribution of the radiation about the axis of symmetry was chosen as

$$\frac{P+1}{2\pi} \cos^P\theta = \text{source distribution; neutrons/steradian/sec} \qquad (1)$$

where θ is the angle measured from the axis of symmetry and P is an arbitrary positive integer.

Located at a distance g from the center of the source sphere was a point detector. The space about the detector was divided into a number of solid angles with apex at the detector point. The number of neutrons coming into each of these solid angles was counted. The solid angles were located by first establishing a coordinate system as shown in Fig. 1. The x axis coincided with the source-detector axis and the orthogonal y axis was in the plane containing the source-detector axis and the axis of symmetry of the radiation. The z axis was orthogonal to the x and y axis. The x axis was chosen as the polar axis for the grid system to establish the solid angle intervals and the usual spherical coordinate system was used. The polar angle was divided into a number of equal angle intervals and the azimuthal angle was divided into a number of equal angle intervals. The meridian and parallels of latitude scribed on a sphere centered at the detector point established the intersection of the set of solid angles with the arbitrary sphere.

UNCLASSIFIED
2-01-059-182

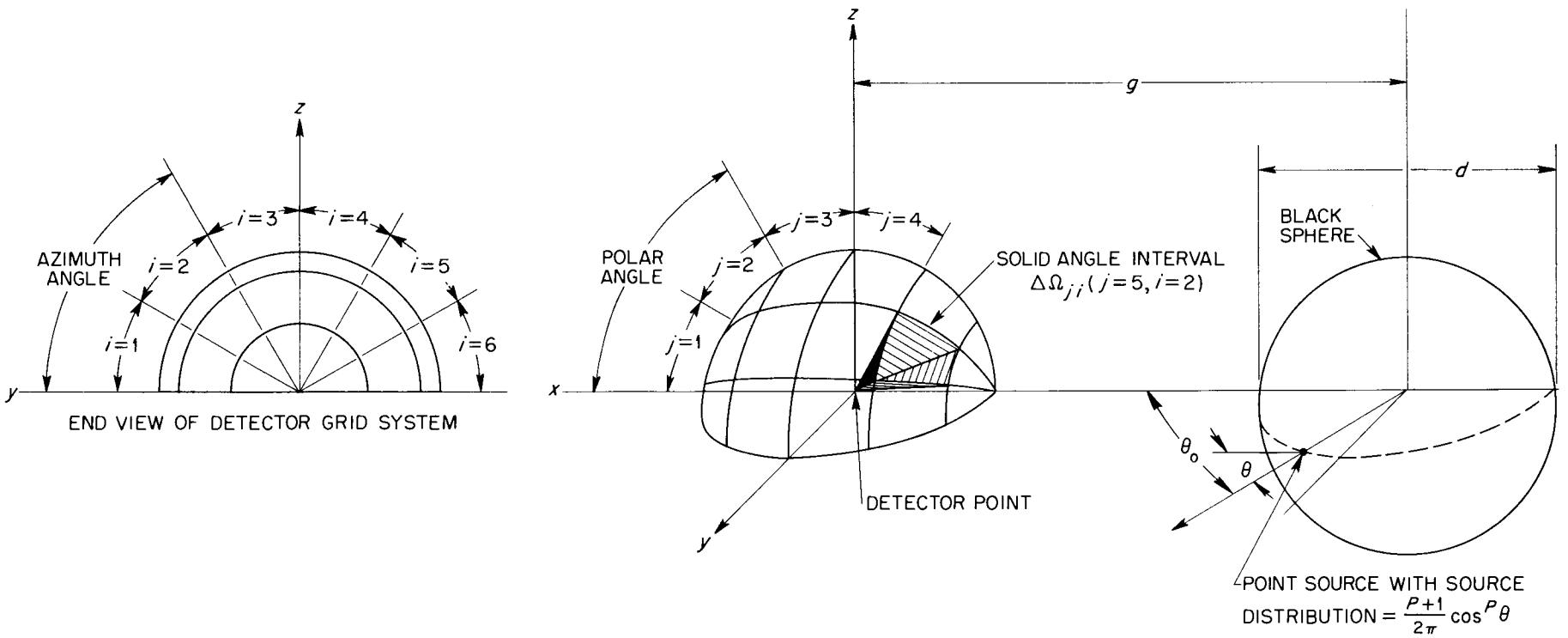

Fig. 1. Source-Detector Geometry Showing a Typical Grid System About the Detector Point Where the Polar and Azimuthal Angles were Divided into 30-deg Intervals.

Because of the symmetry of the geometry it was not necessary to divide the 4π space about the detector point into solid angles but just the 2π space above the x-y plane. The lower 2π space will then be just a reflection of the upper 2π space.

Variables that were determined by input data to the code was the diameter d of the black sphere, the angle θ_o, the number P, the separation distance g, the number of polar and azimuthal angle intervals about the detector point, the density of the dry air and the density of the moisture in the air.

The energy spectrum of the radiation entering each of the solid angle intervals was determined by dividing the energy range from some cut off energy to the source energy into an arbitrary number of equal intervals.

General Formulation of the Monte Carlo Problem

The general problem, as outlined in the geometry section, is an impossible one to attempt using a straight analogue Monte Carlo approach. This is easily seen when one realizes that the fraction of the source particles passing through a sphere having a unit cross sectional area at the detector point at a source-detector separation distance of only 0.3 mfp is in the order of 10^{-7}. The expected standard deviation in this case is approximately

$$\delta = \sqrt{\frac{F(1 - F)}{N}} \qquad (2)$$

where

F = the fraction of the source particles passing through the unit sphere,

δ = standard deviation on the value F,

N = the number of source particles.

If one would be satisfied with a confidence interval such that $\delta/F \cong 0.5$ then the number of source particles required can be determined from Eq. (2) as 4×10^7. One possible way to reduce the number of source particles required is to increase the cross section of the sphere at the detector point and accept an average value answer for the flux; however, it would be necessary to increase the area by a factor of 10^5 before the problem became practical. It seems undesirable to accept an average flux value over such a larger region.

Rather than take the straight analogue approach to the problem, it was decided to solve the Boltzmann Transport equation in its integral form using expected values as described by Kahn.[6] From previous problems it was expected that reasonable statistical accuracy could be achieved with this method with a minimum of sample source particles.

The integral form of the Boltzmann equation is derived in App. A. In what follows it will be presented in such a way as to give the particle current coming into a point located at the origin rather than the current leaving the point. The solution of the equation in this form will provide data which is more easily used when detectors are involved. The equation is

---

6. H. Kahn, Applications of Monte Carlo, RM-1237-AEC (1956).

$$\phi(0,E,\vec{\Omega}) = \int_{\text{All Space}} q(\vec{r}',E,-\vec{\Omega})e^{-\int_0^{r'} \Sigma_T(r''\vec{\Omega}',E)dr''} \frac{\delta(\vec{\Omega}',\vec{\Omega})}{r'^2} d\vec{r}' \qquad (3)$$

where

$\vec{\Omega}$ = a unit vector,

$\phi(0,E,\vec{\Omega})$ = particles per cm^2 per sec per unit energy at energy E per steradian about the negative direction $-\vec{\Omega}$ at the origin,

$\Sigma_T(\vec{r},E)$ = the macroscopic total cross section at position $\vec{r}$ and at energy E (cm^{-1}),

$q(\vec{r}',E,-\vec{\Omega})$ = the source term: particles per cm^2 per sec per unit energy at energy E per steradian about direction $-\vec{\Omega}$ at position $\vec{r}'$,

$d\vec{r}'$ = $r'^2\, d\vec{\Omega}'dr'$

and

$$\delta(\vec{\Omega}',\vec{\Omega}) = 0 \quad \text{if } \vec{\Omega}' \neq \vec{\Omega}$$

$$\int_{\vec{\Omega}'} \delta(\vec{\Omega}',\vec{\Omega})d\vec{\Omega}' = 1 \qquad (4)$$

In the particular case of interest here, the source term is given by

$$q(\vec{r}',E,-\vec{\Omega}) = \frac{S(-\vec{\Omega})\,\delta(\vec{\Omega}_o,\vec{\Omega}')\,\delta(r_o - r')\,\delta(E_o - E)}{r'^2}$$

$$+ \int_{E''}\int_{\vec{\Omega}''} \Sigma_s(\vec{r}',E'')\phi(\vec{r}',E'',-\vec{\Omega}'')f(E,E',-\vec{\Omega},\vec{\Omega}'')dE''d\vec{\Omega}'' \tag{5}$$

where

$\Sigma_s(\vec{r}',E'')$ = the macroscopic scattering cross section at position $\vec{r}'$ and at energy E" (cm^{-1}),

$f(E,E'',-\vec{\Omega},\vec{\Omega}'')dEd\vec{\Omega}$ = the probability of scattering from a direction $\vec{\Omega}''$ at energy E" into the solid angle $d\vec{\Omega}$ about the direction $-\vec{\Omega}$ and into the energy interval between E and E + dE.

The first term on the right of Eq. (5) is for a monoenergetic, anisotropic point source, where

$S(-\vec{\Omega})$ = particles per sec per steradian about the direction $-\vec{\Omega}$,

E_o = the source energy,

r_o = the radial distance to the point source,

$\vec{\Omega}_o$ = the direction to the point source from the origin,

$\delta(x - x')$ = the Dirac delta function.

When Eq. (5) is substituted into Eq. (3) the result is

$$\phi(0,E,\vec{\Omega}) = \frac{S(-\vec{\Omega})\delta(\vec{\Omega}_o,\vec{\Omega})\delta(E_o - E)e^{-\int_o^{r_o}\Sigma_T(r'\vec{\Omega},E)dr'}}{r_o^2}$$

$$+ \int_{\substack{\text{All}\\ \text{Space}}} \int_{E''} \int_{\vec{\Omega}''} \Sigma_T(\vec{r}',E'')\phi(\vec{r}',E'',-\vec{\Omega}'') \frac{\Sigma_S(\vec{r}',E'')}{\Sigma_T(\vec{r}',E'')} f(E,E'',-\vec{\Omega},\vec{\Omega}'')$$

$$e^{-\int_o^{r'}\Sigma_T(r''\vec{\Omega}',E)dr''} \frac{\delta(\vec{\Omega}',\vec{\Omega})}{r'^2} d\vec{r}'dE''d\vec{\Omega}' \qquad (6)$$

The first term on the right of Eq. (6) is the contribution from the unscattered beam and the second term is the contribution of the scattered radiation. The direct beam contribution was calculated directly using the above expression while the Monte Carlo portion of the calculation was done to solve the integral term. In what follows the integral term will be designated ϕ_S.

The function f in ϕ_S can be easily associated with the differential scattering cross section. It is assumed there are m nuclear species in the transport medium with which the neutrons can make an elastic scattering collision. (Inelastic scattering is neglected.) In this case f is given by

$$f(E,E'',-\vec{\Omega},\vec{\Omega}'') = \frac{\sum_{n=1}^{m} \frac{d\Sigma_S^n}{d\Omega}(\vec{r}';E'';-\vec{\Omega}\cdot\vec{\Omega}'',E')\delta(E' - E)}{\Sigma_S^n(\vec{r}',E'')} \frac{\Sigma_S^n(\vec{r}',E'')}{\Sigma_S(\vec{r}',E'')} \qquad (7)$$

where

Σ_S^n = the contribution to the macroscopic scattering cross section by the nth nuclear species,

$\frac{d\Sigma_S^n}{d\Omega}(\vec{r}';E'';-\vec{\Omega}\cdot\vec{\Omega}'',E')$ = the differential macroscopic scattering cross section contributed by the nth nuclear species, cm^{-1}, at position $\vec{r}'$ for scattering from a direction $\vec{\Omega}''$ with energy E" into a unit solid angle about direction $-\vec{\Omega}$ with resultant energy E'.

As described in the geometry section, the space about the point of interest (the detector point) is divided into a number of solid angle intervals determined by dividing the polar angle and the azimuthal angle into a number of equal angle intervals. Let us designate a particular solid angle interval as $\Delta\Omega_{ji}$ where the index j refers to the number assigned to the polar angle interval and the index i to the number assigned to the azimuthal angle interval as shown in Fig. 1. In addition, the energy space between some cut off energy and the source energy is divided into a number of equal intervals with an index k which refers to the number assigned to any particular interval. This indexing will be referred to again when the ORACLE output format is described; however, it is important here because ϕ_S cannot be calculated directly by Monte Carlo, only the quantity

$$D_{jik} \equiv \int_{\Delta\Omega_{ji}} \int_{E_k} \phi_S(0,E,\vec{\Omega})dEd\vec{\Omega} \qquad (8)$$

can be calculated. From Eqs. (6), (7), and (8) a convenient form of D_{jik} can be written as

$$D_{jik} = \sum_{n=1}^{m} \int_{\substack{\text{All}\\\text{Space}}} \int_{E''} \int_{\vec{\Omega}''} \Sigma_T(\vec{r}',E'')\phi(\vec{r}',E'',-\vec{\Omega}'') \frac{\Sigma_S(\vec{r}',E'')}{\Sigma_T(\vec{r}',E'')} \cdot$$

$$\frac{\Sigma_S^{\,n}(\vec{r}',E'')}{\Sigma_S(\vec{r}',E'')} \frac{\frac{d\Sigma_S^{\,n}}{d\Omega}(\vec{r}';E'';-\vec{\Omega}\cdot\vec{\Omega}'',E')}{\Sigma_S^{\,n}(\vec{r}',E'')} \frac{e^{-\int_0^{r'}\Sigma_T(r''\vec{\Omega}',E')dr''}}{r'^2} \cdot$$

$$Q(E',\Delta E_k)Q(\vec{\Omega}',\Delta\Omega_{ji})d\vec{r}'dE''d\vec{\Omega}'' \qquad (9)$$

where

$$Q(E',\Delta E_k) = 1 \text{ if } E' \text{ is in } \Delta E_k$$
$$= 0 \text{ otherwise,}$$
$$Q(\vec{\Omega}',\Delta\Omega_{ji}) = 1 \text{ if } \vec{\Omega}' \text{ has a direction within the bounds of } \Delta\Omega_{ji}$$
$$= 0 \text{ otherwise.}$$

The terms in Eq. (9) have the following physical interpretation: $\Sigma_T\phi$ is the collision density irrespective of the type of collision, Σ_S/Σ_T is the fraction of the collisions which are scattering collisions, $\Sigma_S^{\,n}/\Sigma_S$ is the fraction of the scattering collisions made with the nth nuclear species, $\frac{d\Sigma_S^{\,n}}{d\Omega}/\Sigma_S^{\,n}$ is the probability per steradian that the neutron will be scattered from the nth nuclear species in such a way as to intersect the detector point, $1/r'^2$ is the steradians per cm^2 subtended by the detector,

$\exp\left[-\int_0^{r'} \Sigma_T dr''\right]$ is the probability the neutron headed for the detector will reach it without making another collision, and $Q(E,\Delta E_k)Q(\vec{\Omega}',\Delta\Omega_{ji})$ is the factor which determines whether the particle shall be recorded in the interval designated by the indicies jik.

The unknown in Eq. (9) is the collision density which will be generated by an analogue Monte Carlo technique to be described. The result of the analogue process is a set of numbers $(\vec{r}_\ell, W_\ell, E_\ell, \vec{\Omega}'_\ell)$, $\ell = 1,2,3..$, where $\vec{r}_\ell \equiv r_\ell \vec{\Omega}_\ell$ is the vector position of the ℓth collision, and the weight W_ℓ the energy E_ℓ and the direction $\vec{\Omega}'_\ell$ are the values the particle had before the ℓth collision. The weight W_ℓ is the probability the particle will make the ℓth collision provided at the start W_1 has the value one. With the set of numbers $(\vec{r}_\ell, W_\ell, E_\ell, \vec{\Omega}'_\ell)$ it is possible to approximate Eq. (9) by

$$D_{jik} = \sum_{\ell=1}^{\infty}\sum_{n=1}^{m} W_{\ell+1} \cdot \frac{\Sigma_S^n(\vec{r}_\ell, E_\ell)}{\Sigma_S(\vec{r}_\ell, E_\ell)} \quad \frac{\frac{d\Sigma_S^n}{d\Omega}(\vec{r}_\ell; E_\ell; -\vec{\Omega}_\ell \cdot \vec{\Omega}'_\ell, E')}{\Sigma_S^n(\vec{r}_\ell, E_\ell)}$$

$$\frac{e^{-\int_0^{r_\ell} \Sigma_T(r'\vec{\Omega}_\ell, E')dr'}}{r_\ell^2} \cdot Q(E', \Delta E_k)Q(\vec{\Omega}_\ell, \Delta\Omega_{ji}) \tag{10}$$

where

$$W_{\ell+1} = W_\ell \frac{\Sigma_S(\vec{r}_\ell, E_\ell)}{\Sigma_T(\vec{r}_\ell, E_\ell)} . \tag{11}$$

Since there is a considerable advantage to eliminating the sum over n, this was done by randomly selecting the nth nuclear species for each of the collisions with a probability $\frac{\Sigma_S^n(\vec{r}_\ell, E_\ell)}{\Sigma_S(\vec{r}_\ell, E_\ell)}$ of obtaining any particular n. The nuclear type selected will be designated by n_ℓ. The random process will be described later. The result of selecting n_ℓ reduces Eq. (10) to

$$D_{jik} = \sum_{\ell=1}^{\infty} W_{\ell+1} \cdot \frac{\frac{d\Sigma_S^{n_\ell}}{d\Omega}(\vec{r}_\ell; E_\ell; -\vec{\Omega}_\ell \cdot \vec{\Omega}_\ell', E')}{\Sigma_S^{n_\ell}(\vec{r}_\ell, E_\ell)} \cdot \frac{e^{-\int_0^{r_\ell} \Sigma_T(r'\vec{\Omega}_\ell, E')dr'}}{r_\ell^2} \cdot$$

$$Q(E' \Delta E_k) Q(\vec{\Omega}_\ell, \Delta\Omega_{ji}) \qquad (12)$$

The singularity in Eq. (12) can be eliminated by the obvious restriction that a neutron scattered from the nth nuclear species should pass through the detector point with a probability less than one. In the calculation this was approximately achieved by requiring

$$\frac{d\Sigma_S^{n_\ell}(\vec{r}_\ell; E_\ell; -\vec{\Omega}_\ell \cdot \vec{\Omega}_\ell', E')}{\Sigma_S^{n_\ell}(\vec{r}_\ell, E_\ell)} \quad \frac{e^{-\int_0^{r_\ell} \Sigma_T(r'\vec{\Omega}_\ell, E')dr'}}{r_\ell^2} \leq 1. \qquad (13)$$

If the quantity on the left of Eq. (13) came out to be greater than one it was arbitrarily set equal to one.

The fact that the singularity in Eq. (12) was removed by a realistic approximation does not preclude the statistical problem that still remains for an unusual number of small values of $\vec{r}_\ell$. In fact, the number of small

values of $\vec{r}_\ell$ does not have to be too unusual to obtain quite a deviation from the correct approximation to D_{jik}. This fact alone suggests there has to be a reasonably large number of sample neutrons taken at the source to minimize the deviation.

There is also a problem that occurs when the point source emits a mono-directional beam of neutrons directly at the detector point or very close to that direction. In this case the greatest contribution to D_{jik} is made by the first scattered neutrons, and of the first scattered neutrons, those with small values of $\vec{r}_1$ make the major contribution. This means that the region near the detector point has to be sampled very well for the first scattering locations of the sample neutrons to obtain a very accurate average value of D_{jik}. This is not likely to be achieved without a biased sampling technique and is certainly not achieved by the sampling methods incorporated in this calculation as will be discussed; therefore, such a condition has been avoided in all calculations by not permitting the particular source condition mentioned above to exist.

Distribution Sampling and Generation of a Neutron History

In order to generate a random neutron history, a series of random variables must be selected from the probability distributions governing the life of a neutron. The processes used for selecting the random variable will be described in each case.

In some cases it is necessary to pick a random variable R from the probability density function, p.d.f,

$$g(r) = 1, \; 0 \leq r \leq 1, \tag{14}$$

and obtain a random variable X from the p.d.f. f(x) by the transformation

$$\int_{-\infty}^{X} f(x)dx = \int_{0}^{R} g(r)dr = R \tag{15}$$

The random variables, or so-called pseudo random numbers, R were generated on the ORACLE as they were needed using the method of congruences which has been described by Taussky and Todd.[7] For the ORACLE, this recursion method of generation is

$$R_{i+1} = \frac{R_i R_o \cdot 2^{78} \ (\text{Mod } 2^{39})}{2^{39}} \tag{16}$$

where

$$R_o = 5^{15}/2^{39},$$
$$R_1 = 2^{-39}.$$

The distribution of the neutrons about the source axis of symmetry was chosen as $\frac{P+1}{2\pi} \cos^P\theta$ per steradian; therefore, the p.d.f. for the variable $\cos\theta \equiv u$ is

$$f(u) = (P+1)u^P, \qquad 0 \leq u \leq 1. \tag{17}$$

The random variable U can be picked from the p.d.f. f(u) by using Eq. (15); however, the estimate of D_{jik} can be improved by systematically sampling rather than random sampling.[6] The systematic sampling procedure is given by

---

7. O. Taussky and J. Todd, Generation and Testing of Pseudo-Random Numbers, NBS-3370 (1954).

$$\int_{o}^{U_i} f(u)du = U_i^{P+1} = \frac{i}{N} \quad i = 1,2,\ldots,N, \tag{18}$$

where

N = the number of source neutrons selected,

U_i = the ith value of the $\cos\theta$ selected.

Equation (18) was solved for U_i by Newton's iteration method.[8]

One of the alternate methods of using the ORACLE code includes the option of making the source an isotropic point source. In this case the p.d.f. for u is given by

$$f(u) = \frac{1}{2}, \qquad -1 \leq u \leq 1, \tag{19}$$

and the systematic sampling procedure is given by

$$U_i = \frac{2i}{N} - 1, \qquad i = 1,2,3,\ldots.N. \tag{20}$$

The azimuthal angle ϕ about the source axis of symmetry was picked randomly by first selecting two random numbers R_1 and R_2 from a uniform distribution on the interval (-1, +1) and testing if $R_1^2 + R_2^2 \leq 1$, if the test passed, then $R_1 / \sqrt{R_1^2 + R_2^2}$ was taken as the $\cos\phi$ and $R_2 / \sqrt{R_1^2 + R_2^2}$ was taken as the $\sin\phi$. If the test failed then another two random numbers were selected and the test was made again. This procedure was continued until an R_1 and R_2 were accepted. The angles θ and ϕ established the direction $\vec{\Omega}_1'$.

---

8. A. S. Householder, Principles of Numerical Analysis, McGraw-Hill Publishing Company, New York (1953), p. 122.

In the case where the value of P was chosen as infinity giving a mono-directional beam of neutrons there was no need to sample from the p.d.f. f(u) and systematic sampling was done to obtain the distance to the first collision point. The p.d.f. for the distance in mean free paths (mfp) is given by

$$f(x) = e^{-x}. \qquad 0 \leq x < \infty \tag{21}$$

The systematic sampling could, of course, be achieved by an equation similar to Eq. (18); however, it was very desirable to fix the first collision points by a method which approximated the cumulative distribution function, c.d.f.,

$$\int_0^x f(x')dx' \equiv F(x) \tag{22}$$

more accurately. This was done by first dividing F(x) into N equal intervals as in Eq. (18) but rather than picking the values of x which corresponded to the end points of the intervals, the average value of x within the interval was taken. In the development of the relationship for the average values, the end point values, x_i, of the intervals will be defined by

$$F(x_i) \equiv \frac{i}{N}, \; i = 0,1,2,\ldots\ldots N. \tag{23}$$

The average value $\bar{x}_i$ in the interval (x_{i-1}, x_i) is therefore given by

$$\bar{x}_i = \frac{\int_{x_{i-1}}^{x_i} xe^{-x}\,dx}{\int_{x_{i-1}}^{x_i} e^{-x}dx} = \left(- x_i e^{-x_i} + x_{i-1}e^{-x_{i-1}}\right) N + 1, \quad i = 1,2,3\ldots,N. \tag{24}$$

From Eq. (23) we obtain

$$\frac{N - i}{N} = e^{-x_i}, \tag{25}$$

thus Eq. (24) can be written finally as

$$\bar{x}_i = \left\{\frac{N - i}{N} \cdot \mathrm{Log}\left[\frac{N - i}{N}\right] - \frac{N - (i - 1)}{N} \cdot \mathrm{Log}\left[\frac{N - (i - 1)}{N}\right]\right\} \cdot N + 1$$

$$i = 1,2,\ldots,N. \tag{26}$$

The value of $\frac{N - i}{N}\ \mathrm{Log}\left[\frac{N - i}{N}\right]$ can be saved at each determination of $\bar{x}_i$ and used in the determination of $\bar{x}_{i+1}$ reducing the amount of work required.

In those cases where P was finite, the distance to the first collision was randomly selected from the p.d.f. given in Eq. (21) using the von Neumann technique.[9] This can be most easily summarized by the schematic diagram given in Fig. 2 where X is the randomly selected distance to the first collision in units of mfp and R_i is a random number picked from a uniform distribution on the interval (0, +1). On the average it takes 4.3 random

---

9. J. von Neumann, "Various Techniques Used in Connection with Random Digits," Monte Carlo Method, Applied Mathematics Series 12, A. S. Householder, editor (U. S. Government Printing Office, Washington, D. C., 1951).

UNCLASSIFIED
2-01-059-183

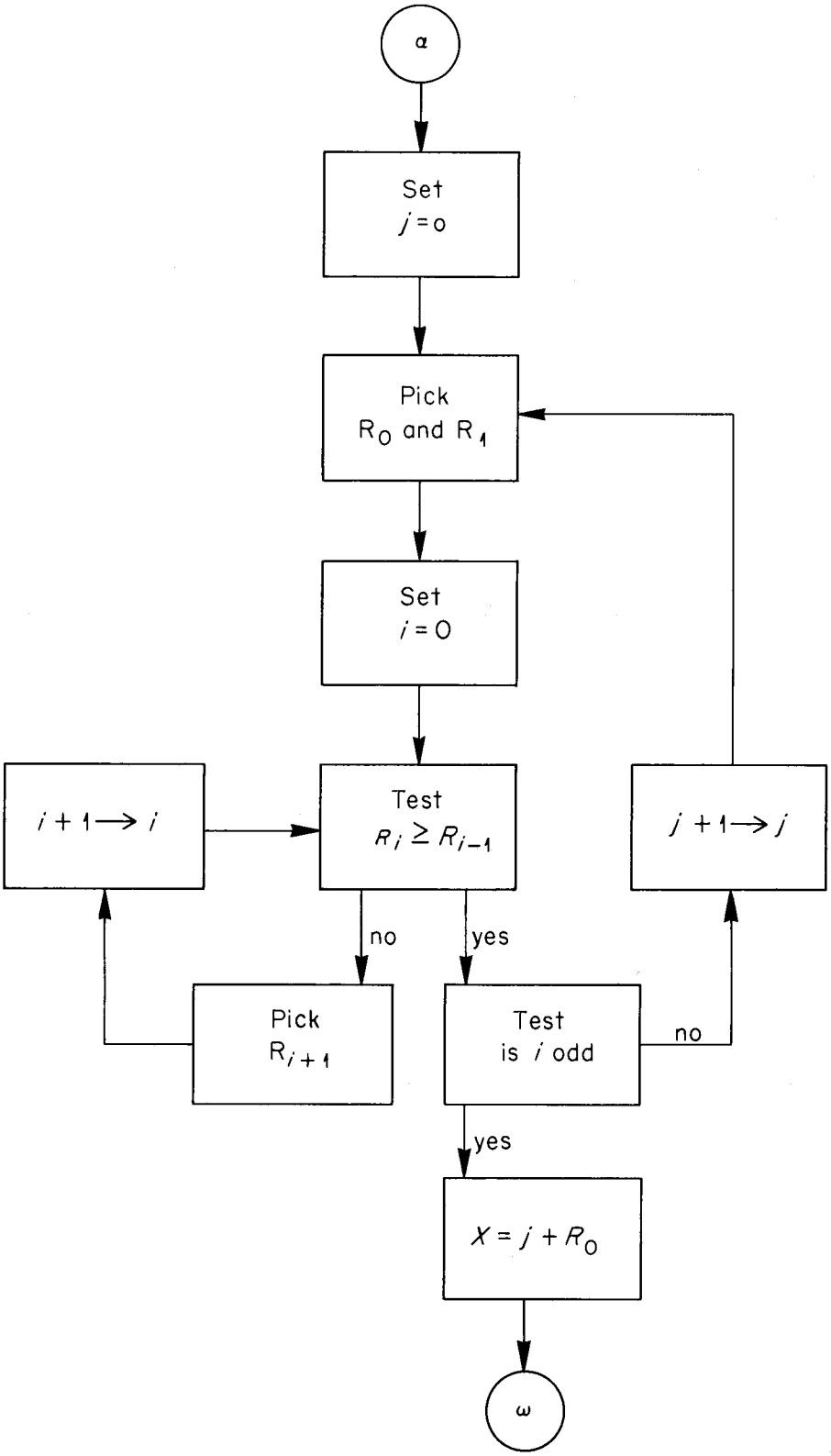

Fig. 2. Schematic Diagram of the von Neumann Method of Selecting a Random Variable X from the Probability Density Function $f(x) = C^{-x}$ Where $0 \leq X < \infty$

numbers to obtain a value of X which takes less time in computation than the logarithm routines available for the ORACLE.

The von Neumann method was also used to obtain distances between successive collisions when the direction of the neutron did not intersect the black source sphere. When it did, however, a truncated p.d.f given by

$$f(x) = \frac{e^{-x}}{1 - e^{-x_1}} \qquad 0 \leq x \leq x_1 \tag{27}$$

was used to randomly select the distance X. The value of x_1 is taken as the distance from the last collision point to the surface of the sphere in units of mfp. The p.d.f. given in Eq. (27) was substituted into Eq. (15) and solved to obtain X. The object of truncating the distribution is to assure that the neutron is not lost from the system since there is information to be gained from each collision if it continues to exist; however, the weight of the neutron has to be reduced by the factor $1 - e^{-x_1}$ which is its probability of not being absorbed by the black sphere.

The the position of a collision $\vec{r}_\ell$ was established by one of the techniques described above, the weight of the neutron was then reduced by its probability of surviving a collision as given in Eq. (11). It was then necessary to determine the nuclear species with which it was assumed there was a scattering collision. This was done by dividing the interval (0,1) into m smaller non-overlapping intervals each of length $\frac{\Sigma_S^n(\vec{r}_\ell, E_\ell)}{\Sigma_S(\vec{r}_\ell, E_\ell)}$ where $\sum_{n=1}^{m} \frac{\Sigma_S^n(\vec{r}_\ell, E_\ell)}{\Sigma_S(\vec{r}_\ell, E_\ell)} = 1$ and then determining in which of the smaller intervals a random number R fell. Since the probability of R falling into the nth

interval is just $\frac{\Sigma_S^n(\vec{r}_\ell, E_\ell)}{\Sigma_S(\vec{r}_\ell, E_\ell)}$, the nth nuclear species was selected with the proper frequency. The particular n selected at each collision was designated n_ℓ.

The direction of scattering was determined under the assumption of isotropic scattering in the C.M. system. The usual collision diagram in the C.M. system is given in Fig. 3 where $\vec{v}_\ell$ is the velocity of the neutron before collision, $\vec{v}_m$ is the velocity of the center of masses, and $\vec{v}'_{\ell+1}$ is the velocity of the scattered neutron in the C.M. system. The relationships that hold in this system are

$$\vec{v}_m = \frac{\vec{v}_\ell}{1 + A_{n_\ell}} \tag{28}$$

and

$$\left|\vec{v}'_{\ell+1}\right| = \frac{A_{n_\ell}}{1 + A_{n_\ell}} \left|\vec{v}_\ell\right| \tag{29}$$

where A_{n_ℓ} is the mass of the nth nuclear species selected at the ℓth collision. The velocity of the scattered neutron in the Laboratory system, $\vec{v}_{\ell+1}$, is given by

$$\vec{v}_{\ell+1} = \vec{v}_m + \vec{v}'_{\ell+1}. \tag{30}$$

The direction of the scattering in the C.M. system was determined by first selecting three random numbers, R_1, R_2, and R_3 from a uniform distribution on the interval (-1, +1) and testing the inequality $R_1^2 + R_2^2 + R_3^2 \leq 1$. If the test failed, another set of three random numbers was generated and the test repeated until the set of random numbers was accepted. When the test passed a vector $\vec{R}$ was established by

UNCLASSIFIED
2-01-059-184

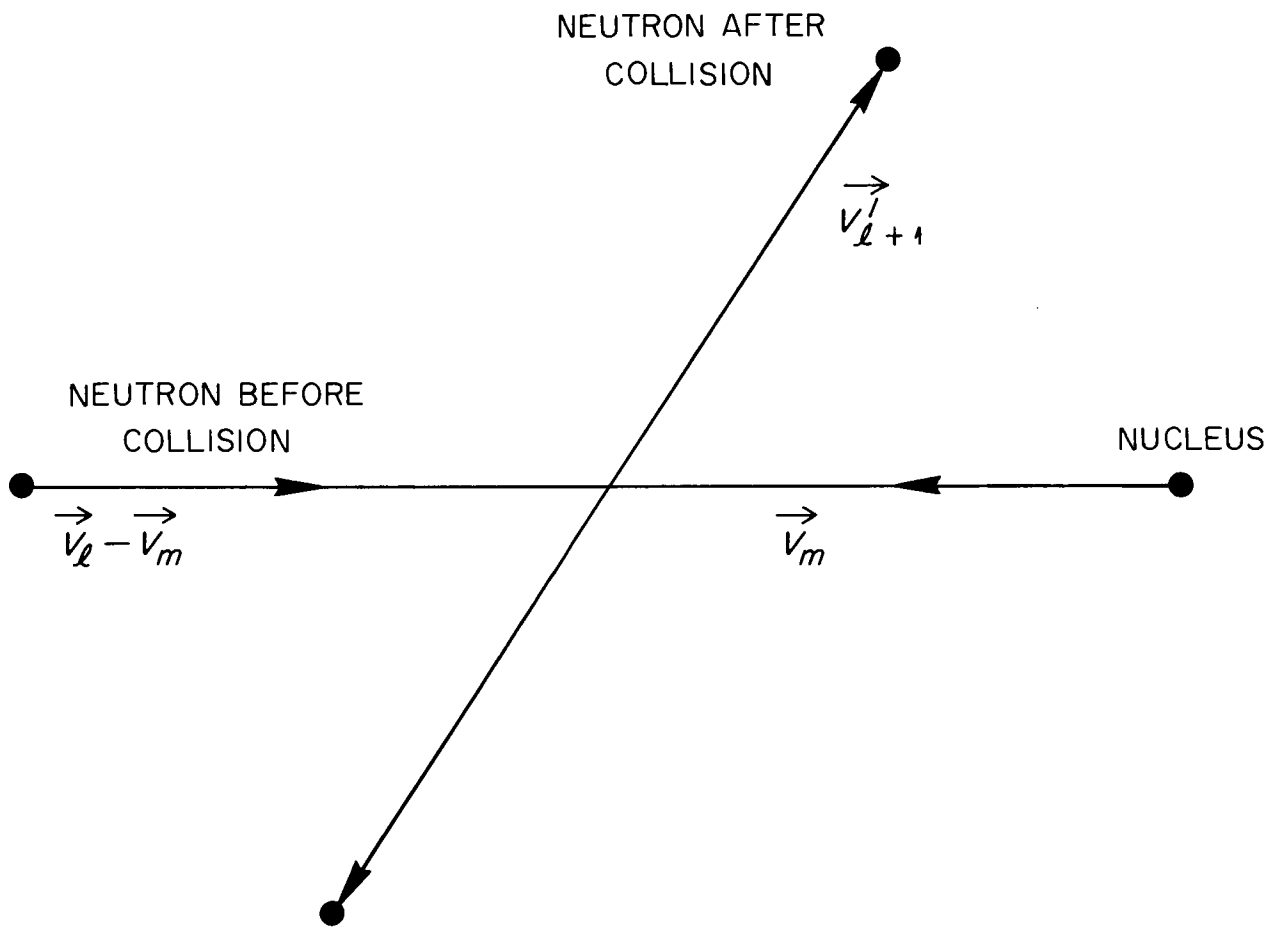

Fig. 3. Collision Diagram in the Center-of-Mass System.

$$\vec{R} = R_1\hat{e}_1 + R_2\hat{e}_2 + R_3\hat{e}_3 \tag{31}$$

where $\hat{e}_i$ is a unit vector along the ith coordinate axis. The vector $\vec{R}$ has an equal probability of pointing in any direction; therefore, it fulfills the meaning of isotropic and can be interpreted as indicating the direction of $\vec{v}'_{\ell+1}$. Thus, one obtains with the use of Eq. (29) that

$$\vec{v}'_{\ell+1} = \frac{A_{n_\ell}}{1 + A_{n_\ell}} \left|\vec{v}_\ell\right| \frac{\vec{R}}{\left|\vec{R}\right|} \tag{32}$$

and with the use of Eqs. (28), (30), and (32)

$$\vec{v}_{\ell+1} = \frac{\vec{v}_\ell}{1 + A_{n_\ell}} + \frac{A_{n_\ell}}{1 + A_{n_\ell}} \left|\vec{v}_\ell\right| \frac{\vec{R}}{\left|\vec{R}\right|} . \tag{33}$$

At this point we can introduce the vector $\vec{\Omega}'_\ell$ through the relation $\vec{v}_\ell = \left|\vec{v}_\ell\right| \vec{\Omega}_\ell'$ to obtain from Eq. (33)

$$\frac{\vec{v}_{\ell+1}}{\left|\vec{v}_\ell\right|} = \frac{\vec{\Omega}_\ell'}{1 + A_{n_\ell}} + \frac{A_{n_\ell}}{1 + A_{n_\ell}} \frac{\vec{R}}{\left|\vec{R}\right|} \tag{34}$$

The energy after scattering is obtained with the use of Eq. (34) from the relation

$$E_{\ell+1} = E_\ell \frac{\left|\vec{v}_{\ell+1}\right|^2}{\left|\vec{v}_\ell\right|^2} , \tag{35}$$

while the direction $\vec{\Omega}'_{\ell+1}$ after scattering is obtained with the use of Eq. (34) from the relation

$$\vec{\Omega}'_{\ell+1} = \frac{\vec{v}_{\ell+1}}{\left|\vec{v}_\ell\right|} \cdot \frac{\left|\vec{v}_\ell\right|}{\left|\vec{v}_{\ell+1}\right|} . \tag{36}$$

At this point the values $W_{\ell+1}$, $E_{\ell+1}$, and $\vec{\Omega}'_{\ell+1}$ have been determined which leaves only to pick the distance to the $\ell+1$ collision by one of the methods described and then determining the position $\vec{r}_{\ell+1}$.

An exception to the above sequence of events occurred when $|\vec{r}_\ell|\cdot\Sigma_T(r\ ,E\ ) > 16$. In this case the weight $W_{\ell+1}$ was set equal to zero and the history was terminated. The reason for this exception was that a neutron which makes a collision at a distance greater than 16 mfp has such a small probability of passing through the detector point on any of its succeeding collisions that it could not contribute significantly to the estimate of D_{jik}.

Computation of the Neutron Current at the Detector Point and Its Variance

In the process of generating a neutron history the process of determining $W_{\ell+1}$ and n_ℓ was described. This leaves only the determination of

$$\frac{\dfrac{d\Sigma_S^{n_\ell}}{d\Omega}(\vec{r}_\ell;E_\ell;-\vec{\Omega}_\ell\cdot\vec{\Omega}'_\ell,E')}{\Sigma_S^{n_\ell}(\vec{r}_\ell,E_\ell)} \quad \text{and } \exp\left[-\int_0^{r_\ell}\Sigma_T(r'\vec{\Omega}_\ell,E')dr'\right] \quad \text{in order to}$$

compute the estimate D_{jik} as given in Eq. (12).

In the case of isotropic scattering in the C.M. system it can be shown that

$$\frac{\dfrac{d\Sigma_S^{n_\ell}}{d\Omega}(\vec{r}_\ell;E_\ell;-\vec{\Omega}_\ell\cdot\vec{\Omega}'_\ell,E')}{\Sigma_S^{n_\ell}(\vec{r}_\ell,E_\ell)} = \frac{1}{4\pi A_{n_\ell}}\left[-2\vec{\Omega}_\ell\cdot\vec{\Omega}_\ell' + B + \frac{(\vec{\Omega}_\ell\cdot\vec{\Omega}'_\ell)^2}{B}\right] \tag{37}$$

where

$$B = \left| \left[A_{n_\ell}^2 - 1 + (\vec{\Omega}_\ell \cdot \vec{\Omega}_\ell{}')^2 \right]^{1/2} \right| \tag{38}$$

with the resulting energy after scattering given by

$$E' = E_\ell \left(\frac{-\vec{\Omega}_\ell \cdot \vec{\Omega}_\ell{}' + B}{1 + A_{n_\ell}} \right)^2 \tag{39}$$

The exponential term left to be computed is straight-forward and was computed as

$$e^{-\int_0^{r_\ell} \Sigma_T(r'\vec{\Omega}_\ell, E')dr'} = e^{-\Sigma_T(E')r_\ell} \tag{40}$$

in all cases except when the path from the detector point to the collision point $\vec{r}_\ell$ passed through the black sphere. In the excepted case

$$e^{-\int_0^{r_\ell} \Sigma_T(r'\vec{\Omega}_\ell, E')dr'} = 0. \tag{41}$$

In those cases where d, the diameter of the black sphere, was chosen to have the value zero, the exponential was always calculated by Eq. (40). This last point is brought up because of some question that may arise in the case where the source beam was monodirectional at 180 deg to the source-detector axis where all 1st scattered contribution to D_{jik} would be removed if the prescriptions for the use of the alternate Eqs. (40) or (41) was followed rigorously.

Although it was not mentioned before, it is convenient here to say something about the total energy current through the detector that was calculated in all cases. For the total energy current Eq. (12) was modified in the following way.

$$\mathcal{E} = \sum_{\ell=1}^{\infty} \frac{E'}{E_1} W_{\ell+1} \frac{\frac{d\Sigma_S^{n_\ell}}{d\Omega}(\vec{r}_\ell; E_\ell; -\vec{\Omega}_\ell \cdot \vec{\Omega}_\ell', E')}{\Sigma_S^{n_\ell}(\vec{r}_\ell, E_\ell)} \frac{e^{-\int_0^{r_\ell} \Sigma_T(r'\vec{\Omega}_\ell, E')dr'}}{r_\ell^2} \tag{42}$$

It is clear that an estimate D_{jik} or $\mathcal{E}$ can be obtained from Eqs. (12) and (42) for each sample neutron for which a history is generated. For the present let us assume the initial weight of the neutron was taken as $W_1 = 1$ so that D_{jik} is normalized to one source neutron and $\mathcal{E}$ is normalized to a unit energy source, then an estimate of the variance on the average value of D_{jik} and the average value of $\mathcal{E}$ is given by

$$V = \frac{\overline{Y^2} - \bar{Y}^2}{N} \tag{43}$$

where

$Y = D_{jik}$ or $\mathcal{E}$,

N = the number of sample neutrons.

Now let Y_n be the estimate made by the nth sample neutron and substitute it into Eq. (43) to get

$$V = \frac{\frac{\sum_{n=1}^{N} Y_n^2}{N} - \left(\sum_{n=1}^{N} \frac{Y_n}{N}\right)^2}{N} \tag{44}$$

Equation (44) is convenient, however, it is desirable in the course of generating a history to start the initial weight as $W_1 = \frac{1}{N}$ giving an estimate

$$Y_n' = \frac{1}{N} Y_n \tag{45}$$

Substituting Eq. (45) into Eq. (44) gives

$$V = \sum_{n=1}^{N} Y_n'^2 - \frac{1}{N}\left(\sum_{n=1}^{N} Y_n'\right)^2 \tag{46}$$

which is the variance on the average value of Y given by

$$\bar{Y} = \sum_{n=1}^{N} Y_n' . \tag{47}$$

The standard deviation calculated is the square root of the variance given in Eq. (46).

Computation of the Tissue Dose Rate at the Detector Point

Provided the conversion factor from neutron energy current to tissue dose rate, P(E'), is known it is very easy to calculate the dose rate in the course of the Monte Carlo computation by an equation similar to Eq. (12). To obtain tissue rate, one need only replace $W_{\ell+1}$ by the factor $P(E')W_{\ell+1}$. The normalization would then be for one source neutron per unit time. This was not done, however, because of space limitations in the fast memory of the ORACLE. Instead, the resulting answers for the various D_{jik} were converted to dose rate after the Monte Carlo calculation was completed.

Two separate tissue dose rate calculations were incorporated into the code. The first, which was designated as Dose 1, used the tissue dose rate conversion factors calculated in the manner described by Hurst and Ritchie[10] for calibration of the Hurst type dosimeter. The second calculation, which

---

10. G. S. Hurst and R. H. Ritchie, A Count-Rate Method of Measuring Fast Neutron Tissue Dose, ORNL-930 (1951).

was designated as Dose 2, used the tissue dose rate conversion factors calculated by Snyder[11] using a Monte Carlo method. The Dose 1 and Dose 2 conversion factors are given in Table 2 and reproduced in part in Figs. 4 and 5. Conversion factors for intermediate values in Table 2 were obtained by linear interpolation on a log-log scale as shown in Figs. 4 and 5.

The method of calculation to convert the quantities D_{jik} to tissue dose rate was to find the average conversion factor $\overline{P}_k$ in the interval ΔE_k by

$$\overline{P}_k \equiv \int_{\Delta E_k} \frac{P(E')dE'}{\Delta E_k} \tag{48}$$

and then computing the quantity

$$D^p_{jik} = \frac{D_{jik}\,\overline{P}_k^{\,p}}{\Delta\Omega_{ji}\,\Delta E_k} \tag{49}$$

where

p = 1 or 2 indicating Dose 1 or Dose 2 calculation, respectively,

$$D^p_{jik} = \frac{\text{dose/hr, steradian, unit energy}}{\text{source neutron/sec}} .$$

Other quantities that are mentioned in App. B are calculated as follows:

---

11. W. S. Snyder, "Depth-Dose Curve for Neutrons with RBE as a Function of LET," Health Physics Semiannual Progress Report for Period Ending July 31, 1956, ORNL-2151 (1956), p. 64.

Table 2. Conversion Factors From Neutron Flux To Tissue Dose Rate

Neutron Energy (Mev)	Conversion Factors Calculated by the Method of Hurst and Ritchie[10] $\left(\frac{\text{rep/hr}}{\text{neutrons/cm}^2\text{-sec}}\right)$	Conversion Factors Taken from the Report of Snyder[11] $\left(\frac{\text{rem/hr}}{\text{neutrons/cm}^2\text{-sec}}\right)$
0.025×10^{-6}	9.72×10^{-13}	3.75×10^{-6}
1×10^{-4}	3.74×10^{-9}	4.84×10^{-6}
1×10^{-3}	3.71×10^{-8}	-
5×10^{-3}	-	4.41×10^{-6}
1×10^{-2}	3.67×10^{-7}	-
2×10^{-2}	-	9.04×10^{-6}
1×10^{-1}	2.43×10^{-6}	3.00×10^{-5}
5×10^{-1}	6.19×10^{-6}	8.33×10^{-5}
1.0	9.36×10^{-6}	1.36×10^{-4}
2.5	1.29×10^{-5}	1.25×10^{-4}
3.5	1.59×10^{-5}	-
5.0	1.70×10^{-5}	1.36×10^{-4}
7.5	1.96×10^{-5}	1.50×10^{-4}
10.0	2.15×10^{-5}	1.50×10^{-4}
12.5	-	1.85×10^{-4}
15.0	2.41×10^{-5}	2.14×10^{-4}

UNCLASSIFIED
2-01-059-185

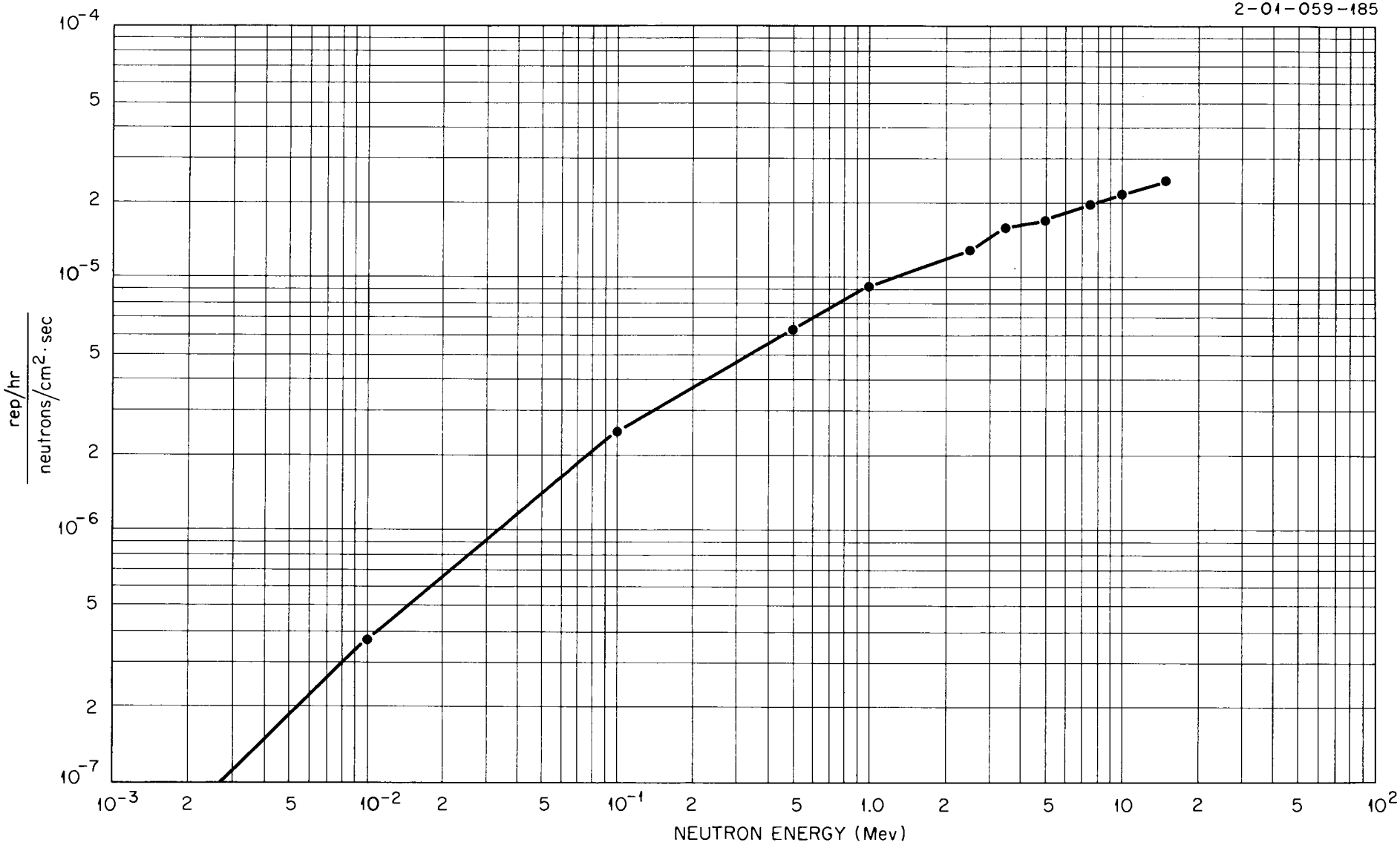

Fig. 4. Neutron Flux to Tissue Dose Rate Conversion Factors Calculated by the Hurst–Ritchie Method[10].

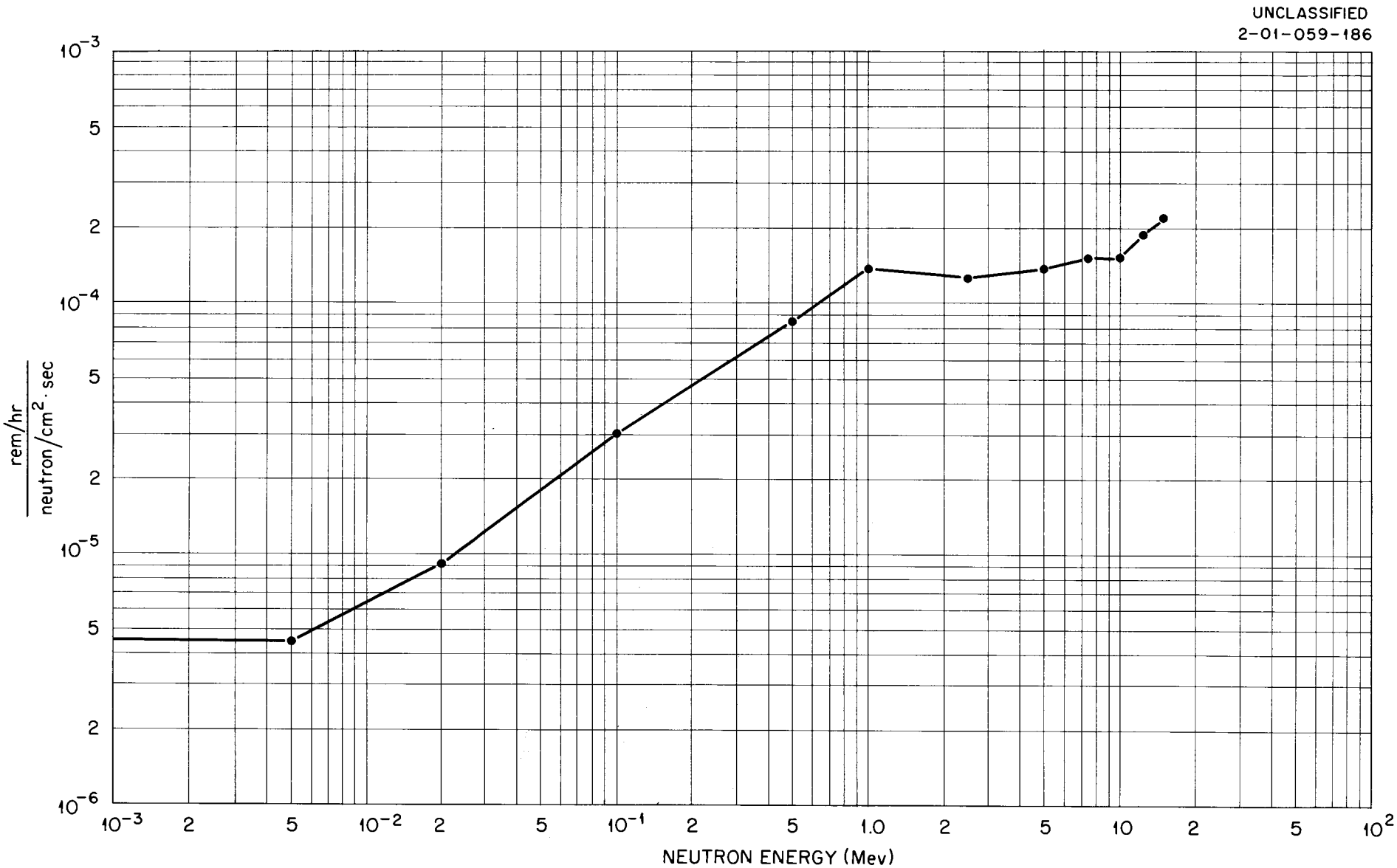

Fig. 5. Neutron Flux to Tissue Dose Rate Conversion Factors, taken from the Report by Snyder[11].

$$D^p_{ji} = \sum_k \frac{D_{jik}\,\overline{P}_k^{\,p}}{\Delta\Omega_{ji}} , \tag{50}$$

$$D^p_j = \frac{\sum_i \sum_i D_{jik}\,\overline{P}_k^{\,p}}{\sum_i \Delta\Omega_{ji}} , \tag{51}$$

and

$$D^p = 2 \sum_j \sum_i \sum_k D_{jik}\,\overline{P}_k^{\,p} \tag{52}$$

where

$$D^p_{ji} = \frac{\text{dose/hr, steradian}}{\text{source neutron/sec}} ,$$

$$D^p_j = \frac{\text{dose/hr, steradian}}{\text{source neutron/sec}} ,$$

$$D^p = \frac{\text{dose/hr}}{\text{source neutron/sec}} .$$

CHAPTER III. TESTING THE CALCULATION

Testing of the Single Scattering Current from a Monodirectional Source

When the point source emits a monodirectional beam of neutrons the distances to the first collision points are selected systematically as discussed in Chapter II. This method is very nearly a numerical integration for the first scattered contribution to D_{jik} with the exception that the nuclear species with which the scattering collisions are made is still done randomly.

A test of the accuracy of the calculation for the first scattered contribution to the detector point can easily be made for the particular conditions where a monodirectional beam of neutrons is directed at 180 deg from the detector point. Here it is assumed that diameter of the source sphere is zero. In this case the analytic expression for the contribution is given by

$$D = \sum_{n=1}^{m} \int_{g}^{\infty} \Sigma_T(E_1) e^{-\Sigma_T(E_1)\cdot(x-g)} \frac{\Sigma_S(E_1)}{\Sigma_T(E_1)} \cdot \frac{\Sigma_S^{\,n}(E_1)}{\Sigma_S(E_1)}$$

$$\frac{\frac{d\Sigma_S^{\,n}}{d\Omega}(\vec{r}_1;E_1;-1,E')}{\Sigma_S^{\,n}(E_1)} \cdot \frac{e^{-\Sigma_T(E')\cdot x}}{x^2}\, dx \qquad (53)$$

which is easily calculated analytically. For the particular case of a separation distance $g = 19.5$ meters, $E_1 = 1$ Mev, and the density of dry

air ρ_A = 0.001293 gms/cm^3, the analytic solution gives a value $D = 2.5644 \times 10^{-9}$. The Monte Carlo solution for the same initial conditions for various sample sizes is shown in Table 3. The error is approximately the same independent of sample size.

The results of this test confirm the expected accuracy for the single scattering contribution. The significant point to be made, however, is that for all cases where a monodirectional beam from the source is used similar accuracy for the first scattering contribution can be expected. The exception to this occurs when the beam points at or nearly at the detector point, but this initial condition has been excluded as discussed in Chapter II.

Comparisons of the Monte Carlo Solution Against Numerical Solutions of the One-Velocity Boltzmann Equation

Numerical solutions of the Boltzmann equation giving the total flux exist only for the one-velocity case of an isotropic point source in an infinite homogeneous medium with isotropic scattering in the Laboratory system. The details and results of this calculation has been given by Case, de Hoffmann, and Placzek.[12] Comparisons with this calculation could be easily made with simple alterations in the ORACLE code to give the isotropic scattering in the Laboratory system without energy degredation. These alterations were the only ones made so the Monte Carlo calculation proceeded as discussed before.

In Table 4 and Fig. 6 is presented the comparison of the calculations for a source energy of E_1 = 1 Mev, and density of dry air ρ_A = 0.001293 gms/cm^3. Under these conditions the macroscopic total cross section was calculated to be $\Sigma_T = 0.0000176607$ cm^{-1}. The top curve in Fig. 6 presents the results

---

12. K. M. Case, F. de Hoffmann, and G. Placzek, Introduction to the Theory of Neutron Diffusion (U. S. Government Printing Office, 1953).

Table 3. First Scattering Contribution to the Detector Point Resulting from a Point, Monodirectional, Monoenergetic Source of 1 Mev Neutrons Directed at 180 Deg from the Detector Point. Density of the Air 0.001293 gms/cm^3. Separation Distance 19.5 Meters

Number of Sample Neutrons	First-Scattered Neutrons per Source Neutron		Percent Error
	Monte Carlo Solution	Analytic Solution	
50	2.5647×10^{-9}	2.5644×10^{-9}	0.01
250	2.5634×10^{-9}	"	0.04
500	2.5646×10^{-9}	"	0.01
1000	2.5638×10^{-9}	"	0.02
2000	2.5637×10^{-9}	"	0.02

Table 4. Solution of One-Velocity Boltzmann Equation for the Flux Contributed by Scattered Neutrons from an Isotropic, 1-Mev Point Source in Infinite Air

Σ_S/Σ_T	Separation Distance (mfp)	Number of Sample Neutrons	Maximum Number of Collisions per History	Neutron Flux Contributed by Scattered Neutrons Normalized to One Source (neutron/sec)		Percent Error of the Monte Carlo Solution Compared with the Numerical Solution
				Numerical Solution	Monte Carlo Solution	
1	0.6	500	15	0.1175×10^{-7}	0.1212×10^{-7}	+3.14
1	0.5	600	13	0.1396×10^{-7}	0.1320×10^{-7}	-5.44
1	0.4	700	11	0.1725×10^{-7}	0.1253×10^{-7}	-27.36
1	0.3	800	9	0.2264×10^{-7}	0.2389×10^{-7}	+5.52
1	0.2	1000	7	0.3329×10^{-7}	0.2943×10^{-7}	-11.56
1	0.1	1500	5	0.6467×10^{-7}	0.5969×10^{-7}	-7.70
1	0.01	2000	4	0.6190×10^{-7}	0.5000×10^{-7}	-19.22
0.9	0.6	500	15	0.7188×10^{-8}	0.6535×10^{-8}	-9.08
0.9	0.5	600	13	0.9037×10^{-8}	0.7126×10^{-8}	-21.15
0.9	0.4	700	11	0.1182×10^{-7}	0.1141×10^{-7}	-3.53
0.9	0.3	800	9	0.1648×10^{-7}	0.1868×10^{-7}	+13.33
0.9	0.2	1000	7	0.2579×10^{-7}	0.2214×10^{-7}	-14.14
0.9	0.1	1500	5	0.5368×10^{-7}	0.5087×10^{-7}	-5.21
0.9	0.01	2000	4	0.5508×10^{-7}	0.4471×10^{-7}	-18.82

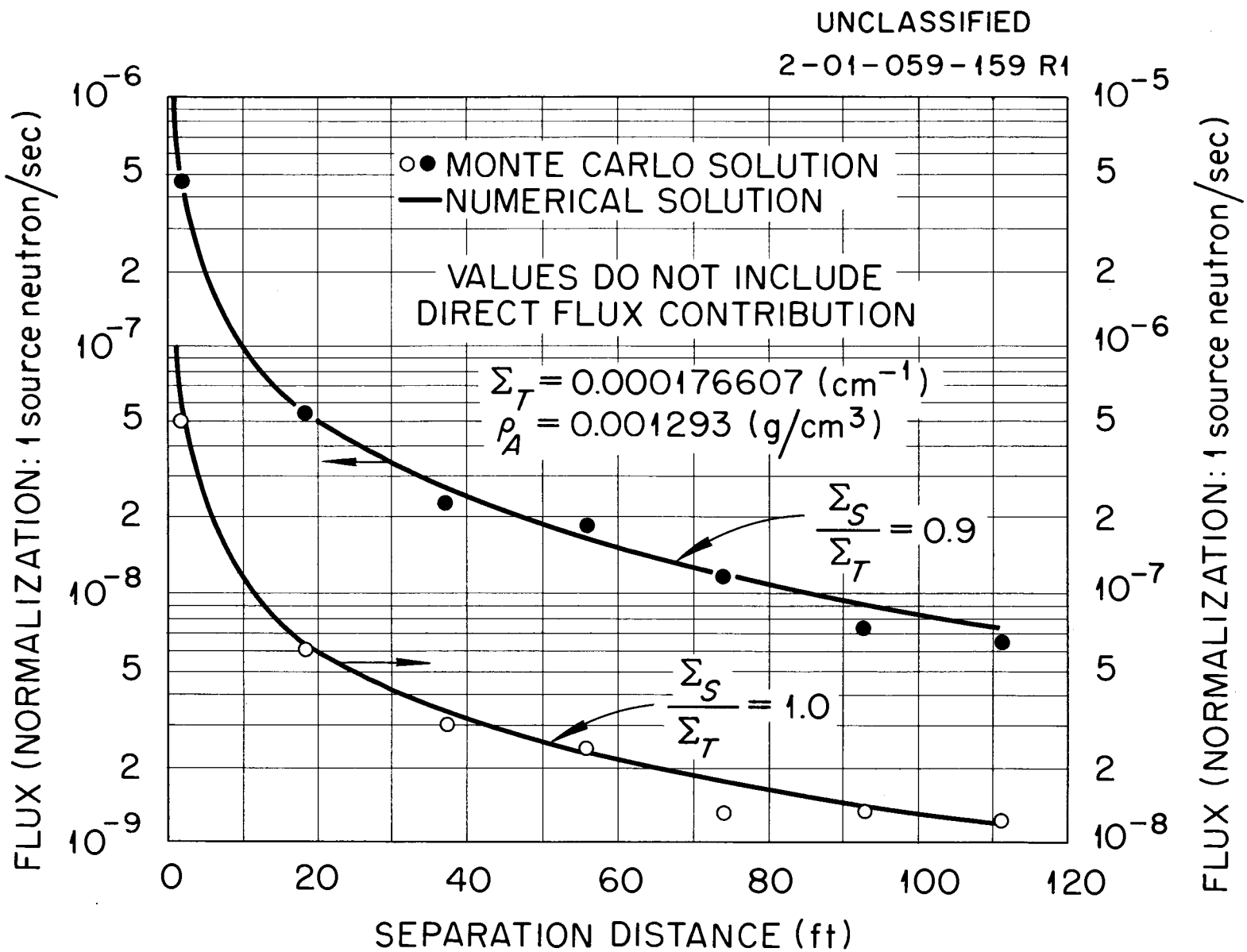

Fig. 6. Solution of the One-Velocity Boltzmann Equation for an Isotropic Point Source of 1-Mev Neutrons in Infinite Air.

for a ratio of $\Sigma_S/\Sigma_T = 0.9$ while the lower curve gives the results for a ratio of $\Sigma_S/\Sigma_T = 1$. Both sides of data represent the flux at the detector point contributed by particles which have made at least one collision, that is, they do not include the direct beam contribution. The solid curves in each case are the results of the numerical solution while the points are the result of the Monte Carlo solution.

As indicated in Table 4 a different number of sample neutrons and maximum number of collisions per history were used at each separation distance. It was observed in some trial calculations that the maximum number of collisions before the remaining collisions made little contribution depended heavily on the separation distance; therefore, when this maximum was a small number, the number of histories was taken large and visa versa. The object of these different sets of histories and collisions was to limit the ORACLE operating time to approximately 25 minutes for each problem and yet obtain maximum accuracy.

The errors in the Monte Carlo solutions indicated in Table 4 are remarkably small considering the number of histories used. As was pointed out at the beginning of Chapter II it would have taken a much larger number of histories to achieve this accuracy if the straight analogue Monte Carlo method had been used. It should be pointed out that in almost every case the error on the Monte Carlo solution for the neutron flux including the direct beam contribution was less than 10 percent. The exceptions to this case for $\Sigma_S/\Sigma_T = 1$ at a separation distance of 0.4 mfp and $\Sigma_S/\Sigma_T = 0.9$ at a separation distance of 0.5 mfp. The errors on the total flux in these cases are 17 percent and 12 percent respectively.

In this particular set of test problems the angular distribution about the source was sampled systematically and the first and succeeding collision points were sampled randomly. For the case of a monodirectional beam source where the first collisions were picked systematically the error on the flux should be less for the same number of sample neutrons.

Comparison of the Monte Carlo Solution against a Moments Method Solution

The only calculation that includes energy degredation which has appeared and provides a means of comparison is the Moments Method solution for an isotropic point source of neutrons in an infinite body of air presented by Holland and Richards.[2] It is of interest to make the comparison of the Monte Carlo calculation against this Moments Method solution for two reasons. The first is because there is a check against the energy spectra for the lower energy sources, and second because one can observe the effects of using isotropic scattering in the center of mass system and neglecting inelastic scattering in the Monte Carlo solution. The Moments solution included the anisotropy of scattering and inelastic scattering.

It was convenient to calculate the neutron flux at the detector point in the dimensionless units used by Holland and Richards for purposes of comparison. In their paper they defined the term

$$K(E,g) = \frac{\lambda^2 E\phi(E,g)}{S} \tag{54}$$

where

λ = a constant approximately equal to a mean free path distance (cm),

E = neutron energy,

$\phi(E,g)$ = neutrons/cm^2, sec, unit energy at energy E and separation distance g,

S = the source strength in neutrons/sec.

The quantity $K(E,g)$ in Eq. (54) can be termed a dimensionless energy flux.

Figures 7 through 12 present a comparison of the Monte Carlo and Moments solutions. Figures 7 through 10 are for a 2 Mev source of neutrons at various separation distances from the detector point, and Fig. 11 is for a 5.15 Mev source of neutrons. All five of these figures indicate there is fairly good agreement between the two methods of solution at the separation distances indicated. It is not expected that this favorable agreement will persist at larger separation distances. Although there is reasonably good agreement at the 5.15 Mev and 2 Mev source energies, at 14 Mev there is a serious disagreement as indicated in Fig. 12. Although the histogram from the Monte Carlo solution, in general, has a tendancy to have hills and vallies at the same energies as the Moments solution the Monte Carlo values are approximately a factor of 50 below for energies below 3 Mev. The surprising thing is the remarkable comparison in the region 8 to 12 Mev. It is very difficult to discover the reason for the disagreement and aggreement in this last case, however, a possible explanation could be that an insufficient number of sample neutrons was taken in the Monte Carlo problem which would give such an underestimate. Other possible explanations dealing with the neglect of inelastic scattering and anisotropy could be given, but, again, it is difficult to analyze the problem without more information.

The comparison at various energies suggests that, in general, the Monte Carlo problem as it is developed in this report should not be used at energies much above 5 Mev.

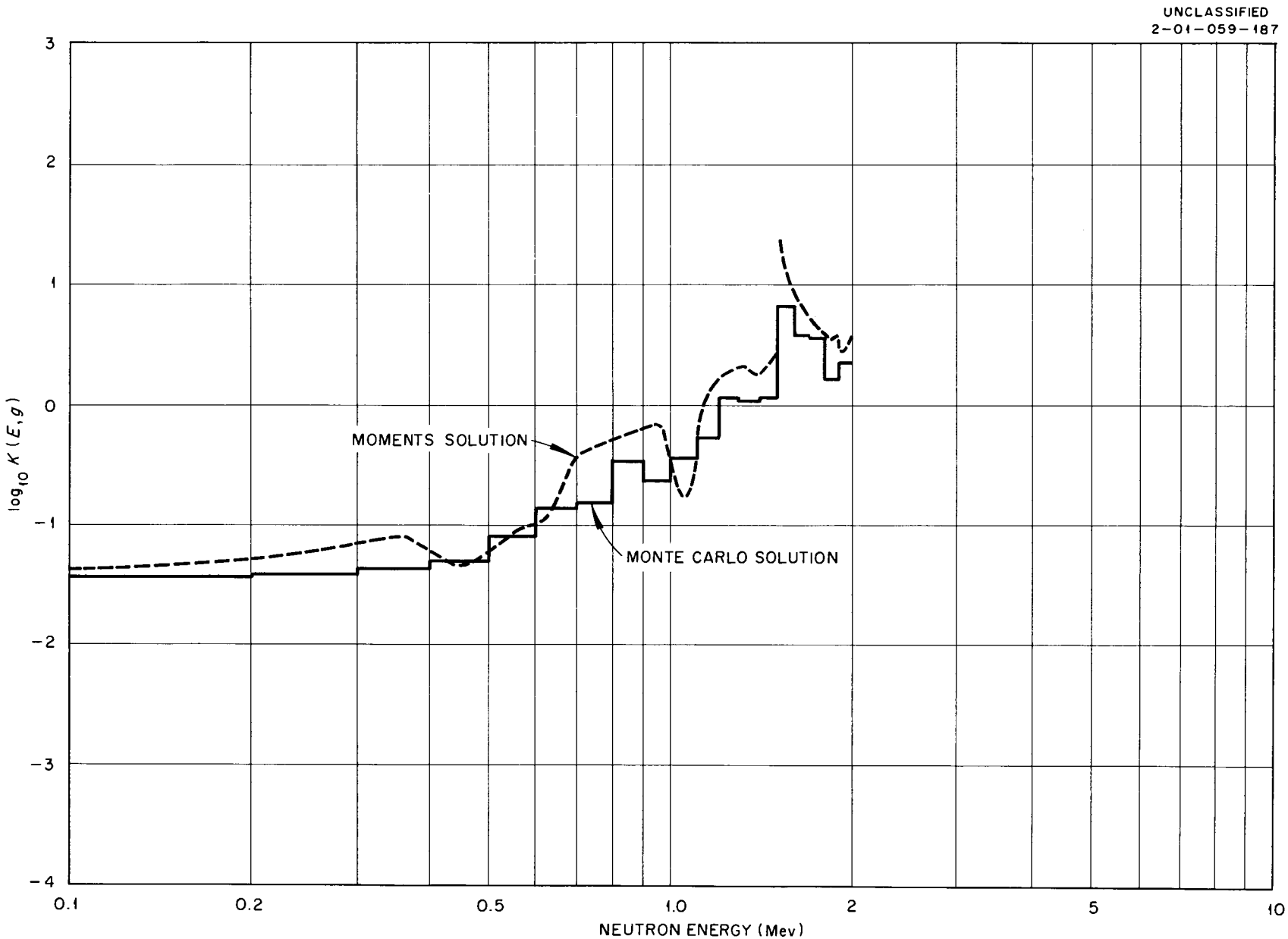

Fig. 7. Dimensionless Flux of Neutrons at Source – Detector Separation Distance $g = 0.1\,\lambda$ ($\lambda = 186$ meters); 2-Mev Point Isotropic Source in Air at STP.

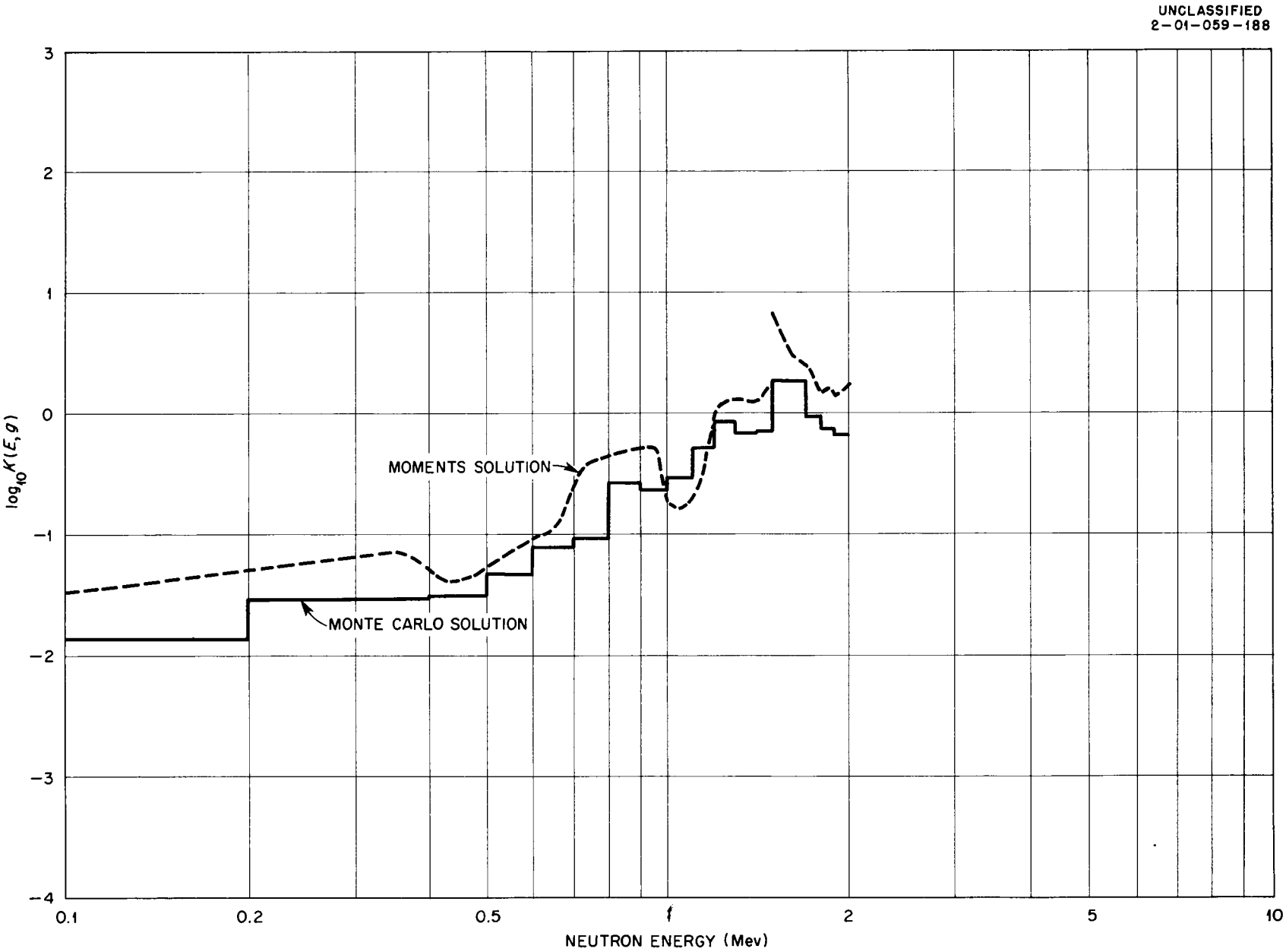

Fig. 8. Dimensionless Flux of Neutrons at Source – Detector Separation Distance $g = 0.2\,\lambda$ ($\lambda = 186$ meters); 2-Mev Point Isotropic Source in Air at STP.

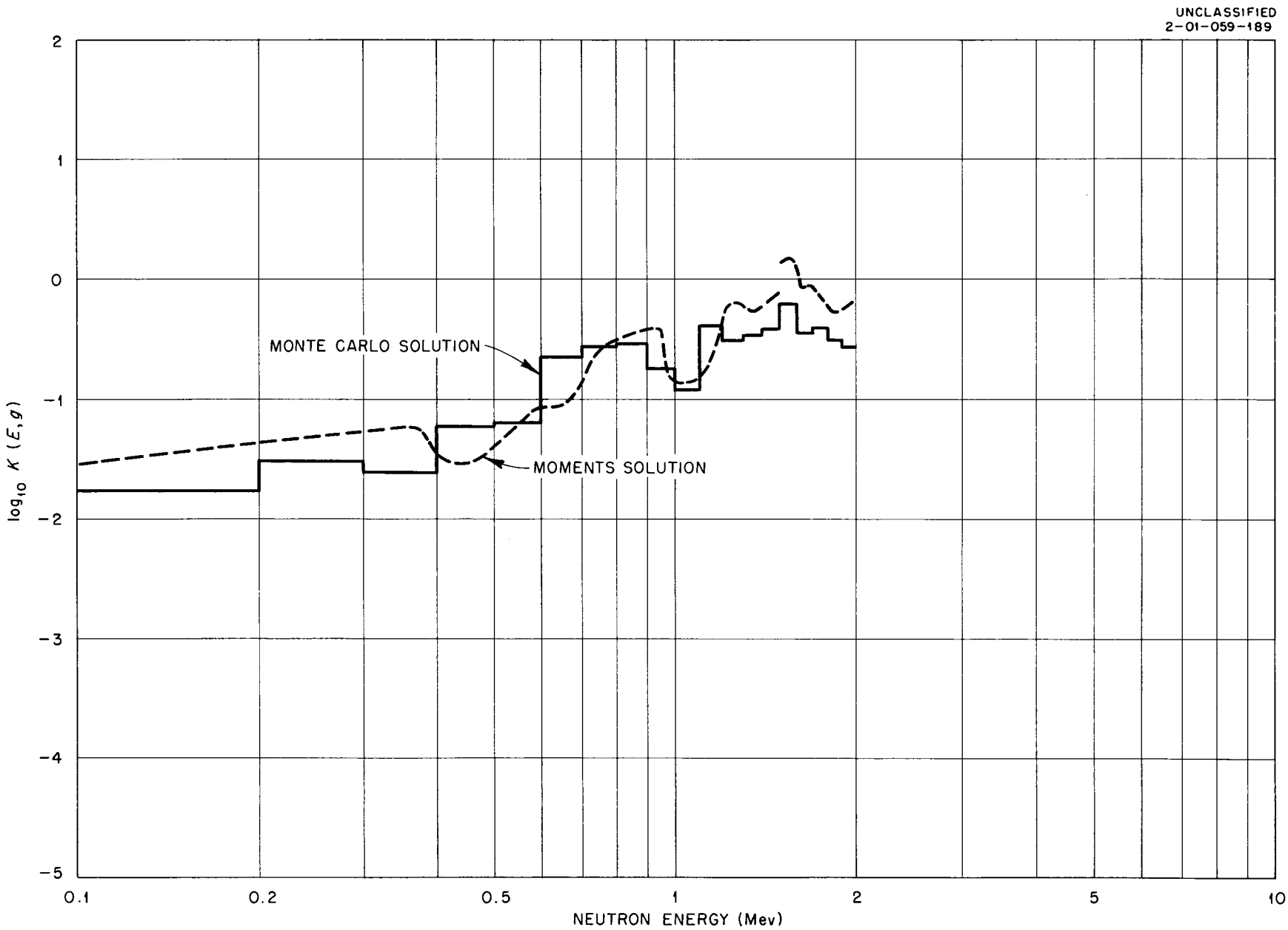

Fig. 9. Dimensionless Flux of Neutrons at Source – Detector Separation Distance $g = 0.4\lambda$ ($\lambda = 186$ meters); 2-Mev Point Isotropic Source in Air at STP.

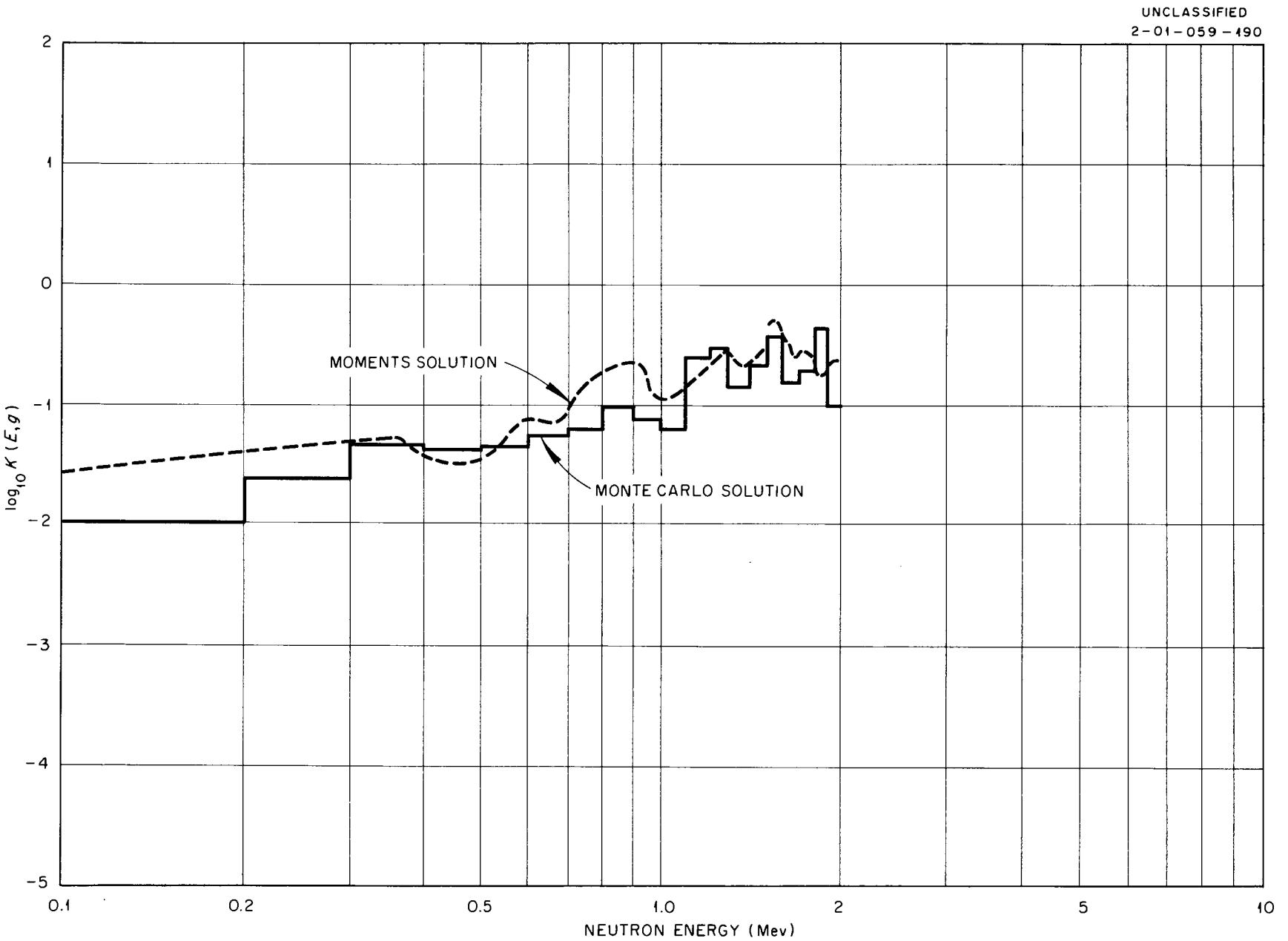

Fig. 10. Dimensionless Flux of Neutrons at Source—Detector Separation Distance $g = 0.7\lambda$ ($\lambda = 186$ meters); 2-Mev Point Isotropic Source in Air at STP.

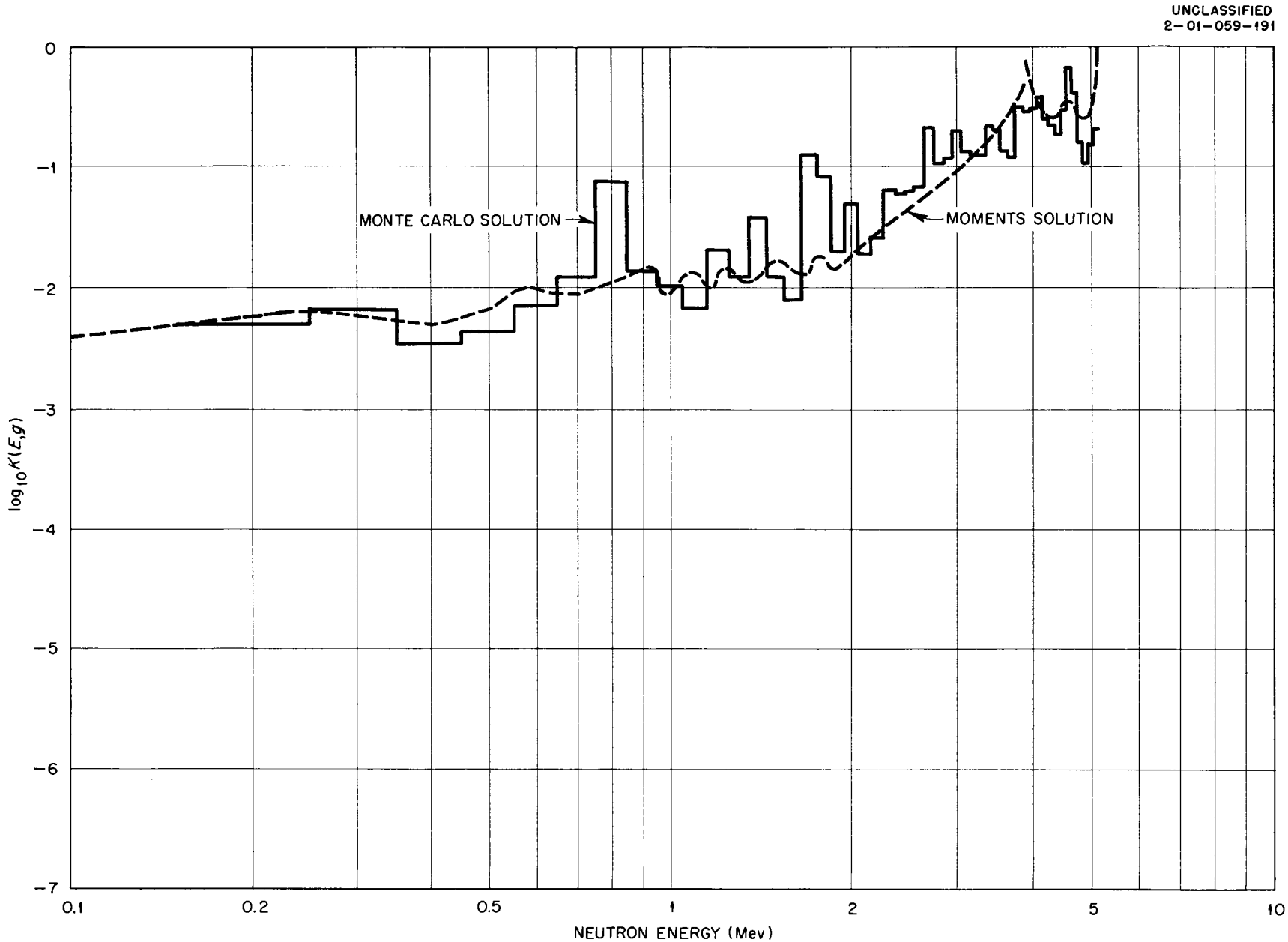

Fig. 11. Dimensionless Flux of Neutrons at Source–Detector Separation Distance $g = 0.5\ \lambda$ ($\lambda = 116$ meters); 5.15-Mev Point Isotropic Source in Air at STP.

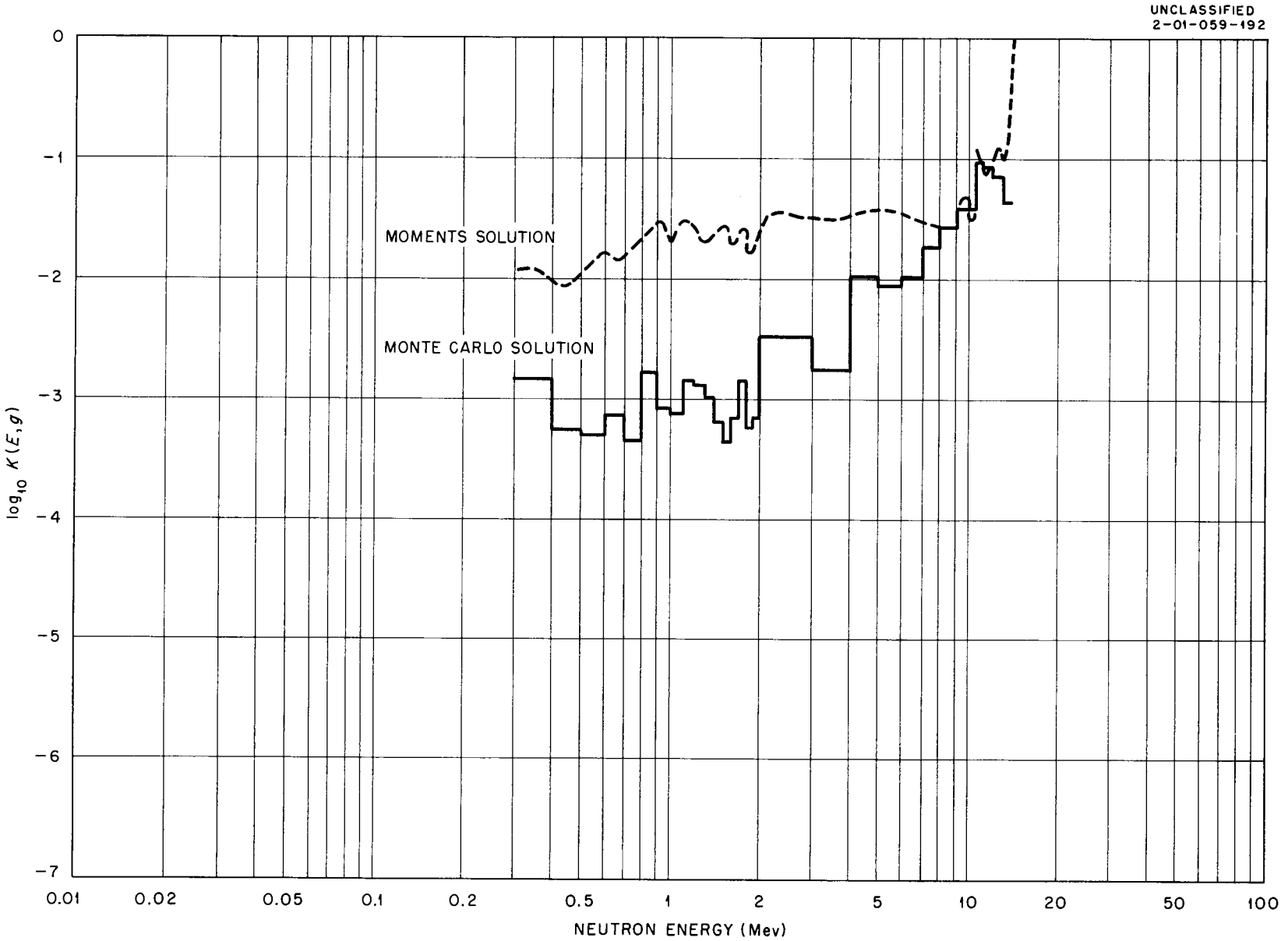

Fig. 12. Dimensionless Flux of Neutrons at Source–Detector Separation Distance $g = 0.5\ \lambda$ ($\lambda = 116$ meters); 14-Mev Point Isotropic Source in Air at STP.

CHAPTER IV. RESULTS

The neutron air scattering problem is of sufficient interest that a complete parameter study was undertaken and completed. For general application it was decided to use a monodirection, monoenergetic point source at several source-detector separation distances. The energies of the source which appeared to be of interest and were within the limits of application of code were 5, 3, 2, 1.2, and 0.55 Mev. These particular values were selected because the cross section at those energies appeared to represent an average within a reasonable energy interval. Beam angles θ_o of 2, 15, 30, 60, 90, 135, and 180 deg were also selected. The density of the dry air used in every problem was 0.00125 g/cm^3. No moisture was included. Since the air density was fixed it was desirable to select several source-detector separation distances at which to do the parameter study. This provides the benefit of obtaining the resulting data at various air densities and separation distances as described in another report.[13] The source-detector separation distances, g, selected were 5, 10, 20, 40, 64, and 100 ft.

As pointed out in Chapter I, the type of source selected does not restrict the application of the results since they can be integrated to form any distributed source.[1]

At the time of this writing it has not been possible to fully analyze the results of the parameter study, so only part of the results are included here. It is intended that graphs of the data will be published at a later date.

---

13. C. D. Zerby, Radiation Flux Transformation as a Function of Density of an Infinite Medium with Anisotropic Point Sources, ORNL-2100 (Oct. 9, 1956).

In Figs. 13 through 22 are given the values of the neutron flux and the Dose 1 results at a separation distance of 64 ft. The energy cut off was taken as 0.1 Mev so the values given are for neutrons between the cut off energy and the source energy. In each of the Figs. 13 through 22 the results are given including all orders of scattering and for comparison what would have been obtained by a single scattering calculation. The curves are smooth fits to the data and are estimated to be within 15 percent of the correct value.

UNCLASSIFIED
2-01-059-193

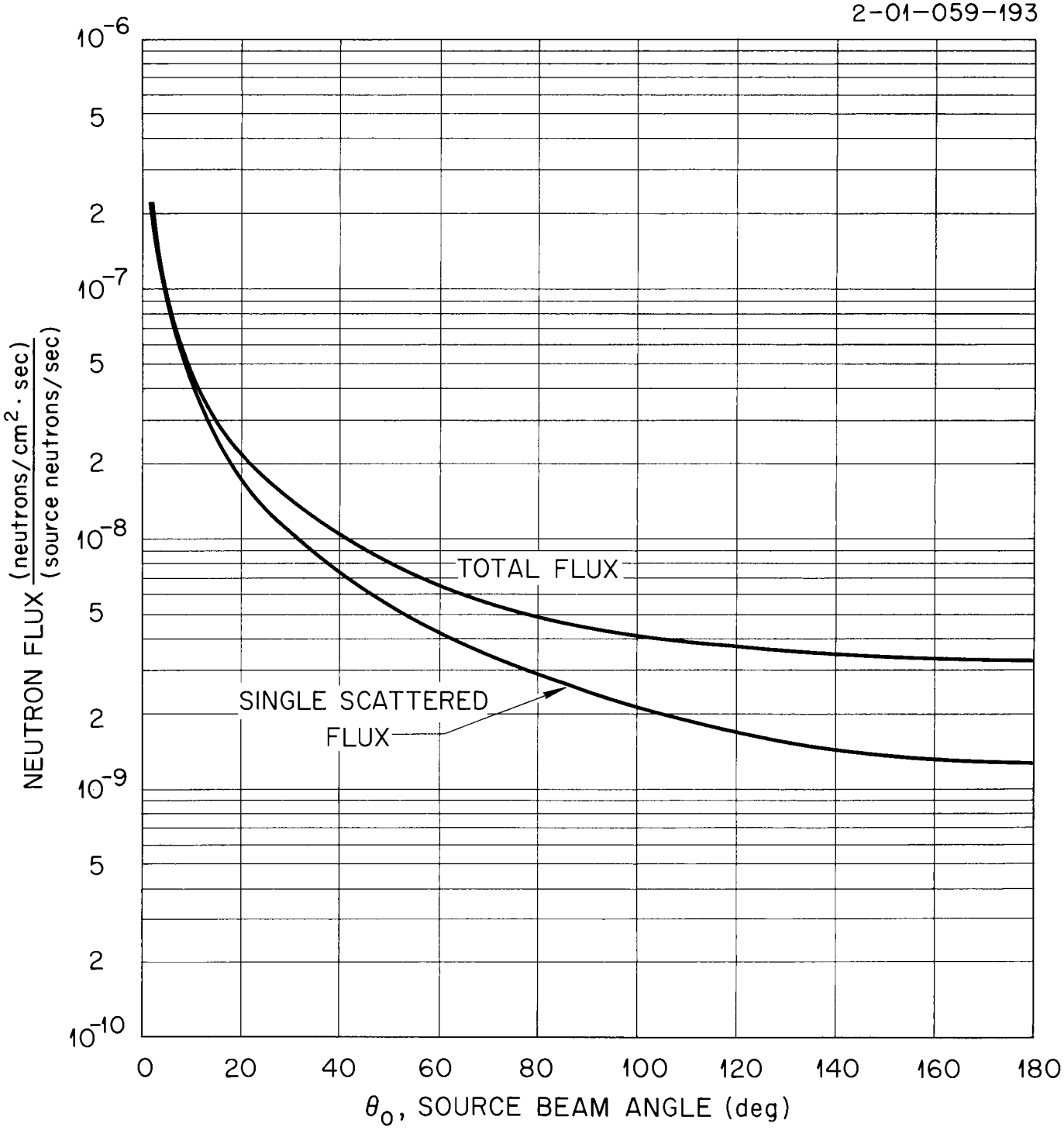

Fig. 13. Flux of Neutrons with Energy Greater than 0.1 Mev in Air at a Source-Detector Separation Distance of 64 ft; 5-Mev Monodirectional Point Source in Air (Air Density = 0.00125 g/cm^3).

UNCLASSIFIED
2-01-059-194

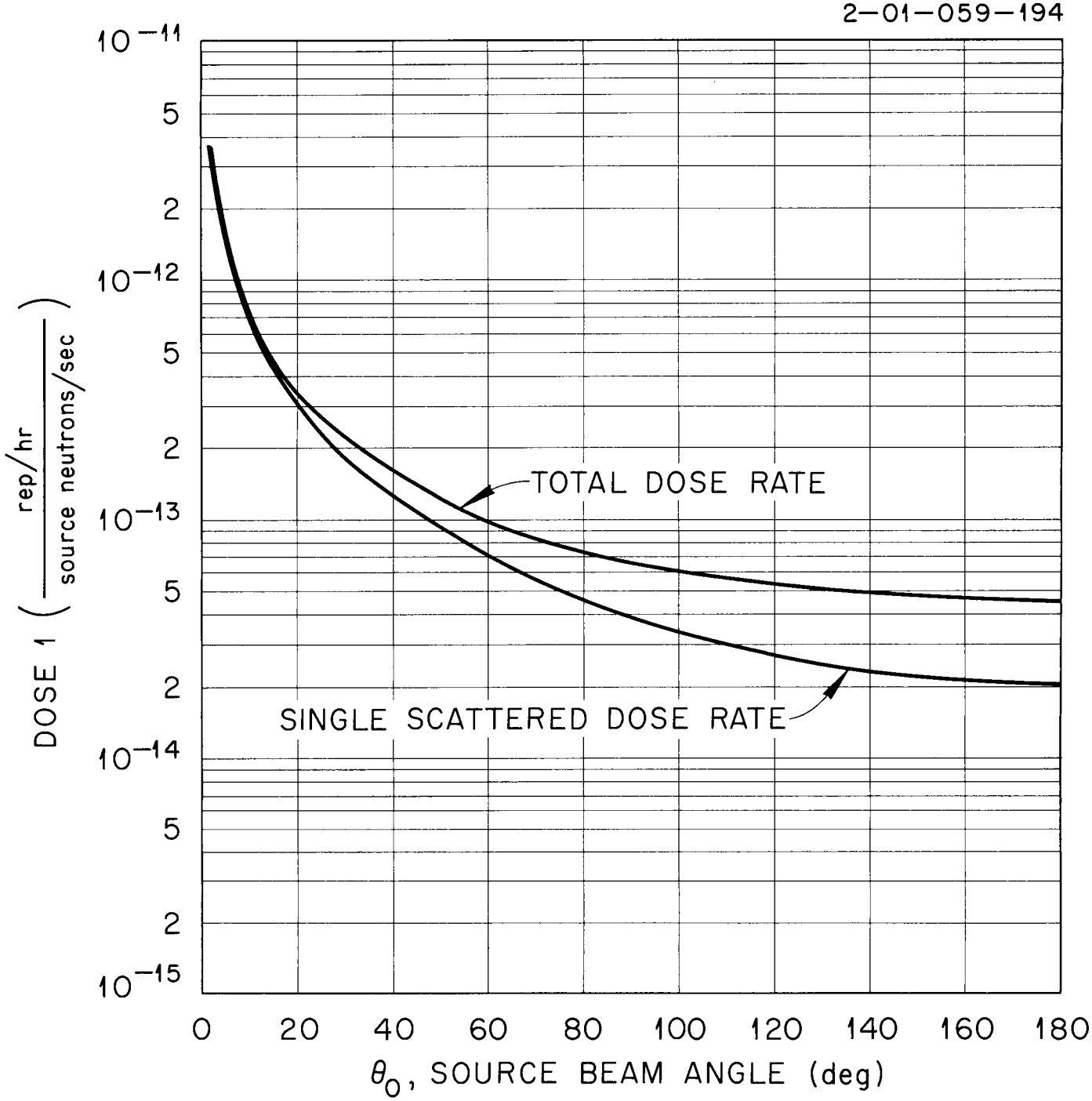

Fig. 14. Tissue Dose Rate in a Point Meatball Detector at a Source—Detector Separation Distance of 64 ft Resulting from Neutrons with Energy Greater than 0.1 Mev; 5-Mev Point Monodirectional Source in Air. (Air Density = 0.00125 g/cm^3)

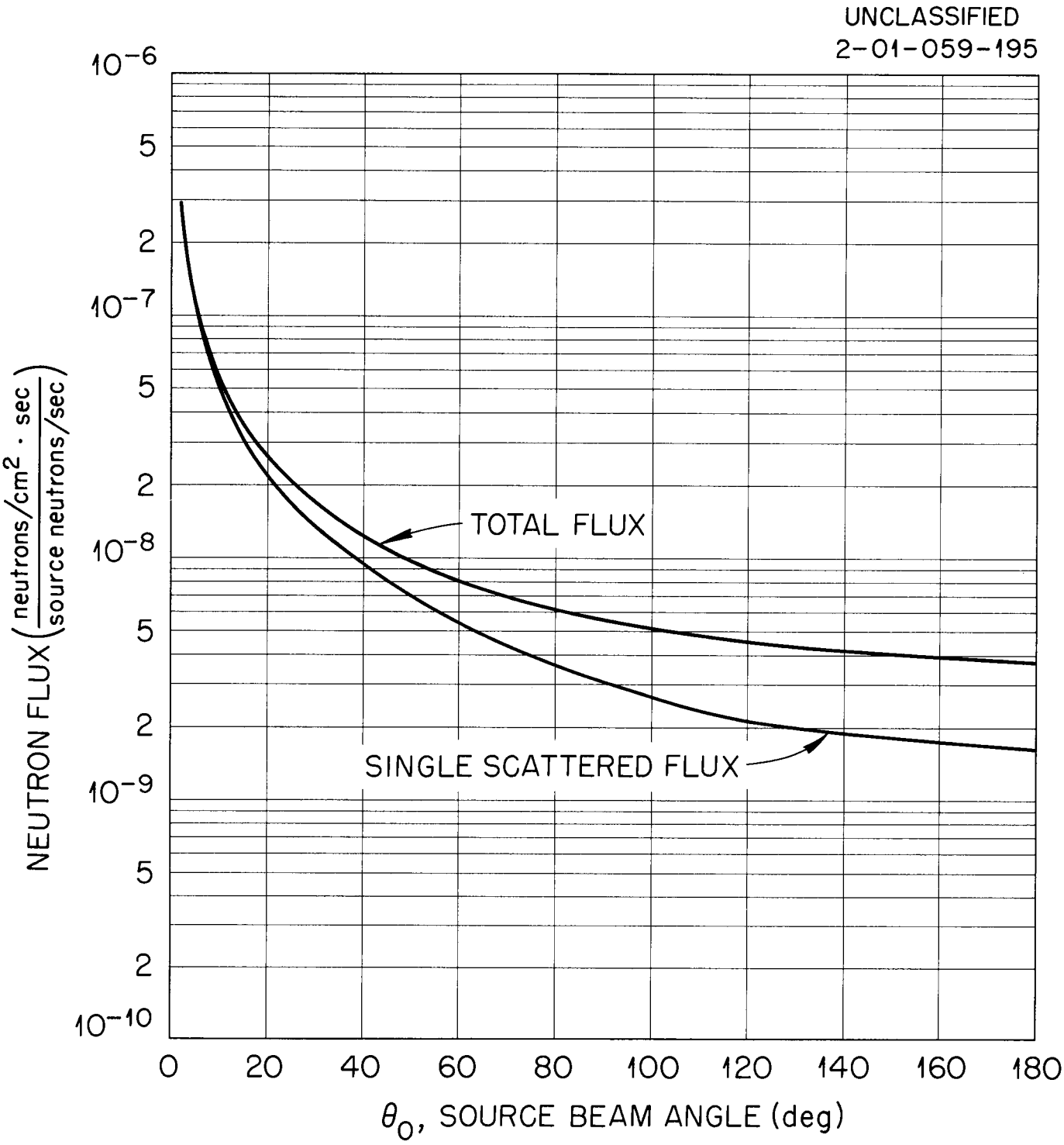

Fig. 15. Flux of Neutrons with Energy Greater than 0.1 Mev in Air at a Source–Detector Separation Distance of 64 ft; 3-Mev Point Monodirectional Source in Air (Air Density = 0.00125 g/cm^3).

UNCLASSIFIED
2-01-059-196

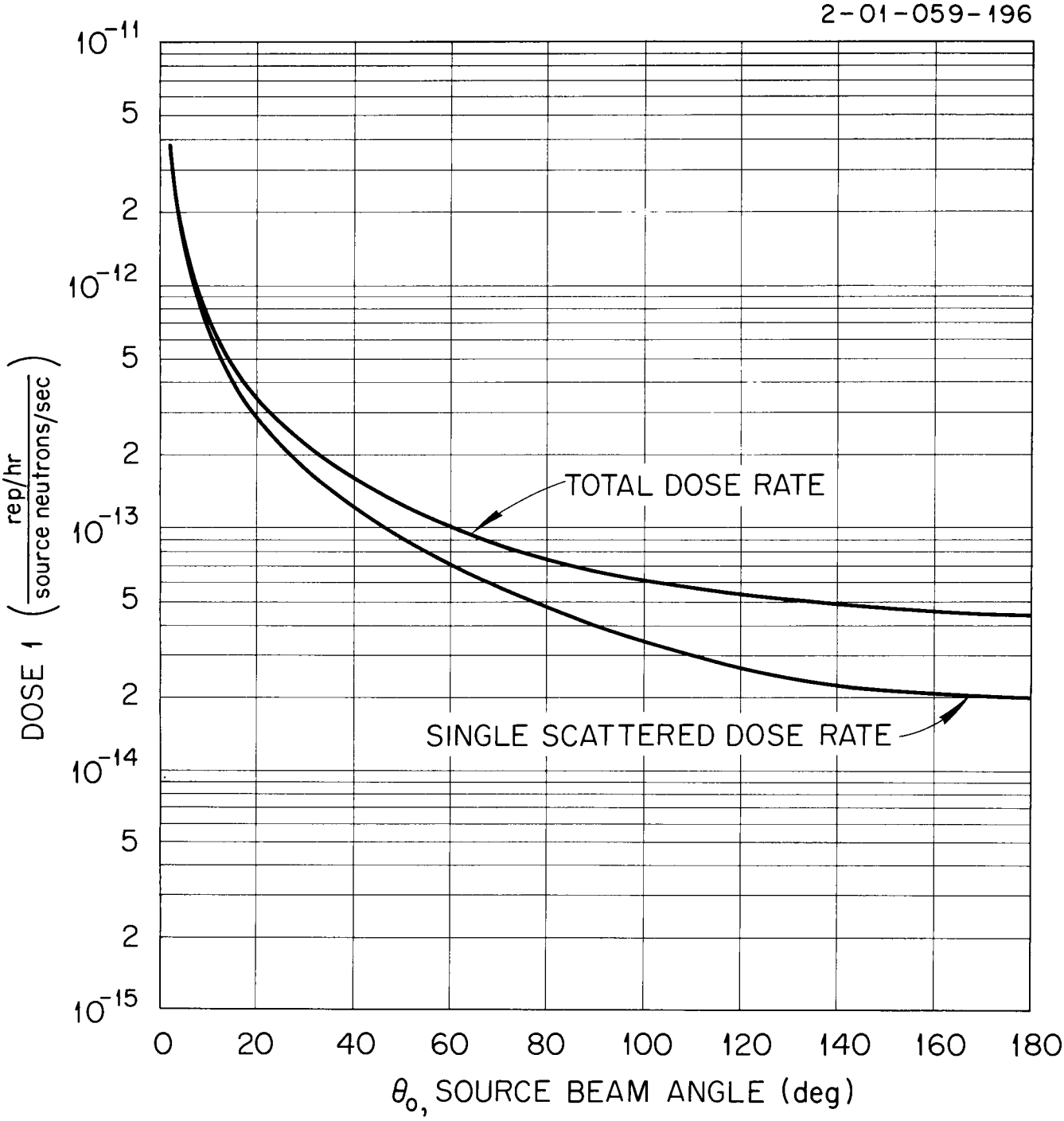

Fig. 16. Tissue Dose Rate in a Point Meatball Detector at a Source-Detector Separation Distance of 64 ft Resulting from Neutrons with Energy Greater than 0.1 Mev; 3-Mev Point Mono-directional Source in Air. (Air Density = 0.00125 g/cm^3).

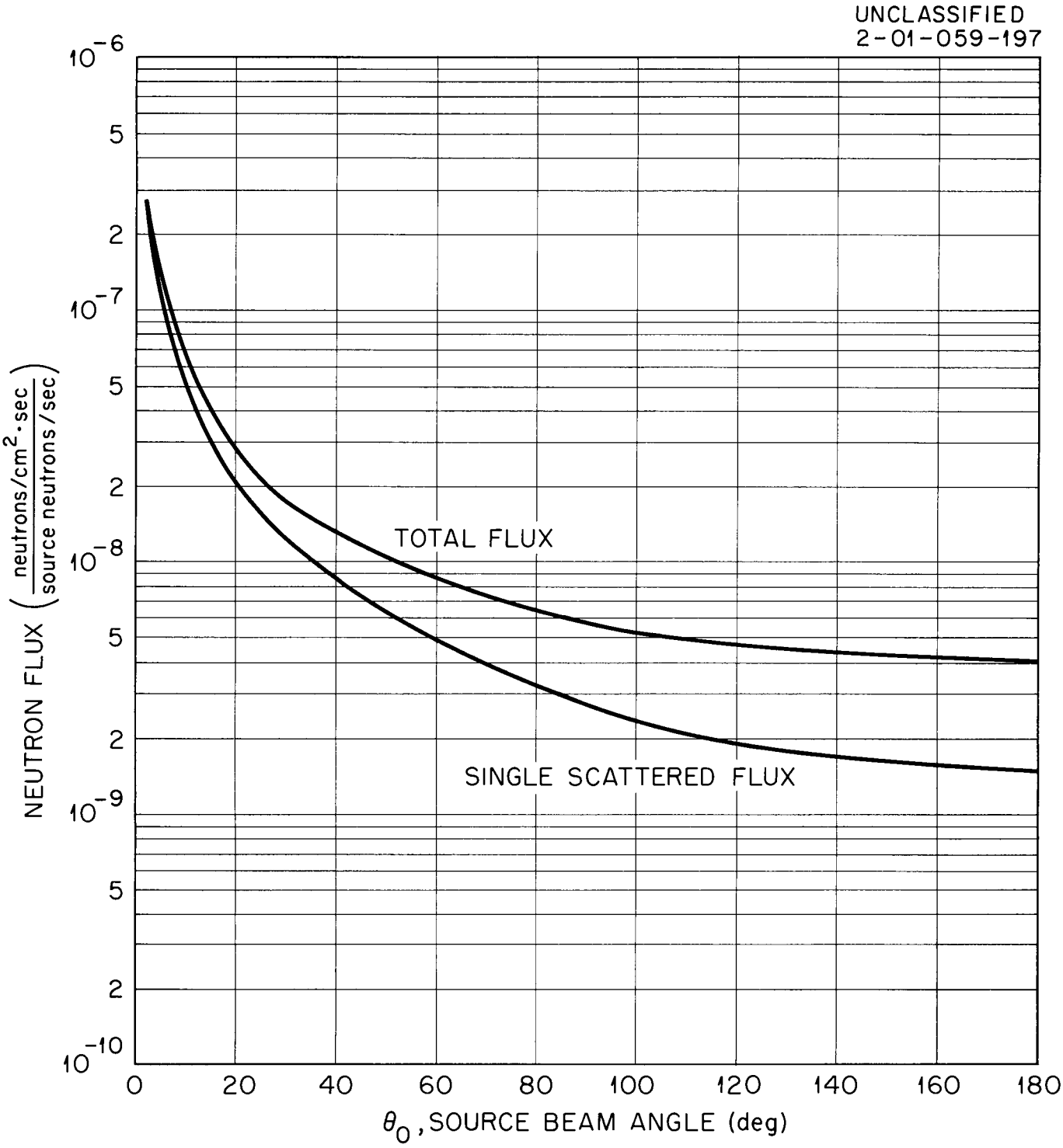

Fig. 17. Flux of Neutrons with Energy Greater Than 0.1 Mev in Air at a Source-Detector Separation Distance of 64 ft; 2-Mev Point Monodirectional Source in Air (Air Density = 0.00125 g/cm^3).

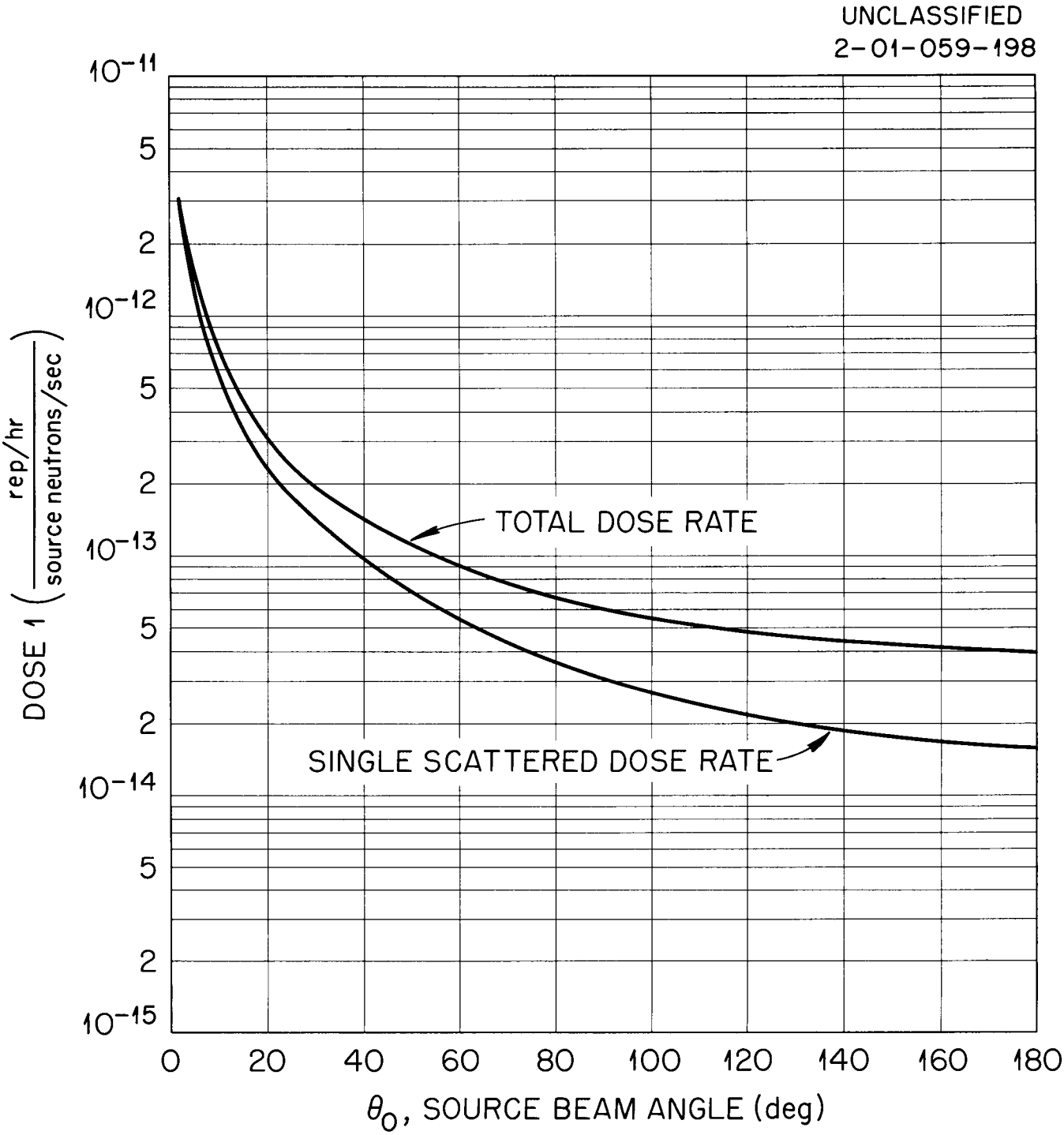

Fig. 18. Tissue Dose Rate in a Point Meatball Detector at a Source–Detector Separation Distance of 64 ft Resulting from Neutrons with Energy Greater than 0.1 Mev; 2-Mev Point Monodirectional Source in Air (Air Density = 0.00125 g/cm^3).

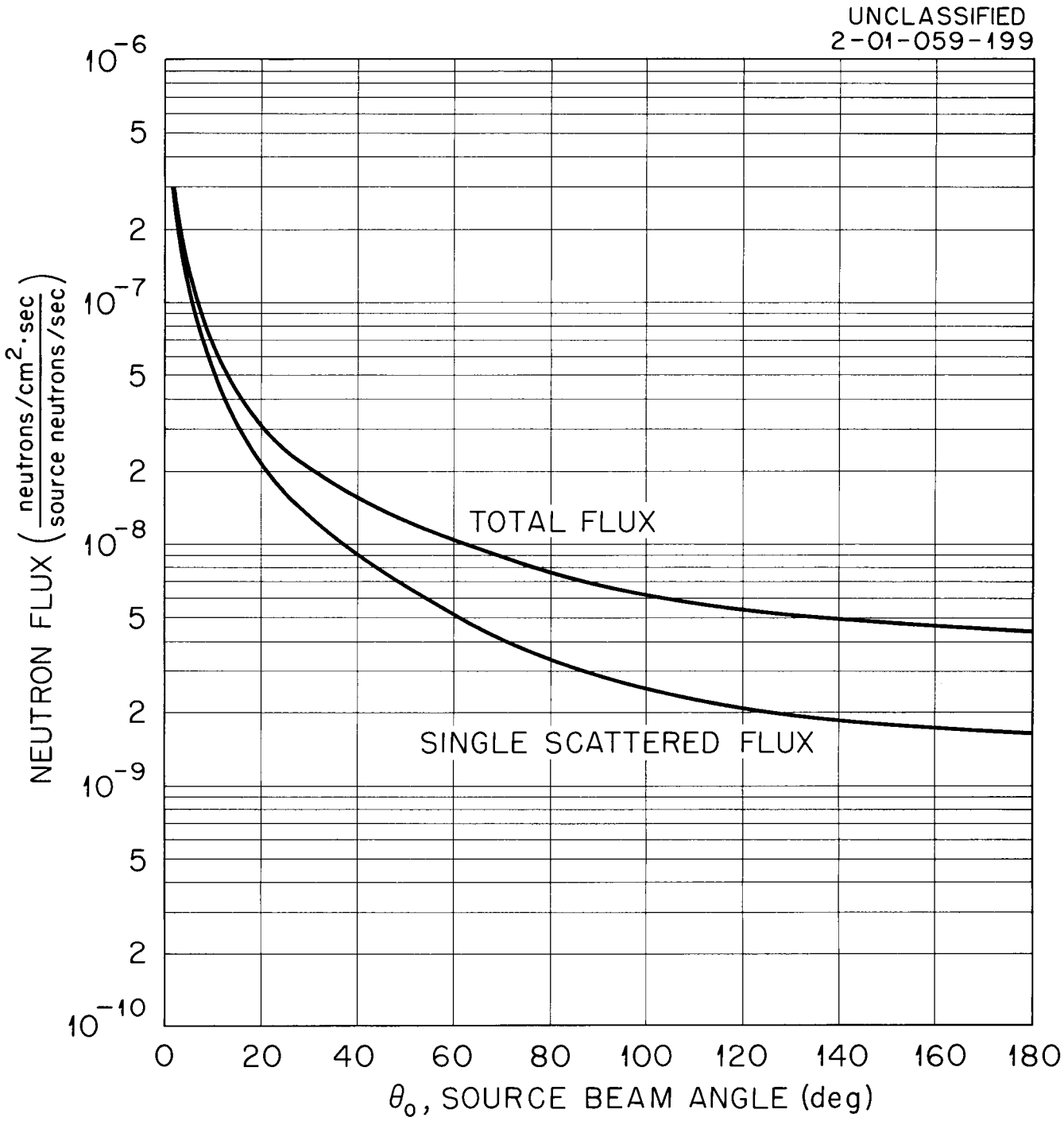

Fig. 19. Flux of Neutrons with Energy Greater than 0.1 Mev in Air at a Source-Detector Separation Distance of 64 ft; 1.2-Mev Point, Monodirectional Source in Air. (Air Density = 0.00125 g/cm^3).

UNCLASSIFIED
2-01-059-200

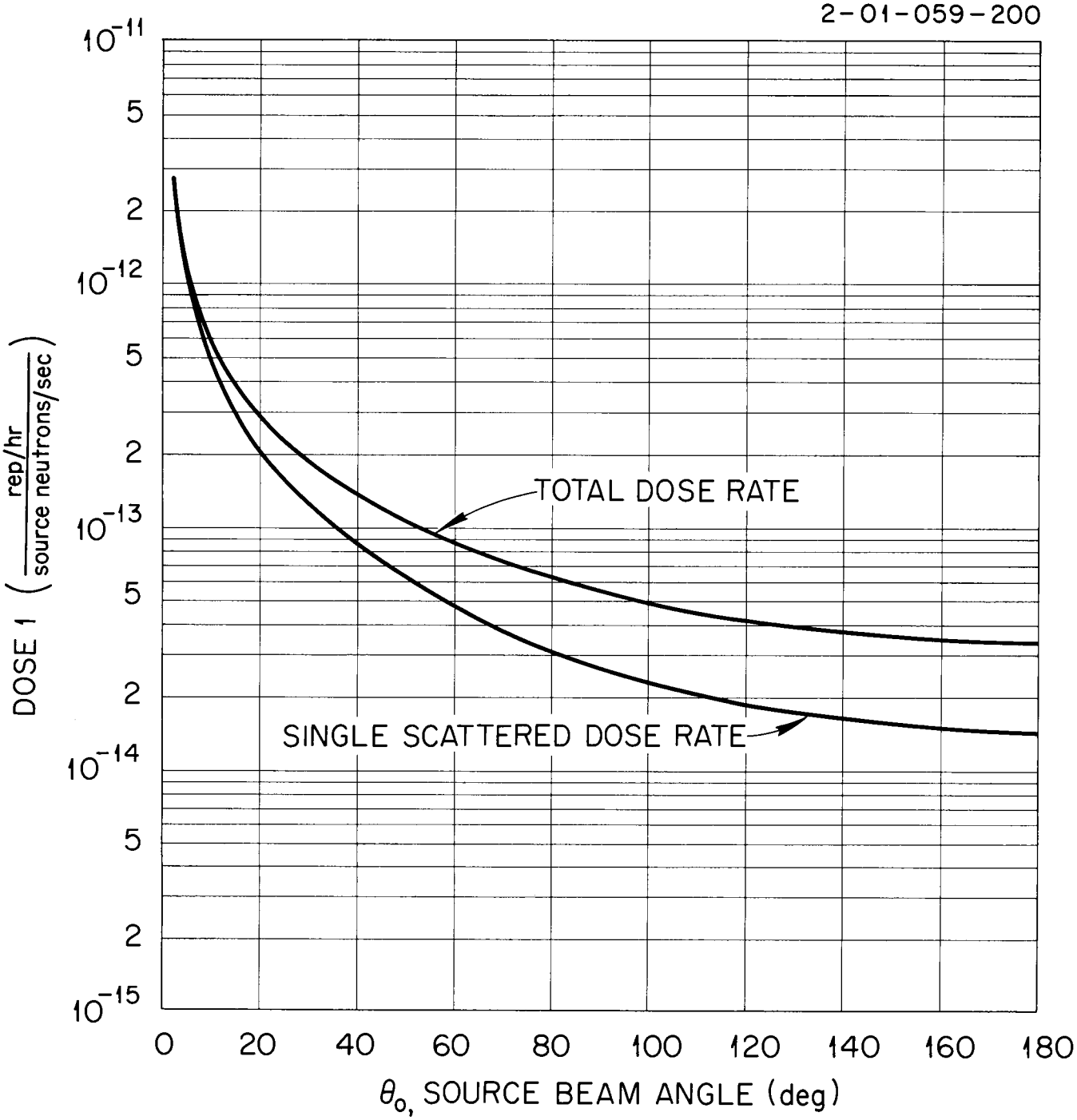

Fig. 20. Tissue Dose Rate in a Point Meatball Detector at a Source-Detector Separation Distance of 64 ft Resulting from Neutrons with Energy Greater than 0.1 Mev; 1.2-Mev Point Monodirectional Source in Air. (Air Density = 0.00125 g/cm^3).

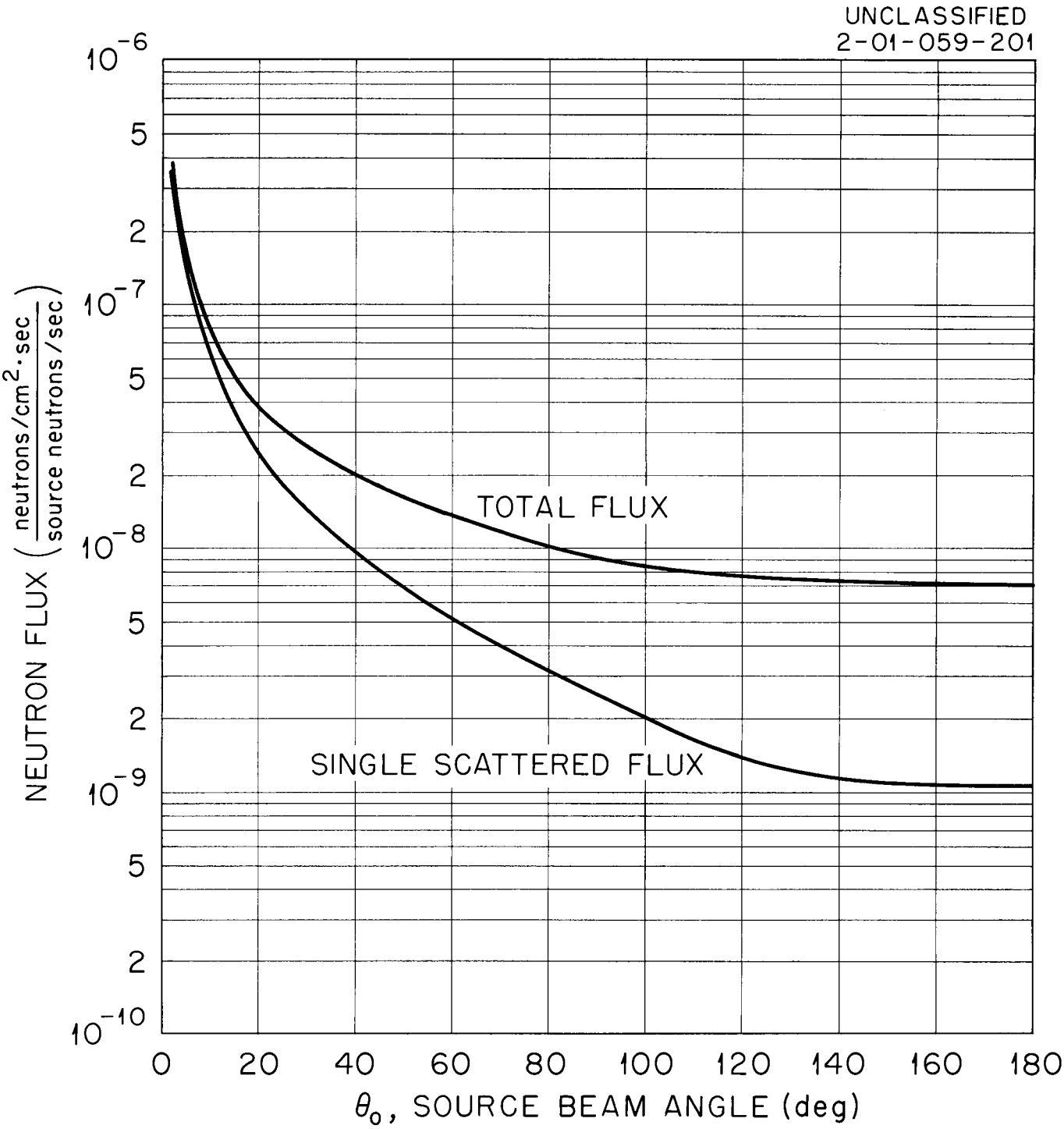

Fig. 21. Flux of Neutrons with Energy Greater than 0.1 Mev in Air at a Source-Detector Separation Distance of 64 ft; 0.55-Mev Point, Monodirectional Source in Air. (Air Density = 0.00125 g/cm^3).

UNCLASSIFIED
2-01-059-202

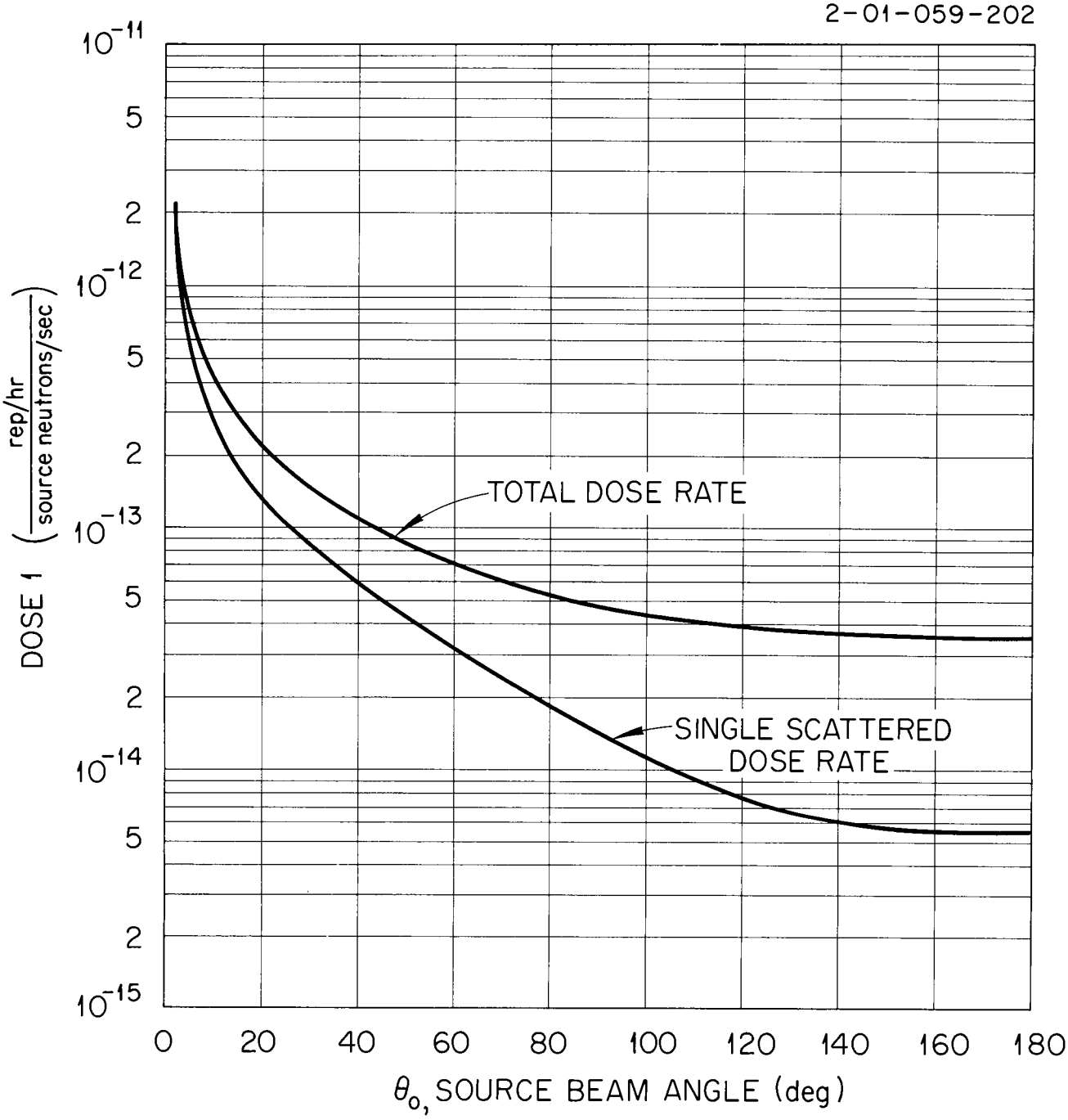

Fig. 22. Tissue Dose Rate in a Point Meatball Detector at a Source-Detector Separation Distance of 64 ft Resulting from Neutrons with Energy Greater than 0.1 Mev; 0.55-Mev Point Mono-directional Source in Air. (Air Density = 0.00125 g/cm^3).

APPENDIX A

The derivation of the integral form of the Boltzmann equation is not usually given. It is presented here because the Monte Carlo method used in this calculation essentially solves the Boltzmann equation in that form.

The Boltzmann transport equation is given as

$$\vec{\Omega}\cdot\vec{\nabla}\cdot\psi(\vec{r}\,',E,\vec{\Omega}) + \Sigma_T(\vec{r}\,',E)\psi(\vec{r}\,',E,\vec{\Omega}) = q(\vec{r}\,',E,\vec{\Omega}) \tag{55}$$

where

$\vec{\Omega}$ = a unit vector,

$\psi(\vec{r}\,',E,\vec{\Omega})$ = particles/cm^2/sec/unit energy at energy E per steradian about direction $\vec{\Omega}$ at position $\vec{r}\,'$,

$\Sigma_T(\vec{r}\,',E)$ = the macroscopic total cross section at position $\vec{r}\,'$ and at at energy E (cm^{-1}),

$q(\vec{r}\,',E,\vec{\Omega})$ = the source term: particles/cm^3/sec/unit energy at energy E per steradian about direction $\vec{\Omega}$ at position $\vec{r}\,'$.

Taking the coordinate system so that the R axis is antiparallel to the direction $\vec{\Omega}$, then

$$\vec{\Omega}\cdot\vec{\nabla} = -\frac{\partial}{\partial R} \quad . \tag{56}$$

Now, letting

$$\vec{r}\,' = \vec{r} - R\vec{\Omega} \tag{57}$$

where $\vec{r}$ is some fixed position, Eq. (55) becomes a partial differential equation in terms of the variable R given by

$$-\frac{\partial}{\partial R}\psi(\vec{r}\,',E,\vec{\Omega}) + \Sigma_T(\vec{r}\,',E)\psi(\vec{r}\,',E,\vec{\Omega}) = q(\vec{r}\,',E,\vec{\Omega}) \tag{58}$$

which can be solved by multiplying through by the integrating factor

$$\exp\left[-\int_c^R \Sigma_T(\vec{r} - R'\vec{\Omega},E)dR'\right]$$ to get

$$-\frac{\partial}{\partial R}\left[\psi(\vec{r}',E,\vec{\Omega})e^{-\int_c^R \Sigma_T(\vec{r}-R'\vec{\Omega},E)dR'}\right] = Q(\vec{r}',E,\vec{\Omega})e^{-\int_c^R \Sigma_T(\vec{r}-R'\vec{\Omega})dR'} \tag{59}$$

where c is an arbitrary constant. Equation (59) can be integrated if it is assumed that the source distribution allows that the quantity in the square bracket on the left of the equation is zero when $R = \infty$. If this assumption holds, as it usually does, then the integration gives

$$-\psi(\vec{r}',E,\vec{\Omega})e^{\int_c^R \Sigma_T(\vec{r}-R'\vec{\Omega},E)dR'} = \int_\infty^R q(\vec{r} - R'\vec{\Omega},E,\vec{\Omega})e^{-\int_c^{R'} \Sigma_T(\vec{r}-R''\vec{\Omega},E)dR''}dR' \tag{60}$$

or

$$\psi(\vec{r}',E,\vec{\Omega}) = \int_R^\infty q(\vec{r} - R'\vec{\Omega},E,\vec{\Omega})e^{-\int_R^{R'} \Sigma_T(\vec{r}-R''\vec{\Omega},E)dR''}dR'. \tag{61}$$

The solution at the position $\vec{r}$ is obtained from Eq. (61) as

$$\psi(\vec{r},E,\vec{\Omega}) = \int_0^\infty q(\vec{r} - R'\vec{\Omega},E,\vec{\Omega})e^{-\int_0^{R'} \Sigma_T(\vec{r}-R''\vec{\Omega},E'')dR''}dR'. \tag{62}$$

To proceed, the following cefinition is made

$$\delta(-\vec{\Omega}',\vec{\Omega}) = 0 \qquad \text{if } -\vec{\Omega}' \neq \vec{\Omega}$$

$$\text{and} \qquad \int_{\vec{\Omega}'} \delta(-\vec{\Omega}',\vec{\Omega})d\vec{\Omega}' = 1 \tag{63}$$

In addition let $\vec{\Omega}'$ be a unit vector directed away from the position $\vec{r}$. With these definitions in mind, Eq. (62) can be written as

$$\psi(\vec{r},E,\vec{\Omega}) = \int_{\vec{\Omega}'} \delta(-\vec{\Omega}',\vec{\Omega})d\vec{\Omega}' \int_0^{\infty} q(\vec{r} - R'\vec{\Omega},E,\vec{\Omega})e^{-\int_0^{R'} \Sigma_T(\vec{r}-R''\vec{\Omega},E)dR''} dR' \tag{64}$$

or

$$\psi(\vec{r},E,\vec{\Omega}) = \int_{\text{All Space}} q(\vec{r} + R'\vec{\Omega}',E,\vec{\Omega})e^{-\int_0^{R'} \Sigma_T(\vec{r}+R''\vec{\Omega}',E)dR''} \frac{\delta(-\vec{\Omega}',\vec{\Omega})}{R'^2} d\vec{R}' \tag{65}$$

where $d\vec{R}' = R'^2 d\vec{\Omega}' dR'$.

In general, when scattering is allowed, the source term is given by

$$q(\vec{r}, E,\vec{\Omega}) = S(\vec{r},E,\vec{\Omega}) + \int_{E'} \int_{\vec{\Omega}'} \Sigma_S(\vec{r},E')\psi(\vec{r},E',\vec{\Omega}')f(E,E',\vec{\Omega},\vec{\Omega}')dE'd\vec{\Omega}' \tag{66}$$

where

$S(\vec{r},E,\vec{\Omega})$ = the extraneous source term: particles/cm^3/sec/ unit energy at energy E per steradian about direction $\vec{\Omega}$ at position $\vec{r}$,

$f(E,E',\vec{\Omega},\vec{\Omega}')dEd\vec{\Omega}$ = the probability of scattering from a direction $\vec{\Omega}'$ at energy E' into the solid angle $d\vec{\Omega}$ about the direction $\vec{\Omega}$ and into the energy interval between E and E + dE,

$\Sigma_S(\vec{r},E')$ = the macroscopic scattering cross section at position $\vec{r}$ and at energy E' (cm^{-1}).

APPENDIX B

This section of the report contains all the instructions and detailed information necessary for using the ORACLE code which has been prepared to solve the neutron air scattering problem. Included is a description of the ORACLE data output and a copy of the complete code. The problem and code are recorded as Problem No. 323 with the Mathematics Panel of the Oak Ridge National Laboratory. The details of the mathematics and physical data included in the code comprise all of Chapter II which should be referred to when necessary.

In the case of this particular section it was necessary to deviate from the style of the rest of the report to make precisely clear the steps necessary for preparing a problem for the ORACLE and operating the machine. The steps of the procedures are given in a series of notes which are cross referenced and writen in the language familiar to those who have become acquainted with the ORACLE. The reader who has not had the acquaintance will find it difficult to understand or follow the instructions and should omit this section.

Notes I through V are the operating instructions for the ORACLE; Notes VI through IX are notes on the preparation of code words and miscellaneous tapes; Note X gives the instructions for preparing the input parameter tape for a problem; Note XI describes the output; and Note XII gives the complete ORACLE code.

In general, it should be noted that it is possible to have the neutron source in H_2O as an alternate to having it in air.

NOTES

I. Loading of fast memory and magnetic tapes from paper tape code and running problems. (The paper tape code is given in Note XII.)

1. Set switch for 2048 word fast memory.
2. Clear fast memory.
3. Put roll 1 of paper tape code under reader.
4. S.O. 90700 (loads tape 1 from roll 1 of the paper tape).
5. S.O. 43700. Stops L-710 (loads all of roll 1).
6. Put the code word for the name in the Q register (see Note IX for the preparation of the code word). If the contents of Q is not altered as indicated in this instruction, the name will be blank on all curve plotter pictures.
7. Go back on continuous operation. Stops R-714.
8. Put roll 2 of paper tape code under reader.
9. Go back on continuous operation. Stops L-71C (this operation will load all of roll 2).
10. Put paper tape date under reader (see Note VII for preparation of tape).
11. Go back on continuous operation. Stops L-000.
12. If corrections are to be made to the Monte Carlo code, do the following:
    a. Put paper tape corrections under reader (see Note VIII for preparation of tape).
    b. Put B/P switch on.
    c. S.O. 4309B. Stops L-09D.

d. Put B/P switch off.

13. To run a problem do the following:

a. Put paper problem parameter tape under reader (see Note X for preparation of tape).

b. Go back on continuous operation.

c. Output may include a curve plotter output. During output, if it is necessary to change film, etc. at the curve plotter, flip on the B/P switch and record where machine stopped. Transfer back in at the same place after manually advancing the film.

d. Machine stops L-000 at end of output (see Note XI for form of output).

14. For each of the remaining problems start at step I-13.

II. Loading of fast memory and magnetic tapes from personal magnetic tape (see Note VI for preparation of personal magnetic tape).

1. Put personal magnetic tape on drive 0.

2. Set all magnetic tape drives to position 0 on the indicator.

3. Manually do the following:

a. 80* $\longrightarrow$ Q.

b. S.O. B0700.

c. S.O. 4372C. Stops L-71C.

4. Continue from Note I-10.

III. Some additional coded stops that may occur are given below. If these stops occur, the code will not accept the input problem parameter tape for the reason given.

L-05D Density of air or moisture in air too great for scaling of the code.

L-082 Too many data spaces asked for (see limits on k given in Table 7).

IV. In case of machine error at any time after computation has started except when writing on any drive

1. Code periodically reads the completed Monte Carlo computation on magnetic tape drive 1 and hunts back. In case of a machine error a problem can be completed without loss of the entire computation by doing the following:

   a. Set drives 1, 2, and 3 to position 0 on the indicators.

   b. Set drive 0 to position 1A on the indicator.

   c. 800* $\longrightarrow$ Q.

   d. S.O. B1000.

   e. S.O. 43107.

   f. Continue as before.

V. In case it is necessary to load the complete code again, start at Note II-2. This instruction is independent of the initial loading as given in Notes I or II.

VI. Preparation of personal magnetic tape.

1. Put personal magnetic tape on drive 0.

2. Complete instructions I-1 through I-9.

3. The first 40 (decimal) blocks of tape on drive 0 will have the complete code. An additional 6 blocks are required on drive 0 during computation making the length of tape 46 (decimal) blocks.

VII. Preparation of paper tape date.

The paper tape date contains one word of ten characters followed by a single or double space. The form of the word is

Month	Day	Year	
xx	xx	xx	0000

where the month, day, and year are designated by decimal numerals, i.e., 0105570000 gives the date 01-05-57.

VIII. Preparation of correction tape for the Monte Carlo code.

The correction tape consists of a series of two word sets. The first word in each set contains the address in which the correction is to be made. The second word is the correction. The address word should be only three Hex characters long. The correction word must be ten Hex characters long. The last set should be followed by a word of all F characters which can be only three Hex characters long. All words are separated by a single space and the last word is followed by a single space. The first of the two word sets must be 65E followed by 25069200AC.

IX. Preparation of name code word.

When curve plotter output is requested, five spaces in the title of the pictures taken will be filled with the name, initials, or some other identification of the person for whom the problem is run. Note I-6 indicates when this identification should be entered into the code. The code word for the identification consists of five groups of two Hex characters making a word ten characters long. Each of the groups of two characters represents a number, letter, or

other symbol as given in Table 5. For example the code word 1318170E1C will cause the name JONES to be reproduced in the title of the curve plotter output.

X. Preparation of problem parameter tape.

The problem parameter tape consists of a series of words on paper tape each of which is ten characters long. These words are separated by a single space except as noted in Table 6. The problem parameter tape contains all the information necessary to run a particular problem including the initial conditions and type of output. Several of the words are code words which will set up certain initial conditions and the type of output. The description of these words are given below or in Table 6. Reference should be made to Fig. 1 for clarification of terms in Table 6. Those words which represent fractional numbers are of the form

$$\left\{\begin{matrix} 0 \\ F \end{matrix}\right\} \quad \text{XXXXXXXXX} \quad \text{representing} \quad \left\{\begin{matrix} + \\ - \end{matrix}\right\} \quad .\ \text{XXXXXXXXX}$$

Each of the characters in these words is a decimal number.

1. Instructions for preparation of the code word P-X indicated in Table 6.

The code word P-X is of the form

$$\underbrace{C_1}_{xx} \quad \underbrace{C_2}_{xx} \quad \underbrace{C_3}_{xx} \quad \underbrace{C_4}_{xx} \qquad A_2 0.$$

This code gives the desired problem code number that will appear on the curve plotter output and also the type of

Table 5. Hex Code for Numbers, Letters, or Other Symbols Which May be Reproduced on the Curve Plotter

Hex Code	Symbol	Hex Code	Symbol
00	0		
01	1	20	W
02	2	21	X
03	3	22	Y
04	4	23	Z
05	5	24	Γ
06	6	25	Δ
07	7	26	π
08	8	27	Ψ
09	9	28	Ω
0A	A	29	Σ
0B	B	2A	α
0C	C	2B	β
0D	D	2C	γ
0E	E	2D	∂
0F	F	2E	δ
10	G	2F	ϵ
11	H	30	E
12	I	31	θ
13	J	32	λ
14	K	33	u
15	L	34	σ
16	M	35	ϕ
17	N	36	ω
18	O	37	Space
19	P		
1A	Q	49	.
1B	R	4A	,
1C	S	4B	:
1D	T	4C	!
1E	U	4D	?
1F	V		

Table 6. Input Paper Tape Problem Parameters

P-X	$\overbrace{xx}^{C_1}\ \overbrace{xx}^{C_2}\ \overbrace{xx}^{C_3}\ \overbrace{xx}^{C_4}\ A_2C$	See Note X-1.
P-0	$A_1 00000 C_1 C_2 C_3 C_4$	See Note X-2.
P-1	$\delta_A \cdot 10^{-9}$	where δ_A is the span of detector azimuth angle intervals. (δ_A = 5, 10, 15, 30, 45, 90, 180 deg)
P-2	$\delta_p \cdot 10^{-9}$	where δ_p is the span of detector polar angle intervals. (δ_p = 5, 10, 15, 30, 45, 90, 180 deg.)
P-3	$N \cdot 10^{-9}$	where N is the number of sample neutrons. ($1 < N < 100{,}000$.)
P-4	$E \cdot 10^{-2}$	where E is the energy of the source neutrons. ($0.025 \cdot 10^{-6} < E < 15$ Mev.)
P-5	$E_c \cdot 10^{-2}$	where E_c is the cut off energy below which the neutrons are not followed. ($E_c < E$ Mev.)
P-6	$J \cdot 10^{-9}$	gives a surface source which emits neutrons per steradian equal to $J + 1/2\pi \cos^J\theta$ where θ is measured from the normal to the surface. ($0 \leq J \leq 14$.)
	FFFFFFFFFF	gives a monodirectional source.
P-7	$d \cdot 10^{-9}$	where d is the diameter of the black source sphere. ($0 \leq d \leq 10^3$ cm.)
P-8	$g \cdot 10^{-5}$	where g is the source-detector separation distance. ($10^{-2} \leq g \leq 10^5$ meters.)

Table 6 (cont.)

P-9	$\theta_o \cdot 10^{-9}$	where θ_o is the angle at which the normal to the surface at the source points with respect to the source detector axis. ($0 \leq \theta_o \leq 180$ deg.)
P-10	ρ_A	where ρ_A is the density of the dry air usually found in nature (gms/cm^3).
P-11	ρ_W	where ρ_W is the density of the moisture usually found in air (gms/cm^3).
P-12	$K \cdot 10^{-9}$	where K is the number of equal energy intervals between E and E_c. See Table 7 for maximum values.
P-13	$L \cdot 10^{-9}$	where L is the maximum number of collisions the neutron can make before it is no longer followed. ($1 \leq L$.)
	FFFFFFFFFF	allows any number of collisions.

Put a CR symbol here for the end of the tape unless it is desired to start with a special random number in which case use a single space and make P-14 the special random number.

P-14		Initial random number (Hex number) from the sequence of congruentially generated numbers.
	CR symbol.	

Table 7. Maximum Number of Equal Energy Intervals

δ_p \ δ_A	180	90	45	30	15	10	5
180	373	186	93	62	31	20	10
90	186	93	46	31	15	10	5
45	93	46	23	15	7	5	0
30	62	31	15	10	4	0	0
15	31	15	7	4	0	0	0
10	20	10	3	0	0	0	0
5	10	1	0	0	0	0	0

output desired. The problem number is limited to four characters (either numerals 1 through 9 or letters A through F) given by $C_1C_2C_3C_4$. In the code word it will take two Hex digits to represent each of the C values. The Hex code is given in Table 5. If the number to be used has less than four digits, fill the remaining C values with the code ,37, for a space. The characters $C_1C_2C_3C_4$ should be the same as in the code word P-0. The value of A_2 determines the type of output as given below. For convenience the output which gives the number of neutrons entering a particular solid angle interval and energy interval will be called a flux output; the dose rate data output will be designated Dose 1 and Dose 2 as defined in Chapter II. See Note XI for a description of the output.

Value of A_2	Type of output.
0	Curve plotter output only.
2	Paper tape output of the flux through the second line of F's and, in addition, curve plotter output.
4	Complete paper tape output of the flux, and in addition, curve plotter output.
8	Complete paper tape output of the flux only.

2. Instructions for the preparation of the code word P-0 indicated in Table 6.

The code word P-0 is of the form

$$A_1 00000 C_1C_2C_3C_4$$

This code word will appear as the first word in the output. The C values should correspond to the values selected in the code word P-X. If any C value is chosen as a space in constant P-X, make it a zero in P-0. The digit A_1 determines the type of problem to be calculated as given below. For each of the different types of problems to be run there are certain conditions placed on the input parameters. These are listed in Notes X-3, X-4, X-5, and X-6.

Value of A_1	Type of problem
0	The medium is air (see Note X-3).
2	The medium is air. The source is a point isotropic source (see Note X-4).
4	The medium is H_2O (see Note X-5).
8	The medium is H_2O. The source is a point isotropic source (see Note X-6).

3. Input for the case $A_1 = 0$, medium: air, source: normal.

   In this case the input parameters are prepared as shown in Table 6.

4. Input for the case $A_1 = 2$, medium: air, source: point isitropic.

   In this case the input parameters are prepared as shown in Table 6 with the exception of the following parameters which are fixed:

P-6	0000000000
P-7	0000000000

5. Input and output for the case $A_1 = 4$, medium: H_2O, source: normal.

In this case all D values, and all energy and number flux data in the output are to be multiplied by 100 to get correct values. The input parameters are prepared as shown in Table 6 with the exception of those shown below.

P-7	$d \cdot 10^{-8}$	where d is the diameter of the black source sphere ($100 \geq d \geq 0$ cm)
P-8	$g \cdot 10^{-4}$	where g is the source-detector separation distance ($10^{-3} \leq g \leq 10^{4}$ meters)
P-10	0000000000	
P-11	$\rho_W \cdot 10^{-1}$	where ρ_W is the density of the water ($1.1 \geq \rho_W \geq 0$ gms/cm^3)

6. Input and output for the case $A_1 = 8$, medium: H_2O, source: point isotropic.

In this case all D values and all energy and number flux data in the output are to be multiplied by 100 to get correct values. The input parameters are to be prepared as shown in Note X-5 with the exception of the following which are fixed:

P-6	00000	00000
P-7	00000	00000

XI. Output

The output consists of three separate sets of data each of which is arranged in a tabular form as shown in Table 8. The first output

Table 8. Output Format

P-0	P-1	P-2	P-3
P-4	P-5	P-6	P-7
P-8	P-9	P-10	P-11
P-12	P-13	Initial Random No. (Hex)	Final Random No. (Hex)
FFFFFFFFFF	FFFFFFFFFF	FFFFFFFFFF	FFFFFFFFFF
M-1	M-2	M-3	M-4
M-5	M-6	M-7	M-8
M-9	M-10	M-11	M-12
M-13	M-14	M-15	M-16
M-17	M-18	M-19	M-20
M-21	M-22	M-23	M-24
FFFFFFFFFF	FFFFFFFFFF	FFFFFFFFFF	FFFFFFFFFF
D^p_1	Std. Dev. on D^p_1	AAAAAAAAAA	AAAAAAAAAA
D^p_{11}	AAAAAAAAAA	AAAAAAAAAA	AAAAAAAAAA
D^p_{111}	D^p_{112}	D^p_{113}	D^p_{114}
⋮	⋮	⋮	⋮
D^p_{11K-1}	D^p_{11K}	BBBBBBBBBB	BBBBBBBBBB
D^p_{12}	AAAAAAAAAA	AAAAAAAAAA	AAAAAAAAAA
D^p_{121}	D^p_{122}	D^p_{123}	D_{124}
⋮	⋮	⋮	⋮
D^p_{12K-1}	D^p_{12K}	BBBBBBBBBB	BBBBBBBBBB
⋮	⋮	⋮	⋮
FFFFFFFFFF	FFFFFFFFFF	FFFFFFFFFF	FFFFFFFFFF
D^p_2	Std. Dev. on D^p_2	AAAAAAAAAA	AAAAAAAAAA
⋮	⋮	⋮	⋮
FFFFFFFFFF	FFFFFFFFFF	FFFFFFFFFF	FFFFFFFFFF

has been termed the flux output and gives the number of neutrons entering a particular solid angle and energy interval. The second output is termed the Dose 1 output which gives the tissue dose rate using the conversion factors calculated in a manner similar to those calculated by Hurst and Ritchie.[10] The third output is termed the Dose 2 output which gives the tissue dose rate using conversion factors calculated by Snyder.[11] Chapter II gives more detail on the methods of calculating the Dose 1 and Dose 2 output.

As described in Note X-1, the output can be obtained on paper tape which should be printed four words to a line as in Table 8, or it can be obtained on the curve plotter. When paper tape output is requested, it is only possible to get the flux output; however, if curve plotter output is requested, all three sets of data will be put on the curve plotter.

The numbers that appear on the output are of two forms. The decimal fraction (d.f.) numbers are of the form

$$\begin{Bmatrix} 0 \\ F \end{Bmatrix} \text{XXXXXXXXXX} \quad \text{representing} \quad \begin{Bmatrix} + \\ - \end{Bmatrix} .\text{XXXXXXXXXX}$$

The decimal floating point (f.p.) numbers are of the form

$$\begin{Bmatrix} 0 \\ F \end{Bmatrix} \text{XXXXXX} \begin{Bmatrix} 0 \\ F \end{Bmatrix} \text{yy} \quad \text{representing} \quad \begin{Bmatrix} + \\ - \end{Bmatrix} .\text{XXXXXX} \cdot 10^{\begin{Bmatrix} + \\ - \end{Bmatrix} \text{y y}}$$

Table 8 gives the format of the output for all three sets of data. The data is separated into sections by a line of F's, the A's and B's

are used as fillers to maintain the organization of the data in the table. The first section marked off by a line of F's is the input data. The second section contains total quantities that will be described below. The remaining sections marked off by lines of F's contain the energy and angular distribution of the neutrons or dose rate as the case may be within each of the polar angle intervals about the detector point. Within each section marked off for each polar angle interval is given the total number of neutrons entering the particular interval followed by subsections for each azimuthal angle interval. In the subsections is given the total coming into the azimuthal angle interval followed by the energy spectra in the particular azimuthal angle interval.

In Table 8 the P quantities in the first section are the same as those put on the problem parameter tape and described in Note X. The remaining quantities have the following meaning:

M-1 Flux at the detector contributed by uncollided neutrons normalized to one source neutron per second (f.p.). When the source is monodirectional and θ_o is zero then the contribution by uncollided neutrons is a (d.f.) number.

M-2 Cosα at which the uncollided neutrons reach the detector (d.f.). The angle α is the polar angle at the detector as indicated in Fig. 1.

M-3 Fraction of source neutrons degraded below the cut off energy E_c per second (d.f.).

M-4 See below.

M-5 Flux at the detector contributed by neutrons which have had at least one collision normalized to one source neutron per second (f.p.).

M-6 Standard deviation on M-5 (f.p.).

M-7 Energy flux at the detector contributed by neutrons which have had at least one collision normalized to a unit energy released at the source per second (f.p.).

M-8 Standard deviation on M-7 (f.p.).

M-9 Fraction of source neutrons escaping the sphere of air about the detector point (d.f.).

M-10 Fraction of the source energy escaping the sphere of air about the detector point (d.f.).

M-11 Blank.

M-12 Blank.

M-13 Fraction of M-5 contributed by 1st collision neutrons (f.p.).

M-14 Fraction of M-5 contributed by 2nd collision neutrons (f.p.).

M-15 Fraction of M-5 contributed by 3rd collision neutrons (f.p.).

M-16 Fraction of M-5 contributed by 1st, 2nd, and 3rd collision neutrons (f.p.).

M-17 Fraction of M-7 contributed by 1st collision neutrons (f.p.).

M-18 Fraction of M-7 contributed by 2nd collision neutrons (f.p.).

M-19 Fraction of M-7 contributed by 3rd collision neutrons (f.p.).

M-20 Fraction of M-7 contributed by 1st, 2nd, and 3rd collision neutrons (f.p.).

M-21 Total number of collisions x 10^{-9} (d.f.).

M-22 Total number of collisions with nitrogen x 10^{-9} (d.f.).

M-23 Total number of collisions with oxygen x 10^{-9} (d.f.).

M-24 Total number of collisions with hydrogen x 10^{-9} (d.f.).

D^p_{jik} (See below) is the quantity in the kth energy interval of the ith azimuthal angle interval of the jth polar angle interval. $k = 1$ represents the highest energy interval.

The flux output will differ from that given above only in the spaces indicated below. Here $D^p_{jik} = D_{jik}$.

M_4 Blank

D_{jik} = the fraction of the source neutrons per cm^2 in the kth energy interval of the ith azimuthal angle interval of the jth polar angle interval.

$D_{ji} = \sum_k D_{jik}$ = the fraction of the source neutrons per cm^2 in the ith azimuthal angle interval of the jth polar angle interval.

$D_j = \sum_i \sum_k D_{jik}$ = the fraction of the source neutrons per cm^2 in the jth polar angle interval.

The Dose 1 and Dose 2 output will differ from that given above only in the space indicated below. Here D^p_{jik} D^1_{jik} for the Dose 1 output and D^p_{jik} D^2_{jik} for the Dose 2 output. The method of calculating all D^p values is given in Chapter II. The dose rate is in units of rep/hr per source neutron/sec for Dose 1 output and rem/hr per source neutron/sec for Dose 2 output.

M-4 = D^p = total dose rate for an infinitesimal meatball detector of tissue at the detector point. This does not include the dose rate contributed by the direct beam.

D^p_{jik} = dose rate/steradian, Mev in the kth energy interval of the ith azimuthal angle interval of the jth polar angle interval.

D^p_{ji} = dose rate/steradian in the ith azimuthal angle interval of the jth polar angle interval.

D^p_j = dose rate/steradian in the jth polar angle interval.

Figures 23, 24, and 25 are examples of all three sets of data from the same problem. In the particular problem shown in Figs. 23, 24, and 25 it was impossible to complete the table as given in Table 8 on one picture so it was continued on the next picture. Each picture in each set of data has the same title and a page number. The numbers run consecutively. In this problem the name entered into the code was ZERBY as indicated in Note I-6. The number 323 is the registered number of the code at the Mathematics Panel of Oak Ridge National Laboratory. The word Flux, Dose 1, or Dose 2 appears in the title to describe the set of data carried on the picture. The problem number 1B3A was entered into the code as part of the input word P-X. The date was entered into the code as described in Note I-10.

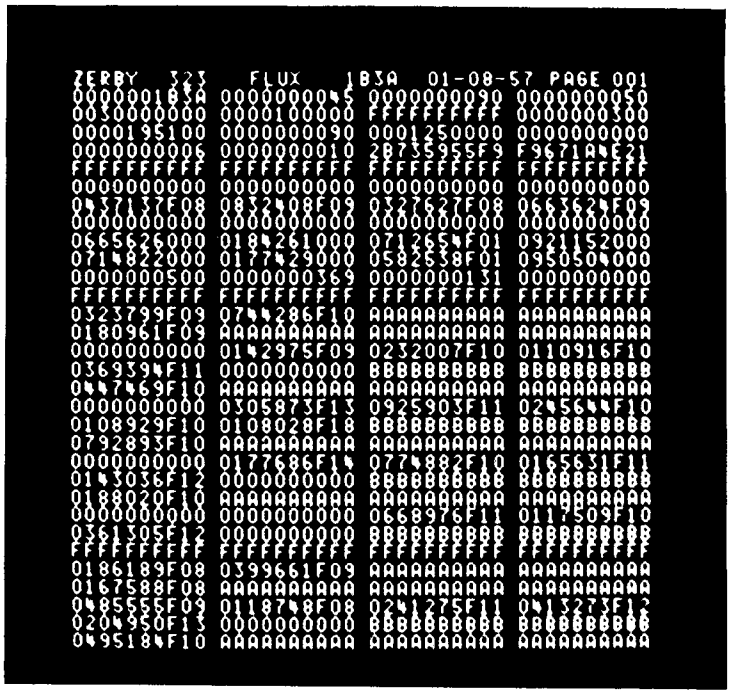

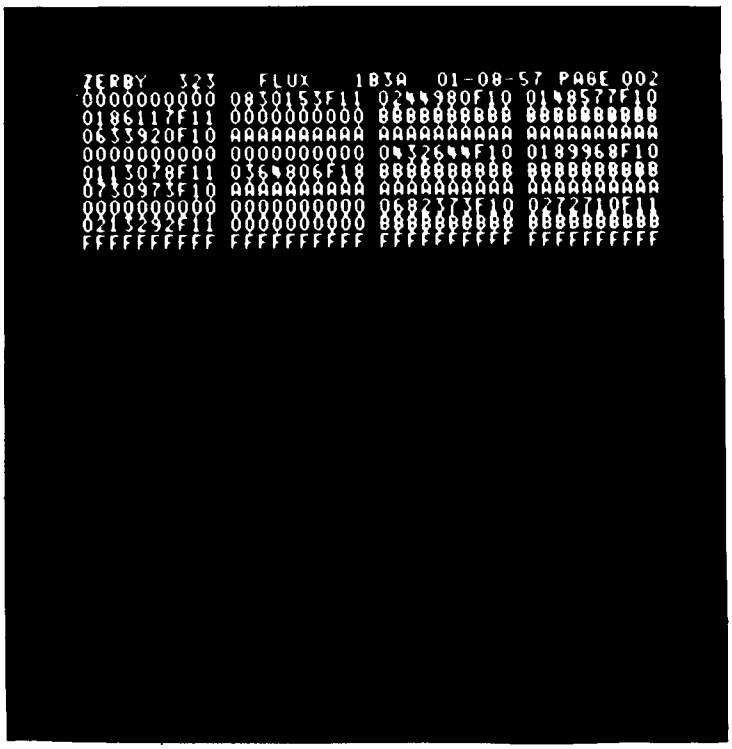

Fig. 23. Sample Curve Plotter Output of the Flux Data

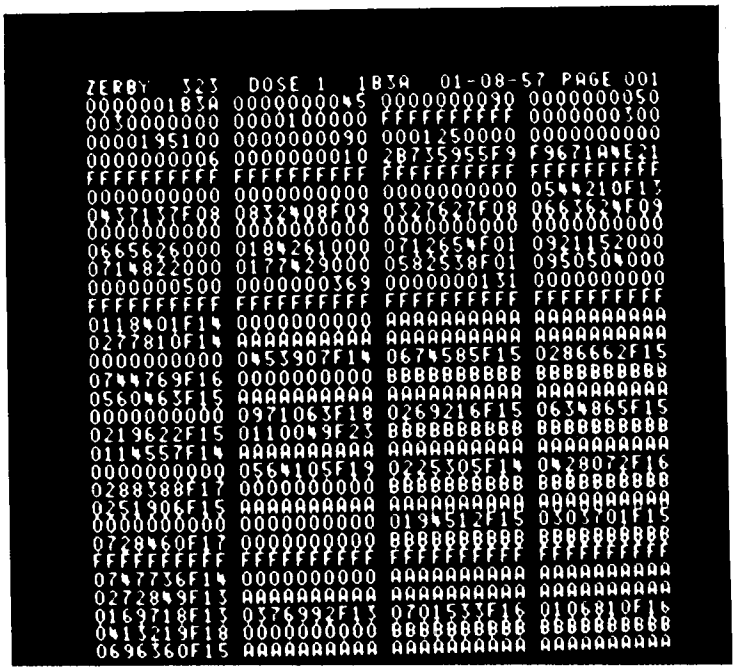

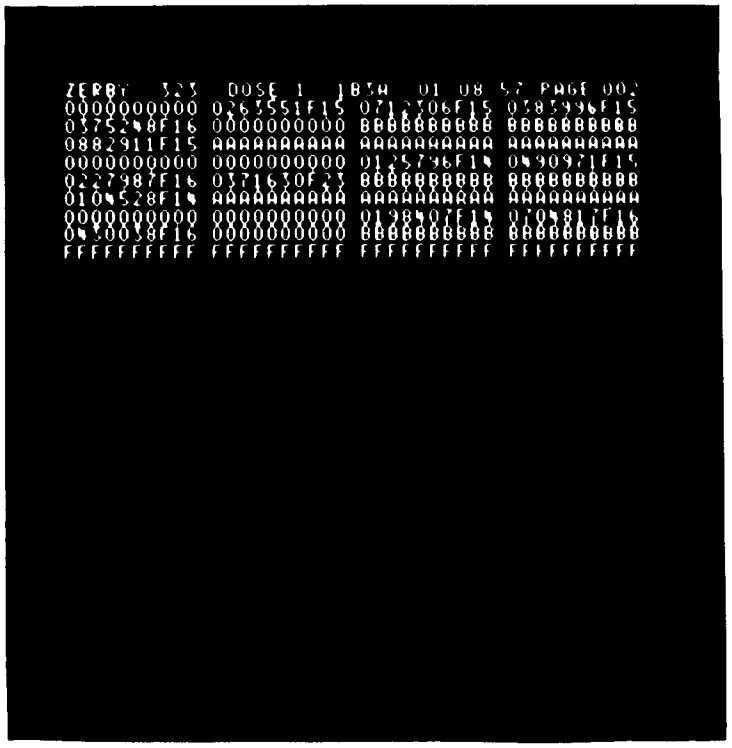

Fig. 24. Sample Curve Plotter Output of the Dose 1 Data

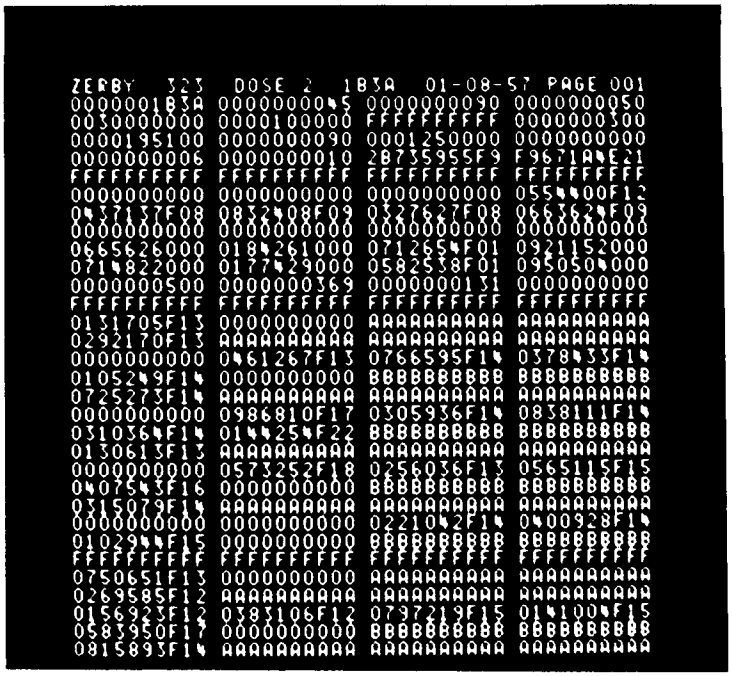

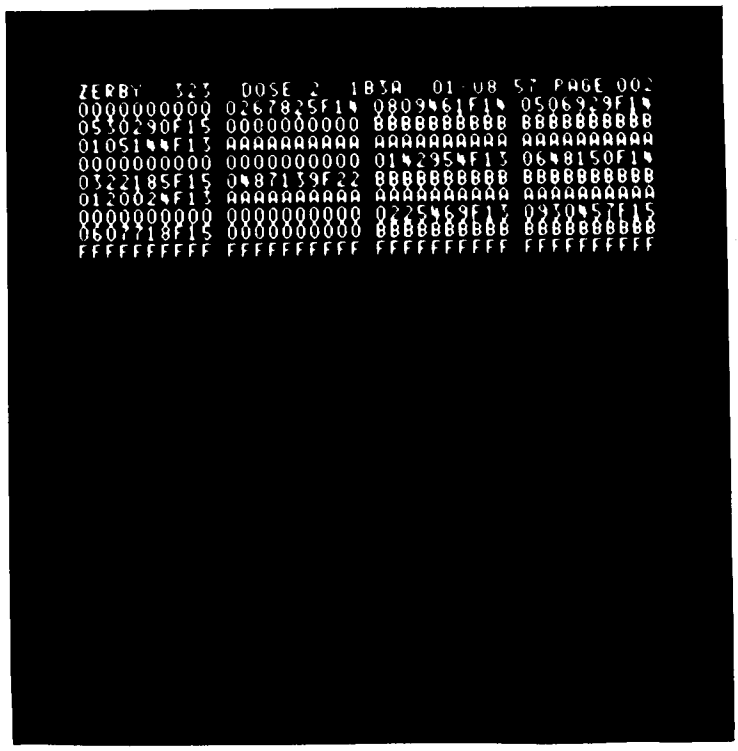

Fig. 25. Sample Curve Plotter Output of the Dose 2 Data

VII. The ORACLE Code

The ORACLE code consists of five tapes which are combined into two rolls of paper tape. The first roll (Roll 1) has the first four of the tapes on a continuous paper tape and the second roll (Roll 2) has the last tape. Each tape ends with a single space followed by a Carriage Return symbol (35). The following pages are printed copies of the code where an address is given in the left hand column to indicate the location of the code word immediately to the right of the address when the code is in the fast memory. After the last word on each tape is written the letters CR to represent the Carriage Return symbol.

In operation the code uses all four magnetic tape drives.

Roll 1

Tape 1

700 6070040080 a070043702 9000043703 6070340800
a300043705 6070540700 a000043707 9000043708
6070840080 a30004370a 6070a40011 af0004370c
6070c40080 a00004370e 900004370f 6074e40000
710 000004374b 6071140400 a000043713 6071340010
ae00000000 907fa43716 6071640800 a100043718
6071840010 ad0004371a 6071a40800 a00004371c
0000040000 947f043743 6071e40400 b27fa41749
720 247f05c131 6072140008 ae00043723 6072340400
a27fa43725 6072540008 ae00043727 6072740800
b100043729 436f400000 0000000000 0000000000
6072c40700 b00004372e 6072e40800 a300043730
730 6073040080 b000043732 6073240080 a300043734
6073440011 af00043736 6073640400 b000043738
6073840400 a20004373a 6073a40008 ae0004373c
6073c40800 b00004373e 6073e40800 a100043740
740 6074040010 ad0004371c 3900003719 1b010247fd
1b00412004 1b00412010 207425f7f1 607f01b010
120185f7f0 4371e247f1 5f06e43720 7f13c40000
6074c40800 a200043711 3737373737 CR

Roll 1

Tape 2

7fa	ffffffffff	0000100001	4000000000	0000000000
	8000000000	0000000001	6000040010	af00043002
	6000240080	b140043004	2440051089	5108f24401
	5108b51091	4308900000	000006009b	2400943142
00a	6009c40000	2400b43142	6009d40000	2400d43142
	2409e18027	3b0d37f0d6	2409e18027	3b0d47f0d7
	240d418027	3b09f7f0d8	600a040000	2401543152
	600a140000	2401743152	2401843168	000ed000ed
01a	000ee000ee	000d5000f0	000d3000f1	807ff000ef
	2401e43100	0f010ef0db	0ed20ab0d9	0ee20ab0da
	0f110ef0dc	0d940da0f2	0f210db0dd	8ac10dc0de
	247fd5f217	16000240d5	180025f0df	7f0e0270e0
02a	4a02d240df	200a212002	5f0e14302f	240df207ff
	120025f0e1	600e1380d6	247fd1c001	7f0f2240f2
	200a35f0e2	4303600000	247fd5f430	247fd5f431
	2403643330	4000040000	247ff5f0e7	2403943168
03a	000e7000f6	807ff000ef	2403c43100	0f610ef0e8
	0ef10ef0f7	0e840f70f8	0e820dd0e9	0d940e90e9
	0f820dd0ea	8d940ea0ea	600a640000	24045431ba
	2404643100	a1a10dd0fa	247fd5f0e3	600e3380e2
04a	1b0275f0f3	240e7227ff	5f0ec270ec	4b05340000
	240f320034	5f051240f3	200355f052	247fd5f458
	247fd5f459	600d8380e3	1b027200a5	5f0f412010
	200f4200d8	1200c203f8	5f05a40000	2405943100

Roll 1

Tape 2 continued

05a	38a43e40e4	0de10e40e5	8ad20e40fe	247ff5f0e6	
	240e6227ff	1c028380e1	1b027200f3	5f0f540000	
	270ec4b066	240f5203f0	5f06540000	247fd5f46c	
	240f5200e7	5f0f9203f1	5f078240f9	1201c203f2	
06a	5f071240f3	1200c200f3	203f35f075	240f51200c	
	200f5203f4	5f07740000	2407043100	47120fa0fb	
	0fb8417417	0fb8417417	0fb10fe097	0978458458	
	0fb20e5097	097846c46c	89710dd471	240d6220e6	
07a	5f0fd270fd	4a07e40000	240e6207ff	5f0e64305e	
	240d7227ff	220e35f0ff	270ff4a083	240e3207ff	
	5f0e343049	240d5220e7	5f0fc270fc	4a08840000	
	240e7207ff	5f0e743039	4309400000	6008940000	
08a	b140041008	6008b40000	ad00041008	2408d4321b	
	0041700417	6008f40000	a140043091	6009140000	
	ad000433fe	0000000150	2409443390	4308d00000	
	0000000000	9a79b3c70f	0000000113	9443043006	
09a	9440143005	244015f0d3	244025f0d4	2440c5f0d5	
	00000000b4	0000000005	244045f0ed	244055f0ee	
	0000000002	0000000008	0000000004	00000000ae	
	240e9432c6	6041784417	6040084400	6043084430	
0aa	6041884418	0763ffffff	0672977319	026487e7c1	
	007ffffffff	007f832767	007e0e410b	007ba39821	
	007847c30d	007401f751	006eda122f	0068d9e83f	
	00620d9945	005a82949b	005246f157	00496b11c7	

Roll 1

Tape 2 continued

0ba	ff7fffffff	ff6c30d307	ff578e9f6b	ff4242070b
	fe58e8a71d	fd59407897	826ce3ee77	fda6bf8769
	fea71758e3	ffbdbdf8f5	ffa8716095	ff93cf2cf9
	ff80000001	00b694ee39	00adb90ea9	00a57d6b65
0ca	009df266bb	00972617c1	009125edd1	008bfe08af
	0087b83cf3	00845c67df	0081f1bef5	00807cd899
	0080000001	000000005a	000000005a	0000000009
	0000000002	0000000002	0000000012	007fffffffd
0da	fd66666665	0448000001	075a000001	fd66666663
	fc477d1693	0000000002	4000000000	0000000010
	0000000028	0000000000	0000000000	a9630aa997
	0000000002	0000000003	0260000001	0059999997
0ea	0066666663	0000000000	0000000002	fa51eb851e
	f74189374c	da40000000	dd48000000	e05a000000
	0000000020	0000000000	00000000ae	0000000038
	db60000000	0140000001	0240000001	000000003a
0fa	f24ea4a385	f24ea4a385	0000000007	0000000000
	5952b66f55	0000000000	207fb54101	2405b5f13e
	5111116001	1b00754108	1b00471105	5f13f240de
	1c0207f13a	5f13b16000	240e41c020	7f13c5f13d
10a	2413f49120	120024911f	1200149135	1200149116
	2513a43130	6013a2413b	1b01f607fa	1b0015f0e5
	4f14024101	207fb54101	2413e4a101	2410154116
	430482713c	481232713a	481112513a	2313c4b11d

Roll 1

Tape 2 continued

11a	2413a14001	5f13a2413b	207ff5f13b	2413a3a13c
	2413b2213d	431102613c	5f13c2713a	4b1246013c
	2413d1b020	4111100000	2713c4a10f	2413b2213d
	4812a5f13f	2413a6013c	5f13c7f13a	2413d5f13b
12a	2613f5112c	221394a10f	2413c14003	2013a4e130
	1c0292413b	207ff43110	5f13a2713a	481112413a
	120014f10f	5f13a2413b	227ff5f13b	411312413b
	2013d5f13b	6013a3813c	5f13a41130	0000000020
13a	477d169300	ffffffffc	0000000000	0000000000
	0de10e40e5	10e40e5000	4a139247fd	4111100000
	207fb54150	7c1447314f	2440c5f7f2	247ff1e003
	5f7f87f7f5	607f21a004	247fd1b001	207f51b002
14a	207f51b001	5f7f5247f8	227ff5f7f8	4a148247f2
	49150247f5	401425f0d5	4300e267f5	4114f00000
	207fb54166	731657c154	244055f7f1	267ff16003
	7f7f55f7f2	607f11a004	247fd1b004	207f55f7f8
15a	12002207f8	120015f7f5	247f2207ff	5f7f24b158
	247fd1b004	207f55f7f8	607f838167	1b00b207ff
	100015f7f2	247f14a165	267f241165	247f25f0ee
	4301800000	44b82fa09b	207fb54169	2403c5f7f1
16a	5416b51178	247ff5f7f2	277f248178	247fd5f7f9
	247f212001	4f1725f7f2	247f9227ff	5f7f94316e
	267ff12008	207f24e177	247f214001	5f7f2247f9
	207ff5f7f9	607f2247f9	1b0205f0ef	24169207fb

Roll 1

Tape 2 continued

17a	541695417c	247f14a169	4303c00000	207fb5417f
	207fb541b2	24361511b5	14014511b0	43338607f1
	277f1481b0	1b01c1200c	5f7f27f7f1	1a004247fd
	1b0045f7f3	12002207f3	120015f7f3	247fd1b004
18a	207f35f7f3	247f14a18d	267f35f7f3	607f3381b9
	1b002207ff	5f7f41b028	10001207fe	5f7f1607f1
	391b85f7f1	267fb14010	5f7f0267f1	5f7f31c027
	3b7f01a001	1c001247f0	207ff7f7f1	4a19b5f7f0
19a	387f341195	247f216004	7f7f57f7f3	180247f7f6
	207f55f7f5	247f3207ff	5f7f3221b6	4a1a5247f5
	16002207f5	160015f7f5	247f64319d	607f5381b7
	1b00a5f7f5	247f24a1a9	267f55f7f5	607f5387f1
1aa	1b0014f1ae	5f7f5247f4	227ff5f7f4	247f5431aa
	1c029247f4	1b01f607fa	1b0015f478	241b0221b5
	4a362241b0	207ff5f1b0	4318100000	1b0015f478
	0000000009	44b82fa09b	58b90bfbe9	6a4d3c25e6
1ba	207fb541eb	7c1be241be	207fb5c1bf	207fb5c1c0
	240e95f212	240ea5f213	240eb5f214	711d3401ba
	241c243100	a134212215	262144b1c7	241e4201f1
	5f1e4431cd	5f21624214	511c9267ff	401ba12000
1ca	207ff5f217	2421612020	202155f215	160007f21a
	160007f219	261f05f216	241d043100	1f22215218
	a1882127f1	241d3432c6	241d443100	20227f1218
	a188219219	241d5201ef	5f1d5241d1	201ef5f1d1

Roll 1

Tape 2 continued

1da	24216207ff	5f2164b1d0	241ed5f1d1	241ee5f1d5
	241de43100	2152219218	218821a21a	a158212212
	24217207ff	5f2174b1ce	411e4241e4	201f15f1e4
	241e643100	a134212215	431ce241e4	221f15f1e4
1ea	2421a401ba	4304600000	0000000000	1f22215218
	20227f1218	0010000000	0000000010	0000400000
	f956d3d9b3	fb7182a67a	fd44cbfcaf	fd7d3ba226
	fe61d2dcc9	ff455fb4cb	ff5bf46a33	ff73d6a14d
1fa	004614af5a	005205cae6	005d50259a	00678b48ce
	0070588bbb	007766806a	007c73eacc	007f52584d
	fa6f376ad3	fb7f7ec68b	fc61713b9e	fc7f9ebcaf
	fd4c97d86f	fd569baeed	fd5d7e31e0	fd60ffaba0
20a	fd60ffaba0	fd5d7e31e0	fd569baeed	fd4c97d86f
	fc7f9ebcaf	fc61713b9e	fb7f7ec68b	fa6f376ad3
	0066666663	0066666663	0000000000	fd66666661
	0000000000	0000000003	eb64a9c709	ee7dd438d3
21a	eb64a9c709	207fb5421d	207fb54251	2421b5421f
	1601454254	2421b1c020	7f7f01c028	38258207ff
	5f7f11b028	10001207fe	5f7f2607f2	392595f7f2
	267fb14010	5f7f3267f2	5f7f41c027	3b7f31a001
22a	1c001247f3	207ff7f7f2	4a22e5f7f3	387f441228
	607f2397f2	5f7f4607f4	397f45f7f2	607f2397f0
	5f7f012002	207f012001	4d2365f7f0	247f1227ff
	5f7f1247f0	49238607fd	43239607fa	257f020257

Roll 1

Tape 2 continued

23a	4e23e247f1	207ff5f7f1	247fc10002	1a01843244
	5f7f026255	5f7f2257f0	14002217f0	1a00410001
	5f7f0247f2	207ff4b23f	247f14b246	247fd41246
	247fa1b004	7f7f216000	7f7f4257f1	222564924c
24a	5f7f1247f4	207ff5f7f4	41248247f4	12004217f1
	12020607f2	1b0084325a	2421f22254	4a21b2421f
	207fb5421f	4321f00000	2421b1c020	0000000006
	000000000a	00000431be	268826a13f	49aec6eed6
25a	2421f5425b	7f00043250	207fb5425e	207fb54283
	602e57425f	2431071282	587f816009	777f87f7f6
	1c002207fc	5f7f4207fe	1b0013b7f4	7f7f47f7f9
	397f41c002	5f7f7247ff	20284537f6	607f7397f9
26a	5f7f91c027	3b7f67f7f5	277f54a26f	207f45f7f4
	247f643268	277f85f7f7	4827724285	5f7f7607f8
	382865f7f8	1b0014f277	5f7f8247f7	227ff5f7f7
	247f843273	247f751278	247f41c004	207f84d27f
27a	5f7f816021	4c282247f8	160014d283	5f7f8247f7
	227ff5f7f7	4127b14001	5f7f8247f7	207ff607f8
	1c0087f2f8	432e6247f7	4128100002	0000000007
	58b90bfbff	207fb542bb	74289712ba	242fe16000
28a	1c0205f7f6	7f7f4257f6	222bd49291	247f64828f
	607fc247ff	432ba247f4	482bd247fd	412ba257f4
	4c295267fc	5f7f4247f6	207ff5f7f6	4128b5f7f1
	247ff12001	207f64829d	5f7f6267f6	5129c602c1

Roll 1

Tape 2 continued

29a	397f15f7f1	607f1247fd	5f7f61c000	432aa512a6
	512a9602c1	387f15f7f7	120011c001	7f7f6602bc
	397f1207f6	5f7f14c2a5	247f7207ff	5f7f7607f7
	247fd1b006	4d28f5f7f6	247f112001	607f71b006
2aa	247f44b2ae	247ff1d001	207f65f7f6	392c0412b0
	267f65f7f6	120011c001	392bf5f7f7	262be5f7f9
	247f71c027	3b7f91b028	227fe5f7f8	247f9207ff
	4a2b95f7f9	607f7387f8	412b200000	607f8247f6
2ba	1b0205f2ff	432ed00000	3700000000	0000000006
	0000000011	58b90bfbe9	a746f40417	5c551d94ae
	10dd0fafff	1b03c542c5	160094b7fd	94fff942c2
	207fb542ee	247ff5f2f1	24300202f1	5f2f21201c
2ca	203f55f2cc	242cb43100	b0247f12f3	242f312009
	4a2d1242f1	207ff5f2f1	432c8402c6	242f212010
	202f2227ff	1200c203f7	5f2d9242f2	227ff1200c
	203f65f2d8	242d743100	7f113012f5	b0213012f6
2da	24301202f1	227ff12014	542e3207fb	542e5402c6
	242de4325c	002f5002f9	242e04325c	002f6002fa
	242e24325c	0030f002f7	242e44325c	00310002f8
	242e643100	2f842f72fb	2f912fa2fc	2fb22fc2fd
2ea	af782fd2fe	602ef402c6	242ec43287	242ff5f7f1
	431d400000	002fe002ff	0000000000	0000000001
	0000000302	0099aaf765	0000000000	01e66ac08d
	e8e5281023	049c0cc9ca	049c0cc9ca	fe5d4abe3d

Roll 1

Tape 2 continued

2fa	05bb7262d7	0000000000	faa8e78181	0000000000
	049c0cc9cb	ee7dd438d1	0000000301	000000030f
	e76b5fca6b	f368db8bad	f951eb851f	fb51eb851f
	fd66666667	ff7fffffff	007fffffff	024fffffff
30a	034fffffff	0377ffffff	044fffffff	0463ffffff
	0477ffffff	ee7dd438d2	ee7dd438d2	ef512e19e9
	ef4a045d6b	f04bccf681	f17dd44135	f357619cc5
	f4477e775d	f44189374b	f4477e775d	f44ea4a8c1
31a	f44ea4a8c1	f4612af965	f4703b961d	0000000000
	0000000000	0000000000	0000000000	0000000000
	0000000000	0000000000	0000000000	0000000000
	0000000000	0000000000	0000000000	0000000000
32a	0000000000	0000000000	0000000000	0000000000
	0000000000	0000000000	207fb54334	247fd5f373
	240d722373	5f37427374	4a03740000	600e238373
	1b0275f375	4334000000	241b051339	4000024000
33a	5f7f141181	207fb5f33f	944584333d	944594333e
	9445a4333f	9445b43340	247fd5f376	240d622376
	5f37740000	273774b350	4334e00000	120142036f
	227fb5f34d	227fb5f34c	227fb5f34b	227fb5f34a
34a	9447c4334b	9447d4334c	9447e4334d	9447f4334e
	24373207ff	5f37343332	600e138376	1b02720375
	5f3784335b	203705f357	207fb5f358	207fb5f359
	207fb5f35a	9446c43358	9446d43359	9446e4335a

Roll 1

Tape 2 continued

35a	9446f4335b	24378200d5	2037153379	5f36124378	
	1201420361	5f36140000	243604317d	0047000478	
	4336600000	220d55f37a	4000040000	2737a4b368	
	24376207ff	5f37643341	24379207ff	5f37912014	
36a	203725f36b	9447b4336c	2437a227ff	5f37a43365	
	944304333d	944304334f	9443443358	0043800437	
	940004336c	0000000002	0000000000	0000000028	
	0000000002	0000000000	0000000038	000000047b	
37a	0000000000	0000000000	0000000000	0000000000	
	0000000000	0000000000	0000000000	0000000000	
	0000000000	0000000000	0000000000	0000000000	
	0000000000	0000000000	0000000000	0000000000	
38a	0000000000	0000000000	0000000000	0000000000	
	0000000000	0000000000	207fb54394	247fd5f3dc	
	240d7223dc	5f3dd273dd	4a00040000	600e2383dc	
	1b0275f3de	12014203de	203d65f39a	243994321b	
39a	0000000000	433a300000	203de203d7	5f3a0207fb	
	5f3a1207fb	5f3a240000	0000000000	0000000000	
	0000000000	247fd5f3df	240d6223df	5f3e040000	
	273e04b3b4	433b200000	5f3e112014	203e1203d8	
3aa	227fb5f3b1	227fb5f3b0	227fb5f3af	227fb5f3ae	
	0000000000	0000000000	0000000000	0000000000	
	243dc207ff	5f3dc43392	600e1383df	1b027203de	
	5f3e212014	203e2203d9	5f3ba5f3e3	243b94321b	

Roll 1

Tape 2 continued

3ba	0000000000	433c200000	207fb5f3bf	207fb5f3c0
	207fb5f3c1	0000000000	0000000000	0000000000
	243e2200d5	203db533e4	5f3c8243e2	12014203c8
	5f3c840000	243c74321b	0000000000	433cd00000
3ca	220d55f3e5	4000040000	273e54b3cf	243df207ff
	5f3df433a4	243e412014	203e4207fb	533e440000
	203da5f3d3	0000000000	243e5227ff	5f3e5433cc
	0043000430	6043184431	6043084430	0043400434
3da	6000084000	0043800437	0000000000	0000000000
	0000000000	0000000000	0000000000	0000000000
	0000000000	0000000000	0000000000	0000000000
	0000000000	0000000000	0000000000	0000000000
3ea	0000000000	0000000000	0000000000	0000000000
	0000000000	0000000000	247fd5f434	89710dd437
	43720fa0fb	0978430430	0978434434	80047f12f3
	7f110002f5	80010002f6	00040000e4	603f94001b
3fa	b3302433fb	603fb40011	af00024093	513ff43002
	603fe40800	b27fa43154	CR	

Roll 1

Tape 3

```
000  e76b610000 f368d50000 f741890000 fa51e50000
     fd66660000 0040000000 0140000000 0250000000
     0270000000 0350000000 0378000000 0450000000
     0478000000 d9445a0000 d9445a0000 e540420000
010  e84f9e0000 eb628f0000 ee51890000 ef67cf0000
     f04e770000 f06c290000 f142b00000 f1474c0000
     f1522d0000 f15a1d0000 f1651f0000 CR
```

Roll 1

Tape 4

```
7fa  ffffffffff 0000100001 4000000000 0000000000
     8000000000 0000000001 601357f7f9 4000040000
     601307f7f6 601317f7f5 247fd607f5 1b00412004
     1b0041200c 1b00412004 1b0042006d 5f7d52406e
00e  5f7d62406f 5f7d77f7d8 247d81f014 1f0047f7f4
     247f61f004 7f7f31f00c 1f00c7f7f2 1f00c7f7f1
     247f312020 5f7f020070 5802c5803f 247f020071
     5803d24072 5f7e6247f4 227ff227ff 4a01b24073
01a  5f7dc43027 227ff4801e 160007f7dc 240735f7dd
     43027227ff 4a02316000 7f7dc24074 5f7dd24075
     5f7de43027 160007f7dc 240765f7dd 240775f7de
     240785f7df 247ff5f7db 267f15f7da 240795f7e3
02a  267f25f7d9 6002b40080 b03004302d 2607a5f7e9
     2402e43058 267f45f7e8 2407b51032 247e12207c
     5f7e124000 5f7e016000 7f7e52407d 5f7e440000
     2403643089 24032207ff 5f032247d9 207ff5f7d9
03a  4b11e247da 207ff5f7da 4903e607db ac000c8000
     430006007e b0300430bb 247db207ff 5f7db247e9
     207ff5f7e9 4b045430cb 2404443058 247e12207c
     5f7e116000 7f7e02407f 5f7e4247e3 5f7ea240ab
04a  5f7e3247fe 5f7e57f7e8 2404c43089 240ad5f7e3
     240ae5f7e0 240af5f7e4 160007f7e5 2405143089
     247ea430b8 247e8207ff 5f7e849032 247e9207ff
     5f7e94b02f c80004382d 207fb5406c 240b05f7e1
```

Roll 1

Tape 4 continued

```
05a 160007f7e0 247e35f7ea 240b15f7e3 247f95f7e4
    247fe5f7e5 2405f43089 240b25f7e0 240b35f7e3
    240b45f7e4 2406343089 240b55f7e0 240b65f7e3
    240af5f7e4 160007f7e5 2406843089 247d8200b7
06a 5f7d8430be 247ea5f7e3 4300000000 0000390000
    3905063719 0a100e0000 b000000000 ac00000000
    0020000000 0000000200 0000000156 00000002ac
    c000000104 0000000208 000000030c 0000000300
07a 000000001f 00000007dc 0000000020 000000000a
    0000000080 0000000005 207fb54088 247e051086
    247e151084 247e220088 51085c1000 4000060000
    40000c3000 3800040000 43000000d0 207fb5409d
08a 267e45f7cb 4a09d247e5 4a08f240a2 51095240a3
    5f7ef43091 240a451095 240a55f7ef 267ef5f7f8
    247e351093 4000024000 5f7c9247c9 400001f000
    7f7e25f7c9 2409743080 247e0200a6 5f7e0247cb
09a 207ff5f7cb 4909d40000 2409c430a7 43000247f8
    207ff5f7f8 4909440000 240a0430a7 4309100000
    0000000008 0000000005 0000000004 000000000a
    0000000018 207fb540aa 247e3207ff 5f7e340000
0aa 4300000000 00000000ac 0b15180c14 00000007e6
    0000000090 0000000003 00000003e0 00000007d0
    0000000270 00000007d5 000000000d 00000003b8
    00000007d8 0010000000 5f7e3247e6 200b75f7e6
```

Roll 1

Tape 4 continued

0ba	4305300000	267f25f7d9	240795f7e3	4304000000
	1b00810004	220ca4b06b	7f7ee247ee	207ff5f7ee
	160001c008	7f7d8247d8	1b00410004	220ca4b06b
	7f7ee247ee	207ff16000	1c0047f7d8	4306b00000
0ca	0a00000000	2607a5f7e9	c800043844	0000000000
	0000000000	0000000000	7c82827c00	0002fe4200
	62928a4600	8cd2a28400	087e08f800	8c9292f400
	0c92927c00	c0a09e8000	6c92926c00	7c92926000
0da	7e88887e00	6c9292fe00	4482827c00	7c8282fe00
	829292fe00	809090fe00	5c92827c00	fe1010fe00
	0082fe8200	fc02020c00	824428fe00	020202fe00
	fe201820fe	fe1860fe00	7c82827c00	609090fe00
0ea	7e868a827c	629498fe00	4c92926400	8080fe8080
	fc0202fc00	e0180618e0	fe083008fe	8244384482
	c0201e20c0	c2b29a8600	c0808080fe	0e32c2320e
	203e203e20	7008fe0870	7a8680867a	c692aac682
0fa	320a3c423c	58a4a47e01	4020107886	7c92920c00
	0c92b24c00	222a2a1c00	8292543800	7c9292927c
	0618688482	f8301830fe	20203c221c	3844fe4438
	1c220c221c	0000000000	10107c1010	1010101010
10a	4428102844	1010541010	2828282800	5454545454
	1038541010	1010543810	0044281000	0010284400
	4020100804	008282fe00	00fe828200	0082827c00
	007c828200	106c828200	82826c1000	0000020200

Roll 1

Tape 4 continued

11a	00001c1200	0000121200	0000fa0000	40a09a8040
	247e322079	2207e4b053	240795f7e3	2402c58124
	247db207ff	5f7db6007e	0030043053	0000000000
	0000000000	0000000000	0000000000	0000000000
12a	0000000000	0000000000	0000000000	0000000000
	0000000000	0000000000	1000000001	0000001004
	0000000000	0000000000	0000000018	0000000018
	230e1b0b22	3737030203	3737370f15	1e21373737
13a	37370d181c	0e37013737	37370d181c	0e37023737
	0015800000	0015c00000	0016000000	c80002413e
	5403e247f0	5613024138	5f7d224139	5f7d3247f1
	5f13443164	601474000f	ae00043149	6014940800
14a	a27fa4314b	241365f7d0	241375f7d1	241345f7d4
	6014e40010	ae00043000	c80002413f	5403e2413a
	5f7d22413b	5f7d34314b	c800024140	5403e2413c
	5f7d22413d	5f7d34314b	6015840001	ad0004315a
15a	6015a40800	b37fa433f9	6015c40001	ad0004315e
	6015e40800	b37fa43000	6016040011	ad00043162
	6016240800	b100043146	6016440001	ad00043166
	6016640002	b17f243168	247f3207ff	400005115c
16a	247f32016c	5116043147	0000000012	CR

Roll 2

Tape 5

7fa	1f00100000	0000100001	4000000000	0000000000
	8000000000	0000000001	0000040000	9064f43002
	6000240010	a164f43004	6000440011	ad00024650
	4b13812001	4d13d12001	4d14024130	5f22924131
00a	5c52e53530	241325c2cd	241335f2ce	240a05f7ef
	2465e5f7ee	160007f7c0	7f7cd7f7d2	7f7df7f7e0
	7f7e17f7e2	7f7e37f7e4	7f7e57f7e6	7f7e77f7e8
	7f7e97f7ed	40000600a1	2401843583	247ff3a7f0
01a	7f7ea247f0	5f7eb607ea	7f7ec4101d	5f7ec600a2
	2401e43594	607f0380a3	5f7c4600a4	2402143583
	247f016000	1c00b7f7f0	7f7f2387f0	5f7c3247f0
	140163a7c4	7f7f1387f1	5f7f1247fc	14001227f1
02a	5f7f1607f1	2402b43490	5f7c6600a5	2402d43583
	247f03a0a7	247fd1c001	380a612001	5f7f5240a8
	400005f7f4	24033435aa	247f85f7d3	247f95f7d4
	607f2387d3	140145f7de	607f2387d4	14014227c4
03a	5f7dd600a9	2403b43594	607f0380aa	120015f7dc
	600ab40000	2403f43594	607f0380aa	120015f7c5
	600ac40000	2404343594	607f0380ad	120065f7d1
	607f0380ae	120065f7d0	600af40000	2404943594
04a	607f0380b0	120065f7f1	207d15f7d1	247f112001
	5f7cf607dc	2404f4337c	607f1387d0	5f7db607f2
	387d15f7da	607dc40000	240544345b	387cf5f7d9
	607cf380b1	5f7f1607d0	380b2207f1	5f7f2247f1

Roll 2

Tape 5 continued

05a	3a7f27f7ce	247f21200a	5f7f24c05d	00000240b3
	3a7dc40000	2405f43490	5f7f1607f1	387f25f7d8
	24656207ff	5f7f0277f0	4a069600b4	2406543583
	247f05f7d7	240bf51103	4306d00000	267ff227fe
06a	5f7d7240c0	511034306d	607ffad000	247fc5f7d5
	5f7d6600b6	2406f43583	247fd607f0	1b0013b0b7
	7f7c8247fd	600b93b7f0	7f7c9600b8	2407543583
	247fd607f0	1b0013b0b7	7f7c7247fd	600b93b7f0
07a	7f7ca600ba	2407b43583	5f7cc607cc	387c91c001
	7f7cb607cb	387ca1c001	7f7f0267f0	200c348082
	000002465d	207ff5f7f1	277f149087	267ff227fe
	5f7c141089	00000600bb	2408843583	5f7c16010a
08a	400007f7c2	240bd5108c	160007f000	2408c207ff
	5f08c517f0	240be227f0	5f7f1277f1	4a0933a001
	4308c00000	60093400c4	b0000430de	277ee4b09e
	607ff43099	0000000000	0000000000	7f65e43000
09a	0000000000	947f54309c	1b0147409d	94fff4309b
	607ee7f65e	4300000000	071afd498d	246535f7f0
	246585f7f0	01312cffe6	246575f7f0	246595f7f0
	6487ed49c5	00000000b4	0000000002	246545f7f0
0aa	6400000000	246555f7f0	2465a5f7f0	01220bc427
	0435bfb19e	2465b5f7f0	0447922480	00a8f5c28f
	038f5c28f5	00000000d6	246565f7f0	0000000113
	246515f7f0	0000000005	246525f7f0	0000000168

Roll 2

Tape 5 continued

0ba	2465c5f7f0	2465d5f7f0	0020c49ba6	00000005c3
	00000007bc	000000010b	000000011b	0000000651
	000000000e	0000000175	24363510c8	510ca267ca
	5f7f4227ff	5f7f316000	7f7f560000	7f7f616000
0ca	400007f000	240c820362	510cd510d1	4000024000
	5f7f740000	240cf43000	7f627f67f8	ff787f8000
	247f3207ff	5f7f3480da	240c8207ff	510c8510ca
	240d643000	ff687f57f5	247f4207ff	5f7f44a294
0da	410c840000	240db43000	7f527f57f5	ff5861d61d
	43101227ff	5f7eb4a0e1	4315240000	247dd5f7e4
	247de5f7e5	247dc5f7e0	247ec5f7ed	160007f7e7
	7f7e6267ff	227fe5f7df	267c15f7c0	247d95f7f2
0ea	5f7f3247da	5f7f1207f3	5f7f3247db	5f7f0207f3
	5f7f35f7e8	4310000000	160001b028	207f220000
	400005f000	1b0295f000	247f3207ff	5f7f34b0d4
	430da5f7f1	2462110001	207f14d0fe	160001b028
0fa	207f22061d	5f61d430fc	1b0295f621	430de607ff
	410f0607ff	410f90002c	241094114b	247c2207ff
	5f7c22210a	4314a43000	160007f7c2	6010540800
	a100043107	6010740010	ad0004114a	000000036a
10a	0000000064	247f35f7f9	4000060364	2410d4352c
	247e85f7f3	247d95f7f2	247da5f7f1	607e2387d3
	5f7f4607e1	387d4227f4	120015f7f4	607e2387d4
	5f7f5607e1	387d3207f5	120015f7e2	247f45f7e1

Roll 2

Tape 5 continued

11a	4327d0000f	247d45f7e1	247d35f7e2	160007f7e3
	607eb387ea	1c0017f7f4	277f448129	241214355f
	140055f7f5	607f5387f4	5f7f42761b	4912a247f4
	3a7ea1b028	2012c5f7e9	247f45f61b	412a62661b
12a	43126247f4	2261b43126	0020000000	0030f0030f
	0029000290	0029f0029f	145f306d97	14001257f5
	1c00a1200a	7f7e7387ce	0a2f9836cb	40000247f5
	1c00812008	7f7e7247e7	241345f229	241355c52e
13a	5353024136	5c2cd5305b	241375f2ce	4300d24130
	5f22924131	5c52e53530	4113a24134	5f22924135
	5c52e53530	4300b00000	6014440039	b00c4430d5
	60146400c4	b000043148	6014840006	ac00043095
14a	4a104247eb	410de51369	4110300000	6014d40800
	a10004326c	0000000000	0000000002	000000001e
	4314d60235	24153430c4	24154430c4	24155430c4
	24156430c4	247d44b175	607c340150	2415943490
15a	5f7bc607bc	387d414013	5f7bd247c4	227bd5f7f1
	247fd607c3	1c0023b7c4	7f7f2247f2	207f11c028
	2416243490	5f7f4607c4	2416443490	607f9387f4
	5f7f1247d9	207da207db	5f7f2607f2	387f11b01a
16a	5f7f640150	2416b434a8	7f7f2387f2	5f7f2607f2
	387f25f7f2	607f2387f2	5f7f2607f2	387f25f7f2
	247d7207ff	4c223247d4	207fc4d177	410de00000
	24176430c4	43197247f2	5f7f06022a	241794350a

Roll 2

Tape 5 continued

17a	6022b430e1	43197607c4	387d41b001	5f7f3267bc
	14015207f3	3a7f141255	247d75f7f4	247fe5f7f5
	247f4227ff	5f7f44b186	607f5387f3	5f7f543182
	267d7227ff	1b02838229	1c003387f5	5f05224150
18a	5f05440000	2418b43043	5f7f3247f1	5f05224151
	5f0544319c	247d4207fc	4e1926022b	430e343197
	247bd14001	227c43a7f1	1b028207ff	5f7f06022a
	241964350a	605cb43198	7f7f06022a	241994350a
19a	16000430e5	4319e00000	2419c43043	5f7f441257
	607cb387ca	1c0017f7f0	2422d511a4	160007f7f1
	247f0227ff	5f7f04b1aa	4000024000	5f7f240000
	241a643000	ff187f27f1	241a4207ff	5f1a4431a2
1aa	241aa43000	5c317f15c3	5c417f15c4	5c517f15c5
	5c585c45c6	5c685c35c6	5d0222f7f5	5c717f55c7
	5c817f55c8	5c917f55c9	5c985c85ca	dca85c75ca
	247ea5f052	160007f054	241b843043	5f7f440000
1ba	241ba43000	7f1122f7f0	7f127f17f1	7f127f47f1
	61d47f17f1	ff122367f1	607f140000	241c143057
	5f7f1245d0	5f7f243237	0000000000	0000000000
	2461c5f7f0	6022c40150	241c84351d	607f0430e7
1ca	246205f7f0	6022c40150	241cc4351d	607f0430e9
	2461f5f7f0	6022c40150	241d04351d	607f0430eb
	2461e5f7f0	6022c40150	241d44351d	607f0430ed
	247ca5f7bf	60235430ef	241d8430c4	241d9430c4

Roll 2

Tape 5 continued

1da	241da430c4	247bf5f7f3	227ff5f7bf	4a1e240000
	601de40080	a1290431e0	24622207ff	510f7430f7
	247cb5f7f1	247ca227f3	5f7f2607f2	387cb1c001
	7f7f3247f3	20231511eb	5f7bc16000	7f7f0247f1
1ea	227ff5f7f1	4b1f124000	5f7f540000	241ed43000
	ff587f07f0	241eb207ff	5f1eb411e9	241f143070
	007f0007f0	24232207f2	511f5411f5	0000024000
	5f7f540000	241f743000	7f027f07f0	7f027f47f0
1fa	ff547f07f5	607f540000	241fc43057	5f7f540000
	241fe43070	007f5007f5	60228430f1	24201430c4
	247c95f7bd	247bd5f7f3	227ff5f7bd	4b1d7247cc
	5f7f1247c9	227f35f7f2	607f2387cc	1c0017f7f3
20a	247f3207bc	5120f51221	160007f7f0	247f1227ff
	5f7f14b215	4000024000	5f7f540000	2421143000
	ff587f07f0	2420f207ff	5f20f4320d	2421543070
	007f0007f0	60228430f3	24218430c4	24219430c4
21a	247cc5f7be	242335f7f2	247be227ff	5f7be4b24d
	247f2227ff	5f7f248221	242335f7f2	4321e24000
	4124800000	43220247d4	207fc4c17b	247fe5f7f5
	4318600000	000000002c	aaaaaaaaaa	145f306d97
22a	00001247f0	f999999999	247f05f7f0	0000000647
	00004247f0	0040000000	240c143070	0000000647
	00000005f6	0000000004	bbbbbbbbbb	ffffffffff
	0340000000	2423743000	5d025d07f3	7f327f47f3

Roll 2

Tape 5 continued

23a	e1a47f37f3	607f340000	2423c43057	5f7f340000
	2423e43070	007f0007f3	605cc7f7f0	605cd7f7f1
	605cf7f7f2	605ce7f7f3	6022e40000	242454350a
	2424643070	005c3005ca	431c65f7f0	2424943070
24a	007f0007f0	24221207ff	5f2214321c	247f2227ff
	5f7f24b203	60234430f5	4324d24000	4000060000
	3b7ea1b028	227f41b028	387ea1b028	431f87f7f3
	247f34b175	43180247f2	5f05216000	7f05440000
25a	2425a43043	5f7f540000	2425c43000	7f317f47f3
	7f317f47f3	ff327f57f3	2423043070	607e07f7bc
	242624337c	607f1387d0	5f7f0607f2	387d15f7f1
	207f05f7bd	277cf5f7f2	4a28e607bc	242694345b
26a	387cf5f7f2	207bd00000	6026c40010	ad00043144
	1b01a5f7f3	4f27d607e5	387e81b01a	5f7f44f27d
	607e6387e8	1b01a5f7f5	4f27d607c4	387e81b01a
	207f35f7f3	607f3387e1	5f7f6607f4	387e2207f6
27a	5f7f6607f5	387e3207f6	5f7f64c2a4	2427d4347f
	412a6607f3	387f35f7f3	607f4387f4	207f35f7f3
	607f5387f5	207f35f7f3	4f27d41332	387c31200a
	227f35f7f4	607f61b001	413345f7f4	4b27d43131
28a	b226143261	24361227e0	4b29924361	5f7e043299
	247bd4126b	5f7e84327d	247f35f7bc	16000777bc
	267bc4a0b0	410b200000	2435b510c8	510ca410c8
	5f61c247c0	207ff5f7c0	4829e41355	2435910014

Roll 2

Tape 5 continued

29a	5326b43261	247ed205cc	5f5cc607df	387ed205cd
	5f5cd430c4	277c3482ed	247e4412f2	160007f7f5
	160007f7f7	4136960364	433534a27d	4127e60366
	ae260607e4	387e81b013	5f7f3607e9	387e1207f3
2aa	120074f29b	5f7f35f7bc	607e5387e8	1b0135f7f4
	607e9387e2	207f412007	4f29b5f7f4	5f7bd607e6
	387e81b013	5f7f5607e9	387e3207f5	120074f29b
	5f7f55f7be	607f4387f4	5f7f7607f5	387f5207f7
2ba	207ff5f7f6	247f714002	3a7f67f7cd	607f3387f3
	207f65f7f6	120005f7bf	4f29b16000	247f31c01a
	3b7e87f7e4	16000247f4	1c01a3b7e8	7f7e516000
	247f51c01a	3b7e87f7e6	247e85f7f3	247e02235d
2ca	4a2d6607df	242cb43490	247d816000	1c00a3b7f9
	7f7e7387ce	5f7f4247f2	227f45f7f2	247f0227e7
	207f45f7f0	207f1207f2	5f7f33a7e8	387ed5f7ed
	247f23a7f3	7f7f2247f1	3a7f37f7f1	607ef387ee
2da	1c0017f7ee	257ee227f2	482df2435e	5f7d22461e
	207ff5f61e	432e6227f1	482e32435f	5f7d22461f
	207ff5f61f	432e624360	5f7d224620	207ff5f620
	40260607f6	242e743490	5f7f616000	1c0193b7e8
2ea	7f7bf247bf	1200a4d352	247c4207e4	4b2f2267e0
	20361492f5	247df5f7f4	267fc14002	5f7f341311
	4329f3a7bf	267ff1b028	207c649352	412ed607be
	387e35f7f1	607bd387e2	207f15f7f1	607bc387e1

Roll 2

Tape 5 continued

2fa	207f140260	3a7f67f7f2	607f2387f2	5f7f312001
	227fc1400d	5f7f4607d2	387d2207f4	5f7f4607f4
	2430243490	5f7f4247f3	1400c3a7f4	7f7f3247f2
	14005227f3	227f414003	3a7d27f7f3	247f214006
30a	5f7f2247f4	227f25f7f2	247fc14006	207d25f7f4
	247f23a7f4	7f7f4387f4	1b028387df	5f7f440000
	247bf5f052	243675f054	2431443043	5f7f5607f3
	3835c1b002	5f05216000	7f05440000	2431943043
31a	5f7f324359	5326b607f4	387dc5f7bc	607bc43262
	1400a3a7e8	387f61200a	4d3525f7f6	24321434a8
	7f05216000	7f05440000	2432443043	5f7bc247ed
	5f05216000	7f05440000	2432843043	5f7f640000
32a	2432a43000	7f527f57f5	7bc27bc7bc	7bc27bc7bc
	7bc27bc7bc	7bc27bc7bc	7bc27f37f3	ff317f57f3
	43290607e8	387e81c028	432857f7f6	387f6207f4
	41288247e4	3a7bf7f7f9	247c75f7f8	24339434b3
33a	607f6387cb	1b0272035a	5f7f2247f6	2036351376
	51379607cd	2433f43490	247e54a342	267f95f7f9
	247c85f7f8	24343434b3	607f6387cc	1b02740260
	207f25f7f2	247dc430b4	5f7f640000	2434943000
34a	7f323687f5	ff587f6000	247f45f052	160007f054
	2434e43043	410bc24369	203655f369	4337600000
	00000432a1	24353434d7	2461c207ff	43296247c5
	227e04b28b	247ed205cb	5f5cb4129e	4328f4331e

Roll 2

Tape 5 continued

35a	0000000647	00000005f5	eba0cf9269	000ccccccc
	01020c49ba	1000000000	0e020c49ba	00000000d6
	0000000025	00000005d1	0000043490	0000000004
	0000000002	000000001d	0040000000	0000043000
36a	2436a43000	7f585c35c3	ff785c75c7	4134f00000
	2436e43000	7f585c45c4	ff785c85c8	4134f00000
	2437243000	7f585c55c5	ff785c95c9	4134f00000
	412a324000	5f7f640000	2437843000	7f587f6000
37a	ff285d05d0	4136900000	207fa5c392	7f7f0247f0
	223ab49392	223ac49385	223ad49382	18022203aa
	43388203ad	5f7f9603bb	387f9203a9	43388203ac
	5f7f9603ae	387f9203a8	51389207ff	5138c2437c
38a	5f7f112014	5f7f21c001	7f7f92437c	227f15f7f8
	387f8207f1	5f7f1607f8	1a014387f9	207f25f7f2
	00000203af	4a3a0203b0	4839d247f0	120065f7f9
	243b13a7f9	7f7f8247f8	14006203b2	5f7f2243b3
39a	3a7f97f7f8	247f814004	203b45f7f1	43392243b2
	5f7f2243b4	5f7f143392	607f0383b5	1b002203b6
	5f7f2607f0	383b71b009	203b85f7f9	607f0383b9
	1b005203ba	3a7f97f7f1	43392203bc	000002041c
3aa	000002044e	0033333333	04cccccccc	0a00000000
	0000000a00	00332617c2	00000bcbe6	00000012ca
	0799999999	00000022e6	1400000000	9fe7663f0a
	0799c0f601	5e380bb6ed	0200000000	696b9ec1c1

Roll 2

Tape 5 continued

3ba	0051ae7ef5	0000000280	08fff06fff	08ccc070a3
	0833307199	07ccc07333	07666074cc	0733307666
	06f0a078a3	06a8f07b85	0666607eb8	0633308428
	05f5c08999	05bd7097ff	05b330b999	0bccc1bfff
3ca	0557018fff	04eb813333	0547a09fff	0499907fff
	0466607333	041eb06b33	031eb06666	0399906333
	050a305fff	04e1405eb8	047ff05e14	0442805e14
	0405105e66	03ccc05f0a	039eb05fff	037ae0623d
3da	034cc06666	030f506b33	02ccc07666	028a3097ff
	01eb80bccc	023330e428	03fff0ffff	0551e0d999
	0451e09ccc	03ae107ccc	03fff07333	0733306a8f
	02fff06666	02fff0647a	02fff06333	02fff060a3
3ea	02e6605fff	030a3061eb	0333307666	03ae10b999
	0699909666	0466605fff	0514705333	04c2804ccc
	0442804999	03f0a047ff	03bd704666	03b8504428
	03d70041eb	047ff040a3	0685103fff	041eb044cc
3fa	03ccc0afff	03ae104fff	03a3d03b33	03b85038f5
	04051037ff	04fae03666	057ff037ff	0466603fff
	03ccc03fff	03a8f044cc	038a305fff	037ae04ccc
	0370a03fff	03666037ff	035c203333	03570030a3
40a	0351e02f5c	0347a02e66	0338502dc2	0333302d70
	0333302ccc	0347a02bd7	0357002b33	038f5029eb
	03ccc027ff	0399902428	0366601e66	032e100fff
	030a3007ff	0305100ae1	02fff018f5	0305101e66

Roll 2

Tape 5 continued

41a 03051021eb 0305102428 0305102614 030a3028f5
030f502999 02b3302999 0333302999 03a3d02999
0357002f0a 03d1e04666 0319905fff 031eb060a3
03b8505999 03a3d05ccc 0366606333 036b805999
42a 0394704999 03ccc03666 039990323d 0366603ccc
0333304ccc 02fff03ccc 02ccc02fff 02a8f03999
029eb02666 02a8f02999 02bd702c28 02ccc02666
02d1e03fff 02d7003333 02dc202999 02e1402666
43a 02e1402199 02dc202fff 02d7004333 02ccc02e66
02ccc03333 02ccc02ccc 02c7a02999 02bd702666
02b850275c 02b3302ccc 02b3301fff 02b33024cc
02b5c02b33 02b8503333 02bd702d70 02c2802fff
44a 02d1e03428 02dc203fff 02e6604ccc 02eb803b33
02eb8034cc 02bd701fff 02bd702bd7 0328f0323d
0328f03333 031c2034cc 030cc034cc 02fff034cc
02f5c03333 02e660323d 02d7003199 02ca3030a3
45a 02bd702f33 7f7f9207fa 5c468247f9 2247a49468
2247b4946f 607f938476 204755f7f7 607f7387f9
2047d5f7f7 60477387f9 204785f7f8 607f8387f9
204793a7f7 7f7f8247f8 4345b247f9 3a47e7f7f9
46a 607f93847c 2047d5f7f7 607f938473 204723a7f7
7f7f8247f8 4346824474 604745f7f8 4346800000
00005d4c8c 011fbaac8d 2800000000 00fbae9154
1079a73b42 fffbbca1cd 000cf8ebb4 00002950cd

Roll 2

Tape 5 continued

47a	0000014f8b	00028e0cb9	0398bbc1e4	0000800000
	000008637c	207fa5f48e	247fd5f7f8	5f7f9607ee
	5f7f7387ef	1c001777f7	777f8387ef	1c001777f9
	247f9227f8	4a48c387ef	1c001777f8	247f8227f9
48a	49484247f7	2048f43482	7f7ee247f7	100035f7e9
	0000000208	0100000000	207fa5c4a5	247fb544a4
	7f7f7267f7	4b497247f7	484a4414a5	5f7f7247fb
	204a45c4a4	247f71b002	4e495604a6	387f7204a7
49a	5f7f8247f7	3a7f87f7f9	247f9207f8	100015f7f8
	247f73a7f8	7f7f9247f9	207f810001	5f7f8247f7
	3a7f87f7f9	247f9207f8	100015f7f9	4300000202
	5200000000	2e00000000	207fa5c4b1	264b25f7f9
4aa	247f61c027	3b7f91b028	227fe5f7f8	247f9207ff
	484b05f7f9	607f6387f8	414aa607f8	0000000000
	0000000011	207fa5c4c4	244c4514be	247fd604d6
	3b7f87f7f7	277f75f7f7	160017f7f6	4a4c4207ff
4ba	5f7f5244be	207f8514be	247f7207ff	5f7f7484c1
	257f922273	484c1247f6	207ff5f7f6	414ba247f9
	4a4c4267f5	227f65f7f6	00000204c4	3fc193b3a6
	3f072085b1	3dd1a21ea3	3c23e18697	39ff583a53
4ca	376d0917d6	346cf41f20	3106cca2db	2d414a4d2a
	292324c836	24b588e368	1fffffffff	1b0c34c1a8
	15e3a7daa4	109081c2e3	0b1d14e3bc	0593dd97f6
	0000000024	734e573502	207fa5c508	607ee387ef

Roll 2

Tape 5 continued

4da	1c0017f7f0	387ef1c001	7f7ee387ee	5f7f1607f0
	387f0207f1	4f4d95f7f2	607ee7f7f1	387ef1c001
	7f7ee387ee	207f24f4d9	5f7f2607f2	244e5434d7
	5f7f2247d2	205095f7f3	247d23a7f3	7f7f424509
4ea	3a7f37f7f5	247f03a7f2	387f414001	5f7f0607e1
	387f5207f0	5f7f0247f1	3a7f2387f4	140015f7f1
	607e2387f5	207f15f7f1	247ee3a7f2	387f414001
	5f7f2607e3	387f5207f2	5f7f2607f0	387f05f7f3
4fa	607f1387f1	207f35f7f3	607f2387f2	207f312002
	5f7f3607f3	387df5f7df	607f3387e0	5f7e0607f3
	24502434d7	5f7f3247f0	3a7f37f7e1	247f13a7f3
	7f7e2247f2	3a7f37f7e3	434d700000	0100000000
50a	207fa5c50f	7350f247fd	1c0147f7f7	247f7227ff
	5f7f74850f	0000000000	5f7f8257f8	5f7f6247ff
	160035f7f9	247f614002	207f61a004	100015f7f6
	247f9227ff	48512247f8	4a51a1a004	267ff1c004
51a	2451a430c4	2450f207ff	5f50f4350d	207fa5c52a
	7c51f73529	2451d5f7f7	4952a2652b	5f7f816000
	7f7f9247f8	207ff5f7f8	48528247f7	1c0273b52b
	7f7f7607f9	1c0047f7f9	41522247f9	100045f51d
52a	430fa00fff	000000000a	73555207fa	5c55e267ea
	14001207d6	5f7f5267d7	4b533257f5	5f7d65f7e1
	5f7d541549	247d7207ff	5f7f616000	1c0057f7f7
	247f514005	3a7f77f7f5	247d73a7f6	7f7f6247d5

Roll 2

Tape 5 continued

53a	5f7d6267d7	5f7f7247f7	207ff5f7f7	4a540607d5
	387d612001	5f7d64153b	257f53a7d6	7f7f7607d5
	387f6207f7	5f7f7267d5	207f74a547	247f75f7d5
	5f7d64153a	607f77f7e1	387d612001	5f7d6607ee
54a	387ef1c001	7f7f5387ef	1c0017f7ee	387ee5f7f6
	607f5387f5	207f64d549	5f7f6607d5	387d55f7f7
	247fc14001	227f75f7f7	4052c607f7	245554352c
	5f7f4607f6	2455553558	245584352c	5f7f6247f5
55a	3a7f6387f4	5f7e2247ee	3a7f6387f4	5f7e34052c
	5f7e3404e2	207fa5c57b	7f7f6277f6	49562247ff
	5f7f6247fc	140055f7f7	247f612001	4d5685f7f6
	247fc14005	207f75f7f7	4356414002	5f7f62057c
56a	5f7f8247f6	2257c3e7f8	7f7f6397f6	5f7f8607f8
	3958220581	5f7f9607f8	397f920580	5f7f9607f8
	397f92057f	5f7f9607f6	397f92057e	5f7f96057d
	397f95f7f9	607f73957d	120015f7f7	247f9227f7
57a	5f7f94055f	4305000000	2d413ccd02	58b90bfbff
	0200000000	0b8aa3b209	03d8e24c81	024e6c2038
	01bcae9688	207fa5c591	7c58573590	245835f7f3
	247ff1e003	5f7f87f7f5	607f31a004	247fd1b001
58a	207f51b002	207f51b001	5f7f5247f8	227ff5f7f8
	4a589247f3	49591247f5	405835f583	43583267f5
	4159000000	0000000000	207fa5c5a8	735a77c596
	000005f7f1	267ff16003	7f7f55f7f2	607f11a004

Roll 2

Tape 5 continued

59a	247fd1b004	207f55f7f8	12002207f8	120015f7f5
	247f2207ff	5f7f24b59a	247fd1b004	207f55f7f8
	607f8385a9	1b00b207ff	100015f7f2	247f14a5a7
	267f2415a7	247f200000	0000000000	44b82fa09b
5aa	205c25c5bc	247fc5f7f6	5f7f9247fd	5f7f8207ff
	5f7f7247f5	1c0273b7f7	397f65f7f6	207f85f7f8
	247f7207ff	5f7f7267f5	1c0273b7f7	397f65f7f6
	207f95f7f9	277f64a5b9	247f7415ad	247fc14002
5ba	5f7f7247f4	227ff5f7f4	00000607f8	397f91b002
	5f7f8607f9	397f9227f7	1b0025f7f9	415ba00000
	2700100000	0000000000	0000000000	0000000000
	0000000000	0000000000	0000000000	0000000000
5ca	0000000000	0000000000	0000000000	0000000000
	0000000000	0000000000	207fb54001	240005f03e
	5101116001	1b00754008	1b00471005	5f03f24000
	1c0207f03a	5f03b16000	240001c020	7f03c5f03d
5da	2403f49020	120024901f	1200149035	1200149016
	2503a43030	6003a2403b	1b01f60042	1b0015f000
	4f04024001	207fb54001	2403e4a001	2400154016
	430002703c	480232703a	480112503a	2303c4b01d
5ea	2403a14001	5f03a2403b	207ff5f03b	2403a3a03c
	2403b2203d	430102603c	5f03c2703a	4b0246003c
	2403d1b020	4101100000	2703c4a00f	2403b2203d
	4802a5f03f	2403a6003c	5f03c7f03a	2403d5f03b

Roll 2

Tape 5 continued

5fa	2603f5102c	220394a00f	2403c14000	2003a4e030
	1c0292403b	207ff43010	5f03a2703a	480112403a
	120014f00f	5f03a2403b	227ff5f03b	410312403b
	2003d5f03b	6003a3803c	5f03a41030	0000000020
60a	0000000000	0000000000	0000000000	0000000000
	0000000000	0000000000	4a039247fd	4101100000
	ffffffffff	207fa5c045	2705249045	0000024052
	1200a4d049	5f05224054	220565f054	4104524052
61a	120014d04d	5f05224054	227ff5f054	4104924052
	100085f052	2405412020	2005243045	0000000000
	0000000000	0000000000	0000000000	0000000000
	000000000a	207fa5c061	7f0671b007	7f06824068
62a	4906124067	1400158067	2406716000	1c02040000
	2405e43490	1400857067	24067407f9	0000024067
	1400c207fb	1200b58067	2406716000	1c020247fd
	1c0014305e	0000000000	0000000000	0000000000
63a	0000000000	0000000000	0000000000	0000000000
	7f06884068	430a500000	207fb54072	207fb540a6
	2400054074	16014540a9	240001c020	7f0691c028
	380ad207ff	5f06a1b028	10001207fe	5f06b6006b
64a	390ae5f06b	267fb14010	5f06c2606b	5f06d1c027
	3b06c1a001	1c0012406c	207ff7f06b	4a0835f06c
	3806d4107d	6006b3906b	5f06d6006d	3906d5f06b
	6006b39069	5f06912002	2006912001	4d08b5f069

65a	2406a227ff	5f06a24069	4908d607fd	4308e60042
	25069200ac	4e0932406a	207ff5f06a	247fc10002
	1a01843099	5f069260aa	5f06b25069	1400221069
	1a00410001	5f0692406b	207ff4b094	2406a4b09b
66a	247fd4109b	240421b004	7f06b16000	7f06d2506a
	220ab490a1	5f06a2406d	207ff5f06d	4109d2406d
	120042106a	120206006b	1b008430d3	24074220a9
	4a00024074	207fb54074	4307400000	240001c020
67a	0000000006	000000000a	00000431be	268826a13f
	49aec6eed6	0000000000	240b043000	ff327f67f3
	41336247f6	5f7f341336	227c55f7f0	607f4387dc
	5f7f8267f8	207c548352	207f03a7f0	387cc207f2
68a	510bb5134b	4000024000	433485f7f4	240bd43000
	7f427f37f2	7f285f55f5	ff223687f7	4137600000
	007f3007f3	4318f00000	207fa5c0cc	24621207ff
	5f6212412d	22623490cc	2462340000	40000540ca
69a	7f00024623	207fb5f623	000007f7f1	2412e5f623
	600ce40080	a1290430d0	24622207ff	5f622607f1
	430c800000	240d3430c4	430a500000	600d540010
	a9000430d7	600d740090	b128f430d9	607ff7f622
6aa	2412f5f623	2411a53621	607ee40000	240dd430c4
	4115216000	240df430c4	4317600000	240e1430c4
	4317b00000	240e3430c4	4119100000	240e5430c4
	4319b00000	240e7430c4	431ca00000	240e9430c4

Roll 2

Tape 5 continued

6ba	431ce00000	240eb430c4	431d200000	240ed430c4
	431d600000	240ef430c4	431d800000	240f1430c4
	4320100000	240f3430c4	4321800000	240f5430c4
	4325000000	600f740000	ad00040000	600f940002
6ca	a1621430fb	600fb40027	b000043006	2428f1c008
	247fd1b004	4000012024	4f01e12001	4f02012001
	4f02343009	246211200c	5f7f02428f	5f7f143000
	6000940780	b27fa43141	246215100e	5f7f924622
6da	5101040000	6000e40000	b130043010	6001040000
	ad00043012	247f9227ff	5f7f94b017	6030084300
	24014207fb	5f01443012	4000043000	6001840012
	ad0004301a	6001a40800	b100043146	0000000018
6ea	0000000009	2401c51017	4300b00000	2401d51017
	4300b00000	0000000030	240225f621	247ff5f622
	2401d51017	4300b00000	606f4400c4	a05d0436f6
	606f640039	a0694436f8	606f840027	a06cd436fa
6fa	606fa400c4	a0000436fc	606fc40006	ac00043095
	CR			